

A Geometric Structure Associated with the Convex Polygon

Kai Jin

The Hong Kong University of Science and Technology
Clear Water Bay, Hong Kong SAR
cscjkk@gmail.com

Abstract

We propose a geometric structure induced by any given convex polygon P , called $\text{Nest}(P)$, which is an arrangement of $\Theta(n^2)$ line segments, each of which is parallel to an edge of P , where n denotes the number of edges of P . We then deduce six nontrivial properties of $\text{Nest}(P)$ from the convexity of P and the parallelism of the line segments in $\text{Nest}(P)$. Among others, we show that $\text{Nest}(P)$ is a subdivision of the exterior of P , and its inner boundary interleaves the boundary of P . They manifest that $\text{Nest}(P)$ has a surprisingly good interaction with the boundary of P . Furthermore, we study some computational problems on $\text{Nest}(P)$. In particular, we consider three kinds of location queries on $\text{Nest}(P)$ and answer each of them in (amortized) $O(\log^2 n)$ time. Our algorithm for answering these queries avoids an explicit construction of $\text{Nest}(P)$, which would take $\Omega(n^2)$ time.

By applying the aforementioned six properties altogether, we find that the geometric optimization problem of finding the maximum area parallelogram(s) in P can be reduced to answering $O(n)$ aforementioned location queries, and thus be solved in $O(n \log^2 n)$ time. This application will be reported in a subsequent paper.

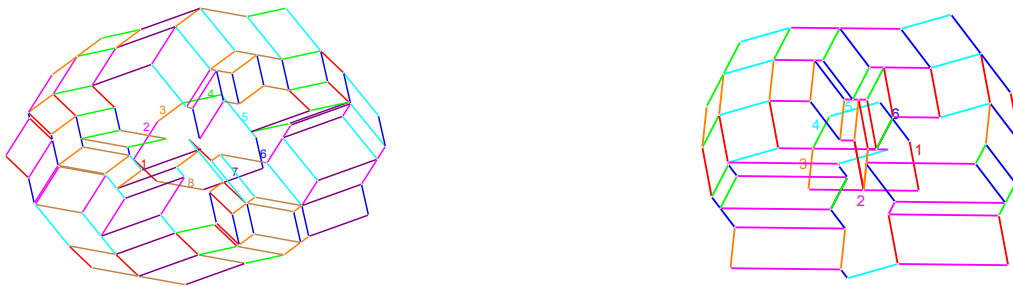


Figure 1: Two examples of $\text{Nest}(P)$. The line segments labeled from 1 to n in clockwise order indicate the n edges of P . The other line segments in the figure are the edges from $\text{Nest}(P)$.

1 Introduction

Geometric structures associated with every instance in a certain space have drawn a lot of attention in discrete and computational geometry. Some prominent representatives are Delaunay triangulation [1], Voronoi diagram [1] (with many variants), and Zonotope [7], which have found enormous applications due to their rich structural properties.

In this manuscript we introduce a geometric structure that is induced by the convex polygons. More specifically, for every convex polygon P , we define a structure called $\text{Nest}(P)$, which is arrangement of $\Theta(n^2)$ line segments, each of which is parallel to an edge of P , where n denotes the number of edges of P . See examples in Figure 1.

The definition of $\text{Nest}(P)$ is roughly as follows. Throughout, regard P as a compact set that contains its boundary and interior. Assume (l, l') is taken over those pairs of nonparallel supporting lines of P with the following property: the intersections $l \cap P$, $l' \cap P$, and $l' \cap P$ lie in clockwise order. Denote by $B_{l, l'}$ the (unique) point in P that maximizes the product $d_l(B) \cdot d_{l'}(B)$, where $d_l(B)$ denotes the Euclidean distance from B to l . Denote $F = \{A + A' - B_{l, l'} \mid A \in l \cap P, A' \in l' \cap P, (l, l') \text{ is taken over the aforesaid pairs of supporting lines}\}$. We call each vertex or edge of P a *unit*, and regard the edges as open, i.e. they do not contain their endpoints. Thus each point in the boundary of P lies in exactly one unit. Observe that we can define a subregion of F by adding a constraint that A, A' lie in a certain pair of units, and we can also define a subregion of F by adding a constraint that $B_{l, l'}$ is restrict to a certain unit. The union of the boundaries of all such subregions is defined to be $\text{Nest}(P)$.

Note: As shown below, to rigorously define $\text{Nest}(P)$ we need several cascading notations, a few of which do not originate in this manuscript but in [3]. However, only in this manuscript, we introduce and study $\text{Nest}(P)$.

This new structure turns out to have a number of surprising properties. In this manuscript, we prove six simple (yet nontrivial) properties of $\text{Nest}(P)$, which all manifest that $\text{Nest}(P)$ has good interactions with the boundary of P (see Theorem 1), e.g. $\text{Nest}(P)$ is a subdivision [1] of the exterior of P . These properties are essentially the properties of the convex polygon P , and hence may be of independent interest in convex geometry. Moreover, we study some computational aspects of $\text{Nest}(P)$. We show that several location queries in $\text{Nest}(P)$ can be answered in $O(\log^2 n)$ amortized time, without having a construction of $\text{Nest}(P)$, which costs $\Omega(n^2)$ time (see Theorem 2).

Application. In a subsequent paper (and also in my PhD. dissertation), we show that computing the parallelograms with the maximum area in convex polygon P (as well as the parallelograms whose areas are locally maximum) reduces to answering $O(n)$ aforementioned location queries on $\text{Nest}(P)$ and hence can be solved in $O(n \log^2 n)$ time by applying Theorem 2. This result is superior than the most related work including $O(n^3)$, $O(n^2 \log n)$, $O(n^2)$, $O(n^2)$, and $O(n^2)$ time algorithms for finding the maximum rectangle [2], maximum similar copy of a given triangle [6], maximum inscribed equilateral triangle and square [5], and maximum parallelogram [3] in a convex polygon. Interestingly, each property in Theorem 1 has a particular value in proving this reduction.

We state our results in this section, state important lemmas in section 2, and outline our techniques in section 3.

1.1 The so-called chasing relation between every two edges and every two units

Edges and vertices. Let e_1, \dots, e_n be a clockwise enumeration of the edges of P . For simplicity of discussion, assume the edges are **pairwise-nonparallel**. Denote the vertices of P by v_1, \dots, v_n such that $e_i = (v_i, v_{i+1})$ (where $v_{n+1} = v_1$). Denote the boundary of P by ∂P . As mentioned above, each point X in ∂P lies in a unique unit; denote the unit by $\mathbf{u}(X)$. Unless otherwise stated, an edge, vertex, or unit refers to an edge, vertex, or unit of P , respectively. Denote by ℓ_i the extended line of e_i .

Chasing relation between edges. Edge e_i is *chasing* e_j , denoted by $e_i \prec e_j$, if the intersection of ℓ_i and ℓ_j lies between e_i, e_j clockwise. Denote by $e_i \preceq e_j$ if $e_i = e_j$ or $e_i \prec e_j$. By the pairwise-nonparallel assumption of edges, exactly one in every pair of distinct edges is chasing the other.

For example, in the left picture of Figure 1, e_2 is chasing e_3, \dots, e_6 , whereas e_7, e_8, e_1 are chasing e_2 .

Backward and forward edges of every unit. The backward and forward edges of v_i are e_{i-1} and e_i , respectively. The backward and forward edges of e_i are e_i itself. Intuitively, if you start at any point in a unit u and move counter-clockwise (clockwise) along ∂P by an infinitely small step, you will be located at the backward (forward) edge of u . Denote the backward and forward edge of u by $\text{back}(u)$ and $\text{forw}(u)$ respectively.

Chasing relation between units. We say unit u is *chasing* unit u' if

$$\text{back}(u) \prec \text{back}(u') \text{ and } \text{forw}(u) \prec \text{forw}(u'). \quad (1)$$

Note: The relation “chasing between units” is a compatible extension of “chasing between edges”.

Note: It may occur that neither u is chasing u' , nor u' is chasing u .

1.2 Define $\zeta(u, u')$ for each unit pair (u, u') in which u is chasing u'

The *distance-product* from point X to lines (l, l') , denoted by $\text{disprod}_{l, l'}(X)$, is defined as $d_l(X) \cdot d_{l'}(X)$.

Z-points [3]. Given two edges e_i, e_j such that $e_i \prec e_j$, it is trivial and proved in [3] that in domain P , function $\text{disprod}_{\ell_i, \ell_j}(\cdot)$ achieves maximum value at a unique point; and this point must lie in ∂P . Denote this maximum value point by $Z_{e_i}^{e_j}$ or Z_i^j for short. We call the $\Theta(n^2)$ points in $\{Z_i^j \mid e_i \prec e_j\}$ the *Z-points*.

Boundary-portions of P . Every continuous portion of ∂P (including a single point of ∂P) is called a *boundary-portion*. If we travel around ∂P from one point X to another point X' clockwise, we pass through a boundary-portion; the endpoints-inclusive and endpoints-exclusive versions of this portion are denoted by $[X \circlearrowleft X']$ and $(X \circlearrowleft X')$ respectively. Points X and X' are referred to as their *starting and terminal points*.

Note: We assume that $[X \circlearrowleft X']$ only contains the single point X but not the entire ∂P when $X = X'$.

We regard every boundary-portion directed and the direction conforms with the clockwise order.

For two points A and B in a boundary-portion ρ , we state that $A <_\rho B$ if A would be encountered earlier than B when we travel along ρ (clockwise), and we state that $A \leq_\rho B$ if $A = B$ or $A <_\rho B$.

We recall a property of the Z-points given in [3]. It is helpful for understanding (2) – the definition of ζ .

Fact 1 ([3] Bi-monotonicity of the Z-points). Given e_s, e_t such that $e_s \preceq e_t$. Let $S = \{(e_i, e_j) \mid e_i \prec e_j, \text{ and } e_i, e_j \text{ both belong to } \{e_s, e_{s+1}, \dots, e_t\}\}$. We claim that all the Z-points in set $\{Z_i^j \mid (e_i, e_j) \in S\}$ lie in boundary-portion $\rho = [v_{t+1} \circlearrowleft v_s]$, and more importantly, they obey the following bi-monotonicity:

$$\text{For } (e_i, e_j) \in S \text{ and } (e_{i'}, e_{j'}) \in S, \text{ if } e_i \preceq e_{i'} \text{ and } e_j \preceq e_{j'}, \text{ then } Z_i^j \leq_\rho Z_{i'}^{j'}.$$

Boundary-portion $\zeta(u, u')$. [3] For every unit pair (u, u') such that u is chasing u' , define

$$\zeta(u, u') := [Z_{\text{back}(u)}^{\text{back}(u')} \circlearrowleft Z_{\text{forw}(u)}^{\text{forw}(u')}]. \quad (\text{See Figure 2 for an illustration.}) \quad (2)$$

Note that when u is chasing u' , we have (1), and thus $Z_{\text{back}(u)}^{\text{back}(u')}$ and $Z_{\text{forw}(u)}^{\text{forw}(u')}$ are both defined.

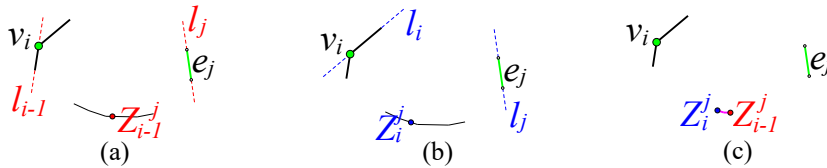


Figure 2: Illustration of (2). Suppose u is a vertex whereas u' is an edge; other cases are similar. Assume $u = v_i$ and $u' = e_j$. First, find the *backward edges* of u, u' , which are e_{i-1}, e_j , and find the point in P with the maximum distance-product to the extended lines of these two edges, i.e., Z_{i-1}^j ; see (a). Second, find the *forward edges* of u, u' , which are e_i, e_j , and find the point in P with the maximum distance-product to the extended lines of these two lines, i.e., Z_i^j ; see (b). Then, $\zeta(u, u')$ is the boundary-portion from the first Z-point to the second; see (c).

Note: When u, u' are both edges, $\zeta(u, u')$ is a point, which equals $Z_u^{u'}$. When at least one of u, u' is a vertex, $\zeta(u, u')$ could be either a boundary-portion that is not a single point, or just a single point – which occurs when the two Z-points $Z_{\text{back}(u)}^{\text{back}(u')}, Z_{\text{forw}(u)}^{\text{forw}(u')}$ coincide. For example, Z_i^j can be equal to Z_{i-1}^j when v_i is chasing e_j .

1.3 Set \mathcal{T} , and blocks and sectors of $f(\mathcal{T})$

Let notation $[\alpha, \beta, \gamma]$ be short for $\{(X_1, X_2, X_3) \mid X_1 \in \alpha, X_2 \in \beta, X_3 \in \gamma\}$. Define $f(X_1, X_2, X_3) = X_1 + X_3 - X_2$, i.e. the unique point X so that $X_1X_2X_3X$ forms a parallelogram. Moreover, for any $S \subseteq [\partial P, \partial P, \partial P]$, let $f(S)$ denote $\{f(X_1, X_2, X_3) \mid (X_1, X_2, X_3) \in S\}$, which is a region in the plane.

We define \mathcal{T}^P , abbreviated as \mathcal{T} when P is clear, as the following subset of $[\partial P, \partial P, \partial P]$.

$$\begin{aligned} \mathcal{T}^P &:= \bigcup_{u \text{ is chasing } u'} [u', \zeta(u, u'), u] = \bigcup_{u \text{ is chasing } u'} \{(X_1 \in u', X_2 \in \zeta(u, u'), X_3 \in u)\} \\ &= \{(X_1, X_2, X_3) \in \partial P^3 \mid \mathbf{u}(X_3) \text{ is chasing } \mathbf{u}(X_1), X_2 \in \zeta(\mathbf{u}(X_3), \mathbf{u}(X_1))\}. \end{aligned} \quad (3)$$

For any unit pair (u, u') in which u is chasing u' , define

$$\text{block}(u, u') := f(\{(X_1, X_2, X_3) \in \mathcal{T} \mid X_3 \in u, X_1 \in u'\}) = f([u', \zeta(u, u'), u]). \quad (4)$$

For any unit w , define

$$\text{sector}(w) := f(\{(X_1, X_2, X_3) \in \mathcal{T} \mid X_2 \in w\}). \quad (5)$$

We call each region in $\{\text{block}(u, u') \mid u \text{ is chasing } u'\}$ a *block* (of $f(\mathcal{T})$) and each region in $\{\text{sector}(w) \mid w \text{ is a unit of } P\}$ a *sector* (of $f(\mathcal{T})$). By the definition of blocks, the union of all the $\Theta(n^2)$ blocks is $f(\mathcal{T})$. Similarly, by the definition of sectors, the union of all the $2n$ sectors is also $f(\mathcal{T})$.

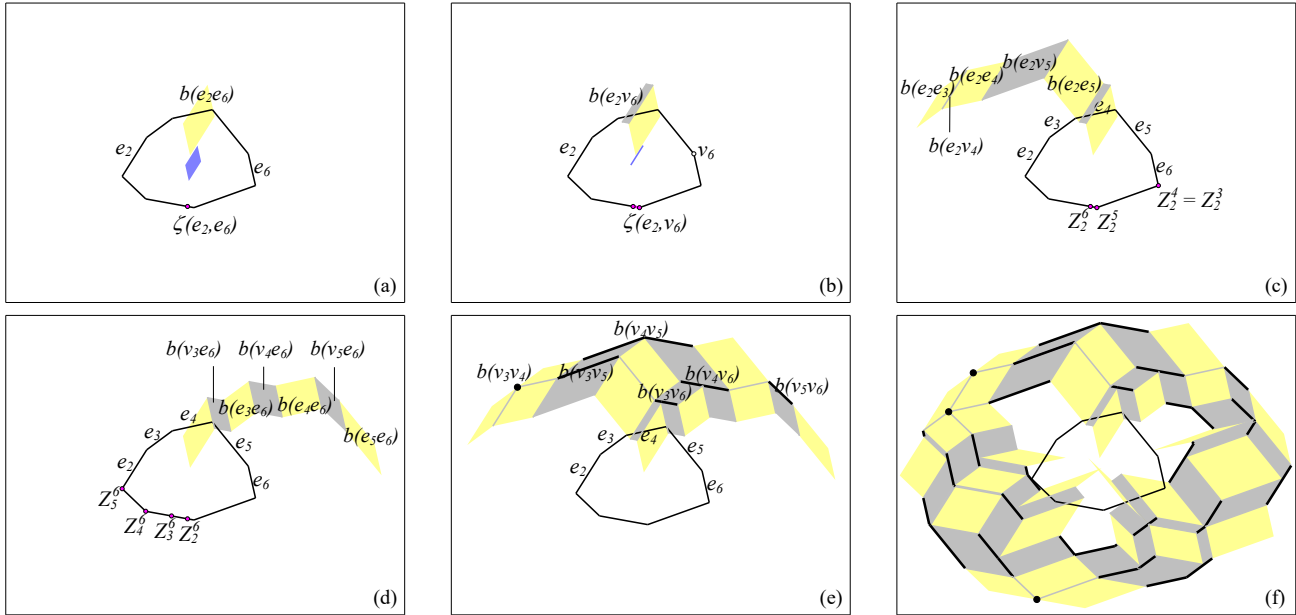


Figure 3: Illustration of (4). In this figure, notation $\text{block}(u, u')$ is abbreviated as $b(uu')$. The region of $\text{block}(u, u')$ is colored yellow, black, or gray, when u, u' are both edges, both vertices, or one vertex and one edge.

We illustrate the definition of the blocks by Figure 3. In this figure, we consider a convex polygon with eight edges. Picture (a) draws $\text{block}(e_2, e_6)$. The blue region contains the midpoints of all those line segments connecting e_2 and e_6 . At each point in this region, draw the reflection of Z_2^6 ; the union of such reflections equals $f([e_6, \zeta(e_2, e_6), e_2])$, namely, $\text{block}(e_2, e_6)$. It is a parallelogram with two sides congruent to e_2 and two sides congruent to e_6 . Picture (b) draws not only $\text{block}(e_2, e_6)$, but also $\text{block}(e_2, v_6)$. The blue segment contains the midpoints of all those line segments connecting e_2 and v_6 . At each point in this segment, draw the reflection of $\zeta(e_2, v_6)$; the union of such

reflections equals $f([v_6, \zeta(e_2, v_6), e_2])$, namely, $\text{block}(e_2, v_6)$. It is again a parallelogram. This parallelogram has two sides congruent to e_2 , and two sides congruent to $\zeta(e_2, v_6)$. (However, because $\zeta(e_2, e_6)$ in general is a polygonal curve that consists of several (possibly zero) line segments, $\text{block}(e_2, e_6)$ in general is a region that consists of several (possibly zero) parallelograms, each of which has two sides congruent to e_2 .) Picture (c) and (d) respectively draw $\{\text{block}(e_2, u') \mid e_2 \text{ is chasing } u'\}$ and $\{\text{block}(u, e_6) \mid u \text{ is chasing } e_6\}$. Notice that $\text{block}(e_2, v_4)$ is a line segment, because $\zeta(e_2, v_4) = [Z_2^3 \cap Z_2^4]$ contains only a single point. Picture (e) draws $\{\text{block}(u, u') \mid u, u' \text{ are in } (v_2 \cap v_7), \text{ and } u \text{ is chasing } u'\}$, where we only show labels of the black blocks. Notice that $\text{block}(v_3, v_4)$ is a single point because $\zeta(v_3, v_4)$ is a single point. Finally, picture (f) draws all the blocks.

The notion “reflection” is formally defined as follows. Given a figure F and a point O , figure F ’s reflection with respect to O is another figure which is congruent to F and is centrally-symmetric to F with respect to O .

Figure 4 (a) below draws the $2n$ sectors for the example given in Figure 3. This picture is drawn according to (5) as follows. Consider any unit pair (u, u') in which u is chasing u' . As shown in Figure 3, each point X in $\text{block}(u, u')$ is a reflection of some point X_2 in $\zeta(u, u')$. If X_2 is from unit u , then we put X into $\text{sector}(u)$.

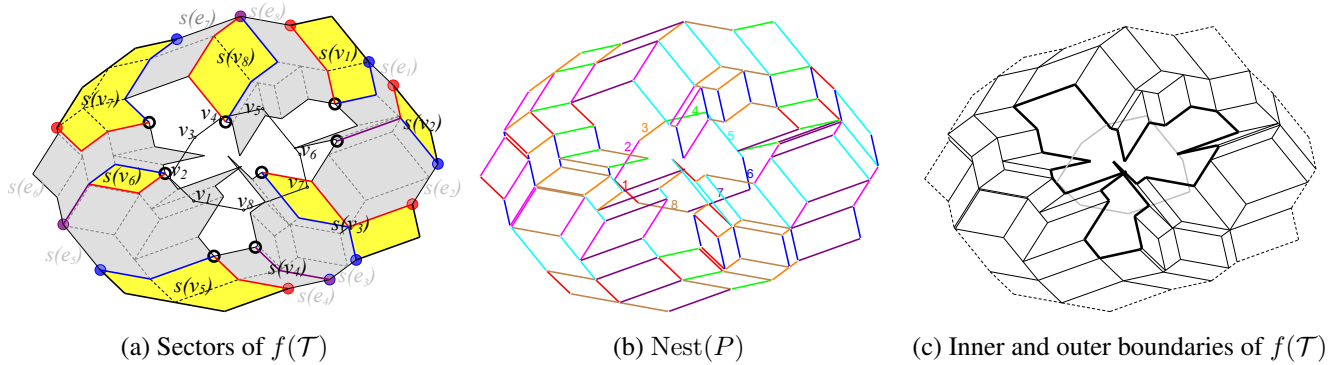


Figure 4: Picture (a) illustrates (5). In this picture, $\text{sector}(w)$ is abbreviated as $s(w)$ and its region is colored yellow or gray, distinguished by whether w is a vertex or an edge. Picture (b) draws $\text{Nest}(P)$ defined below. The bolded and dashed (closed) curves in picture (c) indicate the inner and outer boundaries of $f(\mathcal{T}^P)$ defined below.

It is worthwhile to mention that among the $2n$ sectors, those in $\{\text{sector}(V) \mid V \text{ is a vertex}\}$ are more important (in this manuscript). We will study them more than the other sectors (especially in sections 3 and 5).

1.4 An introduction of $\text{Nest}(P)$ and some additional terminologies

It is not difficult to see that *each block is a connected area bounded by a polygonal boundary*. An explicit definition of the boundary will be given in subsection 2.1. Gladly, the sectors admit the same property; at least, (i) *when w is a vertex, $\text{sector}(w)$ is a connected area bounded by a polygonal boundary*. (When w is an edge, it is also true; yet this result will neither be proved, nor be applied.) However, our proof of fact (i) is complicated and is deferred for a while (sketched in section 3 and fully given in section 5). In the proof, we will explicitly define two simple polygonal curves \mathcal{L}_V^* and \mathcal{R}_V^* for each vertex V (colored red and blue in Figure 4 (a)) and prove that they are on the boundary of $\text{sector}(V)$. Based on those boundaries of the blocks and sectors, we can define $\text{Nest}(P)$.

$\text{Nest}(P)$. We define $\text{Nest}(P)$ as the union of $\mathcal{L}_V^*, \mathcal{R}_V^* \mid V \in \{v_1, \dots, v_n\}$ and the boundaries of the blocks. (Alternatively, we could define $\text{Nest}(P)$ as the union of the boundaries of the blocks and the boundaries of the sectors. Yet in this way we have to define the boundary of $\text{sector}(w)$ for every edge w , which would be more complicated than the case where w is a vertex. So we do not use this definition. The equivalence of the two definitions is useless and unimportant; so proof omitted.) On the terminology, since $\text{Nest}(P)$ captures

all the subregions of $f(\mathcal{T})$ including blocks and sectors, it can be called a **skeleton** of $f(\mathcal{T})$. Moreover, it is an **arrangement** [1] of several line segments, each of which is parallel to an edge of P ; see Figure 4 (b).

Remark 1. *Though $\text{Nest}(P)$ plays an important role in this manuscript, we are not in a hurry to give its full description (which contains the definition of \mathcal{L}_V^* , \mathcal{R}_V^* for example), because for describing our main results in the upcoming subsection, we only need those objects that are already well-defined, e.g., the blocks and sectors, and \mathcal{T} , but not $\text{Nest}(P)$. Besides, it is unwise to give the full description here for the conciseness of this introduction.*

Yet, why do we bother to formally define $\text{Nest}(P)$ below? First, we have to formally define the boundaries of the blocks and sector(V) for any vertex V in order to prove our main results, and defining $\text{Nest}(P)$ does not require any extra work. Second, having a well-defined overall structure $\text{Nest}(P)$ makes it much easier to abstract our work. Briefly, our main result (Theorem 1 below) states that $\text{Nest}(P)$ has a surprising good interaction with ∂P , whereas our secondary result (Theorem 2 below) states that some location queries on $\text{Nest}(P)$ can be answered efficiently.

On the directions of the line segments in $\text{Nest}(P)$. Recall that the boundary-portions of P are all directional. We also regard the boundaries of the blocks and the boundaries of the sectors (\mathcal{L}_V^* and \mathcal{R}_V^*) as directional. So all the line segments in $\text{Nest}(P)$ are directional. The following principle is applied in defining the directions: If a part of boundary (of a block or a sector) α is a copy of a boundary-portion β (perhaps rearranged after the copy), the direction of α will conform with the direction of β . See an example in the first picture of Figure 5. The details can be found at the place where we define the boundaries of the blocks as well as \mathcal{L}_V^* and \mathcal{R}_V^* .

On the size of $\text{Nest}(P)$. The size of $\text{Nest}(P)$ is the number of line segments in $\text{Nest}(P)$, which is obviously $\Omega(n^2)$ since there are $\Omega(n^2)$ blocks. It can also be bounded by $O(n^2)$ easily; see a proof in the appendix. (But the fact that size of $\text{Nest}(P)$ is $O(n^2)$ is unimportant for understanding our two results.)

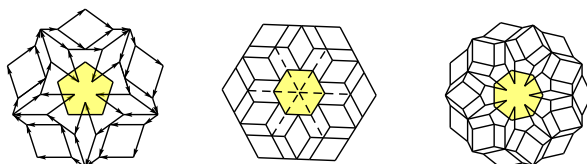


Figure 5: Examples of $\text{Nest}(P)$ for regular n -side polygon for $n = 5, 6, 7$.

Below we give some more notations and terminologies that are important for describing our results.

Subset \mathcal{T}^* . Let \mathcal{T}^* denote the subset of \mathcal{T} that is mapped to ∂P under f .

The inner boundary σP of $f(\mathcal{T})$. As the reader may have noticed, by the definition of chasing, $f(\mathcal{T})$ should be annular – a connected region bounded by two disjoint closed curves, one of which contained in the other; see Figure 4 (a). Thus $f(\mathcal{T})$ has an *outer boundary* and an *inner boundary*; see Figure 4 (c). We denote the inner one by σP . Its direction conforms with the clockwise order. A formal definition is given in subsection 2.1.

Interleaving. Given two oriented closed curves, we say they *interleave* if starting from any intersection between them, no matter we travel around which of them of a cycle, we meet all their intersections in identical order.

1.5 Our results

Theorem 1 (Main result: Six structural properties of $\text{Nest}(P)$). *See Figure 4.*

Block-disjointness. *The intersection of any pair of blocks lies in the interior of P .*

*Be aware that it does **not** state that all blocks are pairwise-disjoint.*

Interleaviness-of- f . The inner boundary of $f(\mathcal{T})$ (i.e. the curve σP) interleaves ∂P .

Reversibility-of- f . Function f is a bijection from \mathcal{T}^* to its image set $f(\mathcal{T}^*) = f(\mathcal{T}) \cap \partial P$.

Henceforth, we denote the reverse function of f on $f(\mathcal{T}) \cap \partial P$ by f^{-1} . Moreover, denote the 1st, 2nd, and 3rd dimension of $f^{-1}(X)$ by $f_1^{-1}(X)$, $f_2^{-1}(X)$ and $f_3^{-1}(X)$ respectively.

Monotonicity-of- f . Function f_2^{-1} , a mapping from $f(\mathcal{T}) \cap \partial P$ to ∂P defined above, is “circularly monotone”: If a point X travels around $f(\mathcal{T}) \cap \partial P$ in clockwise, $f_2^{-1}(X)$ would shift in clockwise around ∂P non-strictly, and moreover, when X has traveled exactly a cycle, $f_2^{-1}(X)$ would also have traveled exactly a cycle.

Sector-monotonicity. The $2n$ districts $\text{sector}(v_1) \cap \partial P$, $\text{sector}(e_1) \cap \partial P$, \dots , $\text{sector}(v_n) \cap \partial P$, $\text{sector}(e_n) \cap \partial P$ are pairwise-disjoint and arranged in clockwise order around ∂P .

Sector-continuity. For any vertex V , the intersection between $\text{sector}(V)$ and ∂P is continuous.

Our proof of these properties is inevitably lengthy, due to the intricacy of $\text{Nest}(P)$. However, it is highly modularized and easy to follow. We sketch the proof in section 3 and then give the full proof in sections 4, 5, and 6.

Remark 2. Among the elements in \mathcal{T} , those in \mathcal{T}^* deserve special attention – all of the properties above essentially concern $f(\mathcal{T}^*)$, rather than $f(\mathcal{T})$. As such, $\text{Nest}(P)$ has a nice interaction with ∂P (beyond our anticipation).

Two more interesting properties. 1. If we travel along the (oriented) segments in $\text{Nest}(P)$ (see the first picture of Figure 5) of one cycle, starting and terminating at the same node, the total distance would be 3 times of the perimeter of P no matter which path we choose. 2. For any non-degenerate linear transformation Γ , it holds that $\Gamma(\text{Nest}(P)) = \text{Nest}(\Gamma(P))$. These properties are not applied in the paper; their easy proofs are omitted.

Theorem 2 (Secondary result: efficient locations on $\text{Nest}(P)$). We can answer each of the following location queries, in (amortized) $O(\log^2 n)$ time, without a full construction of $\text{Nest}(P)$ which takes $\Omega(n^2)$ time.

Sector-intersect-Units Query. Given any vertex V , find the interval of units that intersect $\text{sector}(V)$.

Note: Due to SECTOR-CONTINUITY, those units intersect $\text{sector}(V)$ are indeed an interval of units.

Vertex-in-Sector Query. Given any vertex V , find w so that $\text{sector}(w)$ contains V .

Note: There is at most one such w due to SECTOR-MONOTONICITY. If there is no such w , output NIL.

Vertex-in-Block Query. Given any vertex V , find (u, u') so that $\text{block}(u, u')$ contains V .

Note: There is at most one such (u, u') due to BLOCK-DISJOINTNESS. If no such pair exists, output NIL.

The proof of Theorem 2 is given in section 7, and sketched in section 3.

Remark 3. Among others, BLOCK-DISJOINTNESS, INTERLEAVINESS-OF- f , and Vertex-in-Block query are the most difficult to prove. Our proofs of these three results utilize a group of auxiliary objects called bounding-quadrants (introduced in subsection 2.3), each of which is a relax of a block. These auxiliary objects are so important that it is no exaggerate to credit the most nontrivial step within the entire proof to the introduction of these objects.

Related work. $\text{Nest}(P)$ is novel and has few related work. It has a similar appearance as *Zonotopes* [7] considering that many groups of parallel lines exist. It resembles *Voronoi Diagrams* [1] since they are arrangements of line segments. Whereas a Voronoi Diagram cares the distance, $\text{Nest}(P)$ cares the distance-product.

Organization of this paper. Section 2 formally defines some geometric objects, including the boundaries of the blocks, the inner boundary of $f(\mathcal{T})$ (i.e., σP), and the bounding-quadrants mentioned in Remark 3. It also states seven interesting lemmas that are crucial to our final proof. The proofs of these lemmas are deferred to section 4. Section 3 outlines our techniques for proving Theorems 1 and 2, and its subsequent sections provide the details.

See Figure 39 in appendix for the key geometric objects studied in this manuscript and their relations.

2 Preliminaries: some rigorous definitions and some important lemmas

The following notions will be frequently applied in this section and henceforth.

Region $u \oplus u'$. When unit u is chasing u' , we denote $u \oplus u' = \{(X + X')/2 \mid X \in u, X' \in u'\}$. In particular, for $(u, u') = (e_i, e_j)$ where $e_i \prec e_j$, region $u \oplus u' = e_i \oplus e_j$ is a parallelogram as shown in Figure 6 (a).

k -scaling. Given a figure F , a point O , and a ratio $k > 0$, we define the k -scaling of F with respect to O as the figure F' , which contains point X if and only if F contains $(X - O)/k + O$. See Figure 6 (b).

Inferior portions. We call $[v_i \circ v_{j+1}]$ an *inferior portion* if and only if $e_i \preceq e_j$; see Figure 6 (c) and (d).

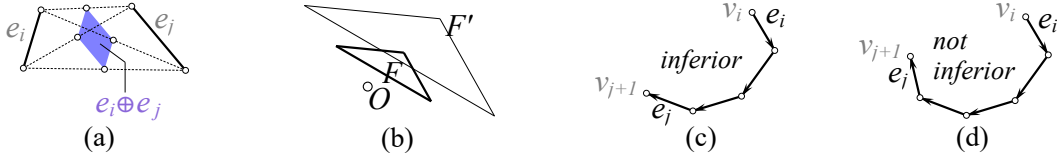


Figure 6: Picture (a) shows $u \oplus u'$ for which $u = e_i$ and $u' = e_j$ are both edges; (b) shows 2-scaling of F with respect to O ; (c) shows a typical inferior portion; whereas (d) shows a boundary-portion that is not inferior.

2.1 The boundaries of the blocks and the inner boundary of $f(\mathcal{T})$

Before defining the boundaries of the blocks, we state two formulas of $\text{block}(u, u')$.

$$\text{block}(u, u') = \bigcup_{X \in u \oplus u'} \text{the reflection of } \zeta(u, u') \text{ with respect to } X. \quad (6)$$

$$\text{block}(u, u') = \bigcup_{X \in \zeta(u, u')} \text{the 2-scaling of } u \oplus u' \text{ with respect to } X. \quad (7)$$

Proof.

$$\begin{aligned} \text{block}(u, u') &= \bigcup_{X_3 \in u, X_1 \in u', X_2 \in \zeta(u, u')} f(X_1, X_2, X_3) \\ &= \bigcup_{X_3 \in u, X_1 \in u'} \bigcup_{X_2 \in \zeta(u, u')} \text{the reflection of } X_2 \text{ with respect to } (X_3 + X_1)/2 \\ &= \bigcup_{X_3 \in u, X_1 \in u'} \text{the reflection of } \zeta(u, u') \text{ with respect to } (X_3 + X_1)/2 \\ &= \bigcup_{X \in u \oplus u'} \text{the reflection of } \zeta(u, u') \text{ with respect to } X. \end{aligned}$$

$$\begin{aligned} \text{block}(u, u') &= \bigcup_{X_3 \in u, X_1 \in u', X_2 \in \zeta(u, u')} f(X_1, X_2, X_3) \\ &= \bigcup_{X_2 \in \zeta(u, u')} \bigcup_{X_3 \in u, X_1 \in u'} \text{the 2-scaling of } (X_3 + X_1)/2 \text{ with respect to } X_2 \\ &= \bigcup_{X_2 \in \zeta(u, u')} \text{the 2-scaling of } u \oplus u' \text{ with respect to } X_2. \end{aligned}$$

□

In the following we define the *borders* of a block. The boundary of a block is the union of its borders.

Definition 1 (Borders and boundaries of the blocks). Assume u is chasing u' .

Case 1 $(u, u') = (e_i, e_j)$. See Figure 7 (a).

By (7), $\text{block}(e_i, e_j)$ is the 2-scaling of $e_i \oplus e_j$ with respect to Z_i^j – a parallelogram whose sides are congruent to e_i or e_j . Each side of this parallelogram is called a *border* of $\text{block}(e_i, e_j)$. Those sides that are congruent to e_i have the same direction as e_i . Those sides that are congruent to e_j have the same direction as e_j .

Case 2 $(u, u') = (v_i, v_j)$. See Figure 7 (d).

By (6), $\text{block}(v_i, v_j)$ is the reflection of $\zeta(v_i, v_j)$ with respect to $(v_i + v_j)/2$. This curve is referred to as the unique border of $\text{block}(v_i, v_j)$, directed from the reflection of Z_{i-1}^{j-1} to the reflection of Z_i^j .

Case 3 $(u, u') = (v_i, e_j)$. See Figure 7 (b).

In this case, by (6) and (7), $\text{block}(v_i, e_j)$ is the region bounded by four curves:

the 2-scalings of segment $v_i \oplus e_j$ with respect to Z_{i-1}^j and Z_i^j , respectively, and

the reflections of $\zeta(v_i, e_j)$ with respect to $(v_i + v_j)/2$ and $(v_i + v_{j+1})/2$, respectively.

Each of these four curves is called a border of $\text{block}(v_i, e_j)$. The first two borders have the same direction as e_j ; whereas the directions of the last two borders are from the reflection of Z_{i-1}^j to the reflection of Z_i^j .

Case 4 $(u, u') = (e_i, v_j)$. See Figure 7 (c). This case is symmetric to Case 3; so we can define four borders.

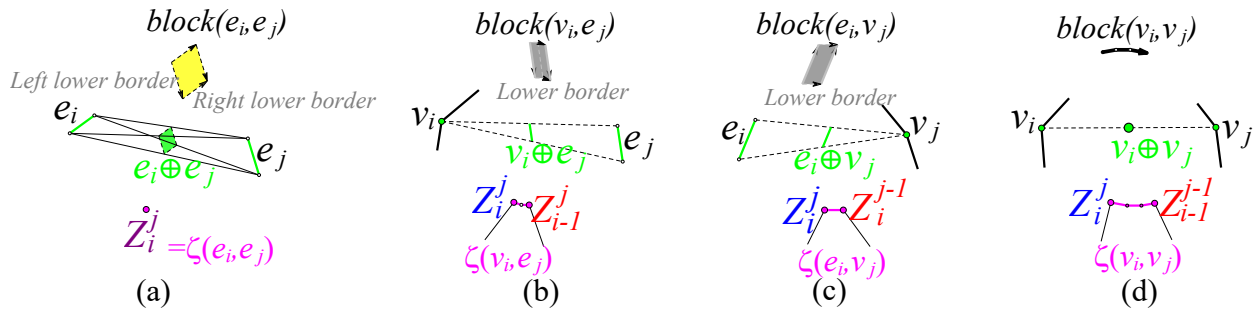


Figure 7: Illustration of the borders of the blocks. The directions of borders are indicated by the arrows. The “left lower border”, “right lower border”, and “lower border” marked in this figure are introduced in Definition 2.

Definition 2. The following terms are applied for defining σP in the next. See Figure 7.

- The left lower border of $\text{block}(e_i, e_j)$ refers to the 2-scaling of $v_i \oplus e_j$ with respect to Z_i^j .
- The right lower border of $\text{block}(e_i, e_j)$ refers to the 2-scaling of $e_i \oplus v_{j+1}$ with respect to Z_i^j .
- The lower border of $\text{block}(v_i, e_j)$ refers to the reflection of $\zeta(v_i, e_j)$ with respect to $(v_i + v_{j+1})/2$.
- The lower border of $\text{block}(e_i, v_j)$ refers to the reflection of $\zeta(e_i, v_j)$ with respect to $(v_i + v_j)/2$.

Outline for defining σP . We first introduce a group of blocks called *frontier blocks* and define the *bottom borders of the frontier blocks*. Briefly, the frontier blocks are those that lie at the inner side of $f(\mathcal{T})$. We will see the frontier blocks have an intrinsic order according to their definitions. We then define the concatenation of the bottom borders of the frontier blocks (in the intrinsic order), which is a closed polygonal curve, to be σP . See Figure 8 (a).

To define the frontier blocks, we define a circular list of unit pairs, called *frontier-pair-list*. It is defined as FPL generated by Algorithm 1. See Figure 8 (b) for an illustration. According to the frontier-pair-list, we can then find out all the frontier blocks — $\text{block}(u, u')$ is *frontier* if and only if (u, u') belongs to this circular list.

Definition 3. Suppose $(u, u') \in \text{FPL}$. The bottom border of $\text{block}(u, u')$ is defined as follows.

- If u, u' are vertices, the unique border of $\text{block}(u, u')$ is also the bottom border of $\text{block}(u, u')$.

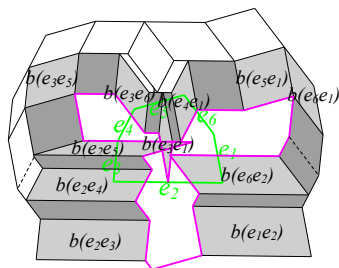
```

1 Let FPL be empty, let  $i = 1$ , and let  $e_j$  be edge that  $e_1 \prec e_j$  but  $e_{j+1} \prec e_1$ ;
2 repeat
3   Add unit pair  $(e_i, e_j)$  to the tail of FPL;
4   if  $e_i \prec e_{j+1}$  then Add unit pair  $(e_i, v_{j+1})$  to the tail of FPL and increase  $j$  by 1;
5   else
6     if  $i + 1 \neq j$  then Add unit pair  $(v_{i+1}, e_j)$  to the tail of FPL and increase  $i$  by 1;
7     else Add unit pair  $(v_{i+1}, v_{j+1})$  to the tail of FPL and increase  $i, j$  both by 1;
8   end
9 until  $i = 1$  and  $e_j$  is the edge that  $e_1 \prec e_j$  but  $e_{j+1} \prec e_1$ ;

```

Algorithm 1: An algorithm for defining FPL

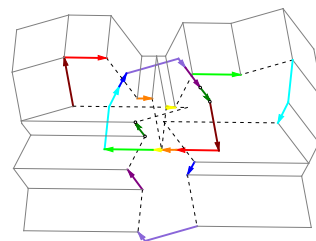
- If u, u' are an edge and a vertex, the lower border of $\text{block}(u, u')$ is also the bottom border of $\text{block}(u, u')$.
- If u, u' are edges, e.g. $u = e_i, u' = e_j$, we define the bottom border of $\text{block}(u, u')$ to be

$$\left\{ \begin{array}{ll} \text{an empty set,} & \text{if } (e_{i-1}, e_j) \in \text{FPL}, (e_i, e_{j+1}) \in \text{FPL.} \\ \text{its right lower border,} & \text{if } (e_{i-1}, e_j) \in \text{FPL}, (e_i, e_{j+1}) \notin \text{FPL;} \\ \text{its left lower border,} & \text{if } (e_{i-1}, e_j) \notin \text{FPL}, (e_i, e_{j+1}) \in \text{FPL;} \\ \text{concatenation of its two lower borders,} & \text{if } (e_{i-1}, e_j) \notin \text{FPL}, (e_i, e_{j+1}) \notin \text{FPL;} \end{array} \right.$$


(a) Frontier blocks

$i \setminus j$	2	3	4	5	6	1	2
1							
2		⊙	⊙	⊙	⊙	⊙	⊙
3			<	⊙	⊙	⊙	⊙
4				<	<	⊙	⊙
5					<	⊙	⊙
6						⊙	⊙

(b) Frontier-pair-list



(c) Function g

Figure 8: Picture (a) shows a convex polygon with six edges and draws all the blocks for this polygon. The frontier blocks are colored dark and light gray. Their bottom borders are pink. Picture (b) illustrates the frontier-pair-list, which indicates the frontier blocks. The table exhibits the chasing relation between the edges of P , where the solid circles indicate the edge pairs in the frontier-pair-list, and the hollow ones indicate other unit pairs in this list. Picture (c) illustrates a function g from σP to ∂P that will be introduced in the next subsection.

The following fact is easy to check: *The starting point of the bottom border of $\text{block}(u_{i+1}, u'_{i+1})$ is the terminal point of the bottom border of $\text{block}(u_i, u'_i)$, when $(u_i, u'_i), (u_{i+1}, u'_{i+1})$ are adjacent pairs in the frontier-pair-list.* Trivial proof omitted. We define the concatenation of the bottom borders (based on the order of FPL) to be σP .

Note 1. When $(e_{i-1}, e_j) \notin \text{FPL}$ and $(e_i, e_{j+1}) \notin \text{FPL}$, the bottom border of $\text{block}(e_i, e_j)$ does not contain the common endpoint of its two lower borders — because these lower borders are open segments. So, in Figure 8, the lowermost corner of $\text{block}(e_3, e_1)$, the leftmost corner of $\text{block}(e_6, e_2)$, and the rightmost corner of $\text{block}(e_2, e_5)$ are not contained in the bottom borders. Therefore, **none of these corner points are contained in σP** . This is important for understanding INTERLEAVITY-OF- f . For example, if the lowermost corner of $\text{block}(e_3, e_1)$ in Figure 8 (a) was counted as an intersecting point of $\partial P \cap \sigma P$, the INTERLEAVITY-OF- f is wrong.

2.2 Miscellaneous

In this subsection we state three lemmas (whose proofs are deferred to section 4) and introduce some notations. Denote

$$\mathcal{T}(u, u') = \{(X_1, X_2, X_3) \in \mathcal{T} \mid X_3 \in u, X_1 \in u'\} = [u', \zeta(u, u'), u]. \quad (8)$$

Lemma 1 (LOCAL-REVERSIBILITY of f). *Function f is a bijection from $\mathcal{T}(u, u')$ to $\text{block}(u, u')$.*

Definition 4 ($f_{u,u'}^{-1}()$ and $f_{u,u'}^{-1,2}()$). *By Lemma 1, there is a reverse function of f on $\text{block}(u, u')$, denoted by $f_{u,u'}^{-1}()$. Moreover, notice that $f_{u,u'}^{-1}(X)$ is a tuple of three points; we denote the second point by $f_{u,u'}^{-1,2}(X)$.*

Extend the domain of $f_{u,u'}^{-1,2}$. By Definition 4, the domain of $f_{u,u'}^{-1,2}$ is $\text{block}(u, u')$, which does not contain the lower border(s) of $\text{block}(u, u')$ in general (unless both u, u' are vertices). For convenience, we extend the domain of $f_{u,u'}^{-1,2}$ to include the lower order(s). Take any point X from the lower border(s) of $\text{block}(u, u')$. If $u = e_i, u' = e_j$, we define $f_{u,u'}^{-1,2}(X) = Z_i^j$. If $u = v_i, u' = e_j$, we define $f_{u,u'}^{-1,2}(X) = X'$, where $X' \in \zeta(v_i, e_j)$ is the reflection of X with respect to $(v_i + v_{j+1})/2$. If $u = e_i, u' = v_j$, we define $f_{u,u'}^{-1,2}(X) = X'$, where $X' \in \zeta(e_i, v_j)$ is the reflection of X with respect to $(v_i + v_j)/2$. If $u = v_i, u' = v_j$, the value of $f_{u,u'}^{-1,2}(X)$ is already defined.

Definition 5 (Function $g: \sigma P \rightarrow \partial P$). *For any point X in σP , assuming it comes from the bottom border of frontier block $\text{block}(u, u')$, we define $g(X) = f_{u,u'}^{-1,2}(X)$. See Figure 8 (c) for an illustration.*

Lemma 2 (LOCAL-MONOTONICITY of f). *When a point X travels along some boundary-portion of P within $\text{block}(u, u')$ (in clockwise), $f_{u,u'}^{-1,2}(X)$ will move along ∂P in clockwise (in the non-strict manner).*

Interleaving. Assume \mathcal{C} is an oriented yet not closed curve. We say \mathcal{C} *interleaves* ∂P , if it is disjoint with ∂P or the following holds. Starting from their first intersection point (the first one that will be encountered when we travel along \mathcal{C} in its positive direction), regardless of whether we travel along \mathcal{C} in its positive direction or along ∂P in clockwise, we encounter the intersection points between \mathcal{C} and ∂P in the same order.

For example, in Figure 9 (a), \mathcal{C} interleaves ∂P . In Figure 9 (b), \mathcal{C} does not interleave ∂P .

Also, recall the definition of *interleaving between two oriented closed curves* in subsection 1.4.

Lemma 3. *Assume a given oriented closed curve \mathcal{C} is cut into $2q$ ($q \geq 3$) fragments: $\beta_1, \alpha_1, \dots, \beta_q, \alpha_q$, such that*

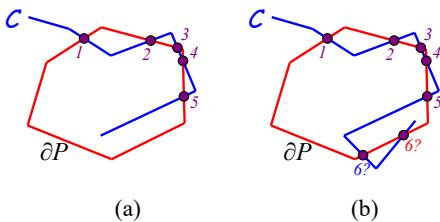
$$\text{for } 1 \leq i \leq q, \text{ the concatenation of } \alpha_{i-1}, \beta_i, \alpha_i \text{ interleaves } \partial P \text{ (where } \alpha_0 = \alpha_q). \quad (9)$$

Further assume that we can find $2q$ points $S_1, T_1, \dots, S_q, T_q$ lying in clockwise order around ∂P which “delimitate” the $2q$ fragments, by which we mean that

$$\text{for } 1 \leq i \leq q, \text{ the intersections between } \beta_i \text{ and } \partial P \text{ are contained in } [S_i \circlearrowleft T_i], \text{ and} \quad (10)$$

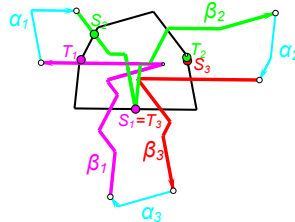
$$\text{for } 1 \leq i \leq q, \text{ the intersections between } \alpha_i \text{ and } \partial P \text{ are contained in } [S_i \circlearrowleft T_{i+1}]. \quad (11)$$

Then, the given curve \mathcal{C} interleaves ∂P . See an example in Figure 10.



(a)

(b)



$$\left\{ \begin{array}{l} C = \beta_1 - \alpha_1 - \beta_2 - \alpha_2 - \beta_3 - \alpha_3; \\ \alpha_1 - \beta_2 - \alpha_2, \alpha_3 - \beta_1 - \alpha_1, \alpha_2 - \beta_3 - \alpha_3 \text{ interleave } \partial P; \\ S_1, T_1, S_2, T_2, S_3, T_3 \text{ lie in clockwise order} \\ \beta_1 \cap \partial P \subseteq [S_1, T_1]; \quad \alpha_1 \cap \partial P \subseteq [S_1, T_2]; \\ \beta_2 \cap \partial P \subseteq [S_2, T_2]; \quad \alpha_2 \cap \partial P \subseteq [S_2, T_3]; \\ \beta_3 \cap \partial P \subseteq [S_3, T_3]; \quad \alpha_3 \cap \partial P \subseteq [S_3, T_1]; \\ \Rightarrow \text{Curve } C \text{ interleaves } \partial P! \end{array} \right.$$

Figure 9: interleaving and not interleaving.

Figure 10: Illustration of Lemma 3. In this example, $q = 3$.

2.3 Introduction of the bounding-quadrants for the blocks

Definition 6 (quad_i^j & $\langle \text{quad} \rangle_i^j$). Assume $e_i \preceq e_j$. let $M = (v_i + v_{j+1})/2$.

Case1: $e_i \prec e_j$; see Figure 11 (a). Make two rays at M , one with the opposite direction to e_j whereas the other with the same direction as e_i . Denote by quad_i^j the **open** region bounded by these two rays (which lies on the left of $\overrightarrow{v_i v_{j+1}}$), and denote by $\langle \text{quad} \rangle_i^j$ the intersection between quad_i^j and ∂P .

Case2: $e_i = e_j$; see Figure 11 (b). Denote by quad_i^j the **open** half-plane that is bounded by the extended line of e_i and lies to the left of e_i , and denote by $\langle \text{quad} \rangle_i^j$ the midpoint of e_i .

Moreover, recall the backward and forward edges of units. For unit pair (u, u') in which u is chasing u' , define

$$\text{quad}_u^{u'} := \text{quad}_{\text{forw}(u)}^{\text{back}(u')}; \quad \langle \text{quad} \rangle_u^{u'} := \langle \text{quad} \rangle_{\text{forw}(u)}^{\text{back}(u')}. \quad (\text{Notice that } \text{forw}(u) \preceq \text{back}(u').) \quad (12)$$

Note: We regard the half-plane quad_i^j as a special quadrant whose apex lies at the midpoint of e_i ; thus all the regions in $\{\text{quad}_i^j \mid e_i \preceq e_j\}$ are quadrants in the plane. The regions in $\{\langle \text{quad} \rangle_i^j \mid e_i \preceq e_j\}$ are boundary-portions of P . It is worthwhile to point out that $\langle \text{quad} \rangle_i^j$ always contains $\text{quad}_i^j \cap \partial P$ for $e_i \preceq e_j$ by the above definition.

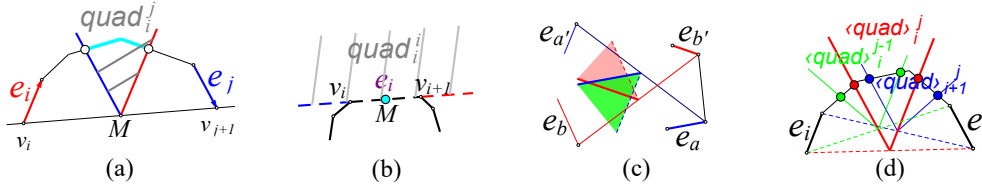


Figure 11: Definition and two properties of the bounding-quadrants (Lemmas 6 and 7).

Lemma 4. For unit pair (u, u') in which u is chasing u' , region $\text{block}(u, u')$ is contained in $\text{quad}_u^{u'}$.

According to Lemma 4, we call $\text{quad}_u^{u'}$ the *bounding-quadrant* of $\text{block}(u, u')$ henceforth.

For the next three lemmas, recall that the borders of blocks are directional, as shown in Figure 7, and recall the relation \preceq_ρ defined on boundary-portion ρ . Also, recall $[v_i \circ v_{j+1}]$ is an inferior portion if and only if $e_i \preceq e_j$.

Lemma 5. Suppose a point X travels along some border of $\text{block}(u, u')$ (in its positive direction) and suppose we stand both in P and in the opposite quadrant of $\text{quad}_u^{u'}$. Then, X moves in clockwise order (**strictly**) around us.

Note: Since $\text{quad}_u^{u'}$ is open, its opposite quadrant is also regarded as **open**; so it does not contain its boundary.

Lemma 6 (Peculiarity of quad). For any a, a', b, b' such that $e_a \preceq e_{a'}$, $e_b \preceq e_{b'}$ and that $e_a, e_{a'}, e_b, e_{b'}$ are not contained in any inferior portion, $\text{quad}_a^{a'} \cap \text{quad}_b^{b'}$ lies in the interior of P , as illustrated in Figure 11 (c).

Lemma 7 (Monotonicity of $\langle \text{quad} \rangle$). See Figure 11 (d). Assume $e_i \prec e_j$. Denote $\rho = [v_i \circ v_{j+1}]$. Then,

$$(\langle \text{quad} \rangle_i^{j-1}).s \preceq_\rho (\langle \text{quad} \rangle_i^j).s \preceq_\rho (\langle \text{quad} \rangle_{i+1}^j).s \quad \text{and} \quad (\langle \text{quad} \rangle_i^{j-1}).t \preceq_\rho (\langle \text{quad} \rangle_i^j).t \preceq_\rho (\langle \text{quad} \rangle_{i+1}^j).t,$$

where $\gamma.s$ and $\gamma.t$ denote the starting and terminal point of γ . Moreover, for a list of m boundary-portions $\langle \text{quad} \rangle_{u_1}^{u'_1}, \dots, \langle \text{quad} \rangle_{u_m}^{u'_m}$, their starting points lie in clockwise order and so do their terminal points, provided that (1) u_1, \dots, u_m lie in clockwise order, (2) u'_1, \dots, u'_m lie in clockwise order, and (3) u_k is chasing u'_k for $1 \leq k \leq m$.

Note: When some objects are said lying in clockwise order, some of them are allowed to coincide.

Lemmas 6 and 7 are proved in subsection 4.3. Lemmas 4 and 5 are proved in subsection 4.4.

3 Technique overview

In this section, we sketch our proofs of Theorem 1 and Theorem 2.

Figure 12 shows how the lemmas given in the last section are applied in our proof of Theorem 1 and illustrates the interconnections between the first five properties of $f(\mathcal{T})$. The last property SECTOR-CONTINUITY is quite independent from these five properties and is not drawn in this figure. As marked in the figure, BLOCK-DISJOINTNESS and INTERLEAVITY-OF- f are strongly connected. Indeed, we will see their proofs are analogous. The easy proofs of REVERSIBILITY-OF- f and SECTOR-MONOTONICITY will not only be sketched but completed in this section.

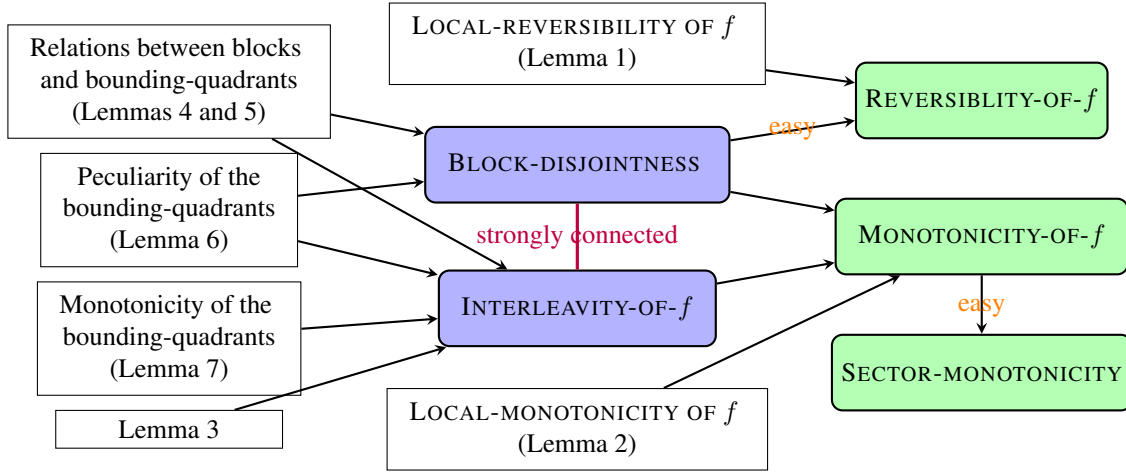


Figure 12: Interconnections between the five properties (not including SECTOR-CONTINUITY).

Technique overview for proving the first five properties.

Definition 7. Denote by $e_i \not\prec e_j$ if e_i is not chasing e_j . Edge pair $(e_c, e_{c'})$ is extremal, if $e_c \prec e_{c'}$ and the inferior portion $[v_c \circ v_{c'+1}]$ is not contained in any other inferior portions. Equivalently, if $e_c \prec e_{c'}, e_{c-1} \not\prec e_{c'}, e_c \not\prec e_{c'+1}$. For example, in Figure 8 (b), the edge pairs indicated by the red solid circles are extremal.

For any extremal pair $(e_c, e_{c'})$, denote

$$\Delta(c, c') := \{(u, u') \mid \text{unit } u \text{ is chasing } u', \text{ and } \text{forw}(u), \text{back}(u') \in \{e_c, e_{c+1}, \dots, e_{c'}\}\}.$$

Proof of BLOCK-DISJOINTNESS (sketch). We regard $(\text{block}(u, u'), \text{block}(v, v'))$ as a **local pair** if the four edges $\text{forw}(u), \text{back}(u'), \text{forw}(v), \text{back}(v')$ are contained in an inferior portion; and as a **global pair** otherwise.

It suffices to prove BLOCK-DISJOINTNESS if we can prove the following results:

- (I) For a global pair $\text{block}(u, u'), \text{block}(v, v')$, their intersection lies in the interior of P .
- (II) For a local pair $\text{block}(u, u'), \text{block}(v, v')$, their intersection is always empty.

We can employ the bounding-quadrants to prove (I) as follows.

Because these blocks are global, $\text{forw}(u), \text{back}(u'), \text{forw}(v), \text{back}(v')$ not contained in any inferior-portion. This means $\text{quad}_{\text{forw}(u)}^{\text{back}(u')} \cap \text{quad}_{\text{forw}(v)}^{\text{back}(v')}$ lies in the interior of P , according to Lemma 6. According to Lemma 4, $\text{block}(u, u') \cap \text{block}(v, v') \subset \text{quad}_u^{u'} \cap \text{quad}_v^{v'} = \text{quad}_{\text{forw}(u)}^{\text{back}(u')} \cap \text{quad}_{\text{forw}(v)}^{\text{back}(v')}$. Together, we get (I).

Be aware of the following equivalent form of (II): For every extremal pair $(e_c, e_{c'})$, the blocks in $\{\text{block}(u, u') \mid (u, u') \in \Delta(c, c')\}$ are pairwise-disjoint. See Figure 13 (a) for an illustration of such blocks. Surprisingly, the monotonicity of the borders stated in Lemma 5 somehow implies this result. Details are given in section 5. \square

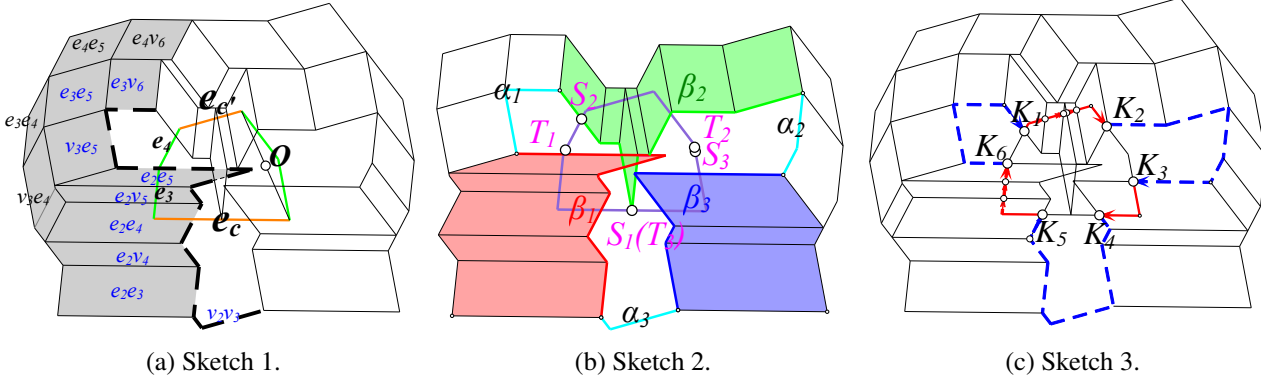


Figure 13: Illustrations of the proof of the properties of $f(\mathcal{T})$.

Proof of INTERLEAVITY-OF- f (sketch). In general, we use Lemma 3 to prove that σP interleaves ∂P .

First, we cut σP into $2q$ fragments $\beta_1, \alpha_1, \dots, \beta_q, \alpha_q$, where q denotes the number of extremal pairs. For every extremal pair $(e_c, e_{c'})$, denote by $\sigma(c, c')$ the concatenation of the bottom borders of the frontier blocks in $\{\text{block}(u, u') \mid (u, u') \in \Delta(c, c')\}$; as shown by the dashed polygonal curve in Figure 13 (a). Denote by $(e_{c_1}, e_{c'_1}), \dots, (e_{c_q}, e_{c'_q})$ an enumeration of the extremal pairs (in the order given by the frontier-pair-list). We define α_i to be $\sigma(c_i, c'_i) \cap \sigma(c_{i+1}, c'_{i+1})$; and β_i to be $\sigma(c_i, c'_i) - \alpha_{i-1} - \alpha_i$. See Figure 13 (b) for an illustration.

As an easy corollary of the monotonicity of the borders stated in Lemma 5, $\sigma(c_i, c'_i)$ interleaves ∂P . In other words, the first condition (9) listed in Lemma 3 holds, since the concatenation of $\alpha_{i-1}, \beta_i, \alpha_i$ equals $\sigma(c_i, c'_i)$.

We then select $2q$ points $S_1, T_1, \dots, S_q, T_q$ from ∂P . Denote by $\text{block}(u, u')$ and $\text{block}(v, v')$ the first and last frontier blocks whose bottom borders contribute to β_i . We define the starting point of $\langle \text{quad} \rangle_u^{u'}$ and the terminal point of $\langle \text{quad} \rangle_v^{v'}$ to be S_i and T_i , respectively. Applying the properties of the bounding-quadrants (Lemmas 6 and 7), it can be proved that $S_1, T_1, \dots, S_q, T_q$ lie in clockwise order around ∂P , and moreover, the conditions (10) and (11) listed in Lemma 3 hold, namely, $\beta_i \cap \partial P \subset [S_i \cup T_i]$ and $\alpha_i \cap \partial P \subset [S_i \cup T_{i+1}]$.

At last, apply Lemma 3 and we obtain that σP interleaves ∂P . See the details in section 5. \square

As a summary, the INTERLEAVITY-OF- f follows from two facts: (I) locally, every local fraction of σP (i.e. $\sigma(c_i, c'_i)$) interleaves ∂P , and (II) globally, all these local fractions are well-scattered around ∂P .

The REVERSIBILITY-OF- f follows from the BLOCK-DISJOINTNESS and LOCAL-REVERSIBILITY OF f .

Proof of REVERSIBILITY-OF- f . Recall $\mathcal{T}(u, u')$ in (8). For each unit pair (u, u') in which u is chasing u' , we call $\mathcal{T}(u, u')$ a component of \mathcal{T} . Notice that each element of \mathcal{T} belongs to exactly one component.

Now, consider any two elements in subset \mathcal{T}^* . If they belong to the same component, their images under function f are distinct according to the LOCAL-REVERSIBILITY OF f (Lemma 1). If they belong to distinct components, their images under f do not coincide, since otherwise there would be two distinct blocks with an intersection on the boundary of P , which contradicts the BLOCK-DISJOINTNESS. Therefore, f is a bijection from \mathcal{T}^* to $f(\mathcal{T}^*)$. \square

Proof of MONOTONICITY-OF- f (sketch). See Figure 13 (c). Let K_1, \dots, K_m denote all the intersection points between σP and ∂P , where K_1, \dots, K_m lie in clockwise order around ∂P . These intersection points divide ∂P into m boundary-portions, each of which is called a K -portion. We state three crucial observations:

- (i) The outer boundary of $f(\mathcal{T})$ is a simple closed curve whose interior contains P .
- (ii) Points $f_2^{-1}(K_1), \dots, f_2^{-1}(K_m)$ lie in clockwise order around ∂P .
- (iii) Function $f_2^{-1}(\cdot)$ is monotone on any K -portion that lies in $f(\mathcal{T})$.

The proof of observation (i) is trivial. Observation (ii) follows from three facts: (a) It always holds that $g(K_i) = f_2^{-1}(K_i)$ (recall g in Definition 5); (b) g is a circularly monotone function from σP to ∂P ; and (c) Points K_1, \dots, K_m lie in clockwise order around σP . Facts (a) and (b) are due to the definition of g . Fact (c) follows from the INTERLEAVITY-OF- f and the assumption that K_1, \dots, K_m lie in clockwise order around ∂P . Observation (iii) follows from LOCAL-MONOTONICITY OF f (Lemma 2), which states a similar property about $f_{u,u'}^{-1,2}()$.

Combining the INTERLEAVITY-OF- f with observation (i), a K -portion either lies in or lies outside $f(\mathcal{T})$. Now, suppose a point X travels in $f(\mathcal{T}) \cap \partial P$ in clockwise. Observation (iii) assures that $f_2^{-1}(X)$ is monotone inside each K -portion. Observation (ii) assures that it is monotone between the K -portions. Details are given in section 6. \square

The SECTOR-MONOTONICITY follows from the MONOTONICITY-OF- f immediately.

Proofs of SECTOR-MONOTONICITY. For any unit w , we have

$$\begin{aligned} \text{sector}(w) \cap \partial P &= \{f(X_1, X_2, X_3) \mid (X_1, X_2, X_3) \in \mathcal{T}^*, X_2 \in w\} \\ &= \{Y \in f(\mathcal{T}) \cap \partial P \mid f_2^{-1}(Y) \in w\} = \{Y \in f(\mathcal{T}) \cap \partial P \mid \mathbf{u}(f_2^{-1}(Y)) = w\}. \end{aligned}$$

Consider the points in $f(\mathcal{T}) \cap \partial P$. Clearly, $\mathbf{u}(f_2^{-1}())$ is a function on these points that maps them to the $2n$ units of P . Following from the MONOTONICITY-OF- f , function $\mathbf{u}(f_2^{-1}())$ is circularly monotone on these points. So, $\mathbf{u}(f_2^{-1}())$ implicitly divides $f(\mathcal{T}) \cap \partial P$ into $2n$ parts which are pairwise-disjoint and lie in clockwise order around ∂P . Moreover, according to the above equation, these $2n$ parts are precisely $\text{sector}(v_1) \cap \partial P$, $\text{sector}(e_1) \cap \partial P$, \dots , $\text{sector}(v_n) \cap \partial P$, $\text{sector}(e_n) \cap \partial P$. Therefore, we obtain the SECTOR-MONOTONICITY. \square

Technique overview for defining \mathcal{L}_V^* , \mathcal{R}_V^* and for proving the SECTOR-CONTINUITY

Assume V is a fixed vertex of P . In the following, we depict the general shape of $\text{sector}(V)$ and define explicitly its two boundaries \mathcal{L}_V^* , \mathcal{R}_V^* mentioned in section 1, and then sketch how do we prove the SECTOR-CONTINUITY.

Recall $u \oplus u' = \{(X + X')/2 \mid X \in u, X' \in u'\}$. The following formula of $\text{sector}(V)$ follows from (3) and (5):

$$\text{sector}(V) = 2\text{-scaling of } \left(\bigcup_{u \text{ is chasing } u', \text{ and } \zeta(u, u') \text{ contains } V} u \oplus u' \right) \text{ with respect to } V. \quad (13)$$

Based on (13), in order to know the shape of $\text{sector}(V)$, it is important to study the structure of Λ_V , where

$$\Lambda_V := \{(u, u') \mid u \text{ is chasing } u', \text{ and } \zeta(u, u') \text{ contains } V\}. \quad (14)$$

In the following we first introduce some symbols or notions and then introduce a structural property of Λ_V .

Delimiting edges e_{s_V} and e_{t_V} . Two particular edges of P will be specified as e_{s_V} and e_{t_V} , for each vertex V .

Note that the exact values of s_V and t_V however will not be defined in this overview section, because the definition is involved and needs additional notations to explain, as we will see in section 6; and also because there is no need to know the exact values s_V and t_V for understanding the following notations and facts within this section. Indeed, only in the proofs of the following facts will we look at the exact values of s_V, t_V .

We abbreviate s_V, t_V as s, t when V is clear, and call e_s, e_t the *delimiting edges*. Two crucial facts are:

- (i) $e_s \preceq e_t$. Moreover, the inferior portion $[v_s \circlearrowleft v_{t+1}]$ does not contain V .
- (ii) If $(u, u') \in \Lambda_V$, units u, u' both lie in $[v_s \circlearrowleft v_{t+1}]$. (This suggests the name ‘‘delimiting’’.)

Incident relation. Each unit has two *incident units*: e_i has v_i, v_{i+1} ; whereas v_i has e_{i-1}, e_i .

In particular, pay attention that e_i, e_{i+1} are **not** regarded as incident.

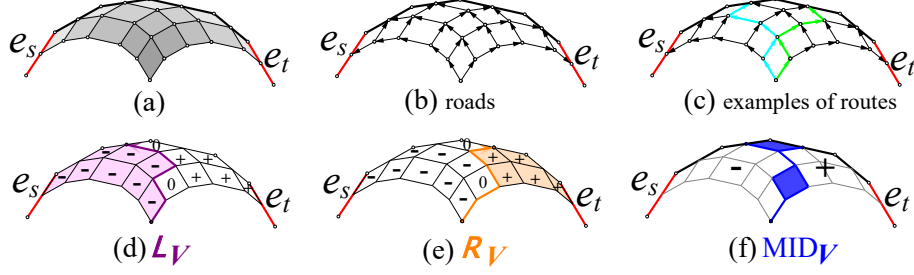


Figure 14: Illustration of the definition of curves $\mathcal{L}_V, \mathcal{R}_V$ and region mid_V .

Δ_V – **A superset of Λ_V .** Notice that there is an order, denoted by ' $<$ ', among the units in $[v_s \circ v_{t+1}]$ conforming to the clockwise order. We denote $\Delta_V = \{(u, u') \mid u, u' \in [v_s \circ v_{t+1}], u < u', \text{ and they are not incident}\}$.

Note: By fact (ii), Δ_V is a superset of Λ_V .

Note: By fact (i), $e_s \preceq e_t$, hence those regions $u \oplus u' \mid (u, u') \in \Delta_V$ are pairwise-disjoint. See Figure 14 (a).

Roads & routes. See Figure 14 (b). For any $(e_i, v_j) \in \Delta_V$, we assume segment $e_i \oplus v_j$ has *the same* direction as e_i ; for any $(v_i, e_j) \in \Delta_V$, we assume segment $v_i \oplus e_j$ has *the opposite* direction to e_j ; and we refer to these segments as *roads*. See Figure 14 (c). By concatenating several roads, we may obtain directional polygonal curves starting from $(v_s + v_{t+1})/2$ to some point in $[v_s \circ v_{t+1}]$; such curves are called *routes*.

$\mathcal{L}_V, \mathcal{R}_V$. Denote $\rho = [v_{t+1} \circ v_s]$. For any edge pair (e_i, e_j) in Δ_V , we mark region $e_i \oplus e_j$ by '-' if $Z_i^j <_\rho V$; '+' if $V <_\rho Z_i^j$; and '0' if $V = Z_i^j$. By the bi-monotonicity of the Z -points (Fact 1), there exists a unique route, \mathcal{L}_V , which separates the regions marked by '-' from the regions marked by '+/0'. Similarly, there exists a unique route, \mathcal{R}_V , which separates the regions marked by '+' from the regions marked by '-/0'.

A region mid_V . By the definitions of $\mathcal{L}_V, \mathcal{R}_V$ and bi-monotonicity of the Z -points (Fact 1), the region bounded by $\mathcal{L}_V, \mathcal{R}_V$ and ∂P is well-defined (see Figure 14 (f)); we denote it by mid_V .

Note: To be more clear, mid_V contains its two boundaries \mathcal{L}_V and \mathcal{R}_V .

Note: For the special case $s = t$, we will have $\mathcal{L}_V = \mathcal{R}_V = \text{mid}_V = v_s \oplus v_{t+1}$.

$\mathcal{L}_V^*, \mathcal{R}_V^*, \& \text{mid}_V^*$. Denote the 2-scalings of $\text{mid}_V, \mathcal{L}_V, \mathcal{R}_V$ with respect to V by $\text{mid}_V^*, \mathcal{L}_V^*, \mathcal{R}_V^*$ respectively.

We now describe the aforementioned structural property of Λ_V .

(iii) Because mid_V is the union of several (disjoint) regions $u \oplus u'$ for which $(u, u') \in \Delta_V$, it defines a subset of Δ_V . To be clear, this subset contains (u, u') if and only if $u \oplus u' \subseteq \text{mid}_V$. Now, remove from this subset those unit pairs (u, u') in which u is not chasing u' , the remaining subset (of Δ_V) is exactly Λ_V .

The proof of fact (iii) again requires the definitions of e_s and e_t and is thus omitted in this overview section.

Notice that $\text{sector}(V) = 2\text{-scaling of } (\bigcup_{(u, u') \in \Lambda_V} u \oplus u')$ with respect to V , by combining (13) with (14). Now, connecting this equation of $\text{sector}(V)$ with the structural property of Λ_V given in fact (iii), we get:

(iv) Region $\text{sector}(V)$ equals the 2-scaling of $(\text{mid}_V - \epsilon_V)$ with respect to V , where ϵ_V denotes the union of those $u \oplus u'$ for which $(u, u') \in \Delta_V$ and u is not chasing u' .

We remark that ϵ_V and mid_V are such regions whose shapes are easy to understand. Therefore, based on fact (iv) it is easy to understand what the shape of $\text{sector}(V)$ could be.

Two boundaries of $\text{sector}(V)$ and the proof of SECTOR-CONTINUITY (overview). Following fact (iv), we can further prove that *the closed set of $\text{sector}(V)$ equals mid_V^** , which implies that mid_V^* and $\text{sector}(V)$ have the same boundaries. Further since $\mathcal{L}_V^*, \mathcal{R}_V^*$ are boundaries of mid_V^* , they are boundaries of $\text{sector}(V)$ indeed as we mentioned. Moreover, we observe that either of $\mathcal{L}_V^*, \mathcal{R}_V^*$ has at most one intersection with ∂P (see Figure 4 (a)); so $\text{mid}_V^* = [\mathcal{L}_V^* \cap \partial P \circlearrowleft \mathcal{R}_V^* \cap \partial P]$. Following this equation and the fact that mid_V^* is the closed set of $\text{sector}(V)$, we see $\text{sector}(V) \cap \partial P$ is a boundary-portion from $\mathcal{L}_V^* \cap \partial P$ to $\mathcal{R}_V^* \cap \partial P$. Thus SECTOR-CONTINUITY holds.

Remark 4. *Although the particular values of s_V, t_V are of no use for understanding the contents sketched in this overview section, defining s_V, t_V is the most nontrivial step in the entire proof of the SECTOR-CONTINUITY.*

A slightly modification on the directions of the roads. Recall that $\text{Nest}(P)$ is defined as the union of the boundaries of all blocks and $\mathcal{L}_{v_1}^*, \dots, \mathcal{L}_{v_n}^*$ and $\mathcal{R}_{v_1}^*, \dots, \mathcal{R}_{v_n}^*$, where $\mathcal{L}_V^*, \mathcal{R}_V^*$ are 2-scalings of $\mathcal{L}_V, \mathcal{R}_V$ with respect to V , and where $\mathcal{L}_V, \mathcal{R}_V$ consist of several roads. Previously we assume road $e_i \oplus v_j$ has the same direction as e_i , whereas road $v_i \oplus e_j$ has the **opposite** direction to e_j . This is convenient for proving the SECTOR-CONTINUITY. However, when defining $\text{Nest}(P)$, it is more reasonable to assume that $v_i \oplus e_j$ has the **same** direction as e_j .

Open problem. Can we find a structure similar to $\text{Nest}(P)$ in a higher dimensional space?

Technique overview for proving Theorem 2

Theorem 2 states that we can answer in (amortized) $O(\log^2 n)$ time *Sector-intersect-Units*, *Vertex-in-Sector*, and *Vertex-in-Block*, which ask the interval of units that intersect $\text{sector}(V)$, or the sector or the block that contains V .

1. Compute the endpoints of $\text{sector}(V) \cap \partial P$ for a given vertex V . According to the proof sketch of SECTOR-CONTINUITY above, computing the endpoints of $\text{sector}(V) \cap \partial P$ reduces to computing $\mathcal{L}_V^* \cap \partial P$ and $\mathcal{R}_V^* \cap \partial P$. Recall that either of $\mathcal{L}_V^*, \mathcal{R}_V^*$ is a polygonal curve and has at most one intersection with ∂P . Moreover, it is not difficult to generate an arbitrary edge of \mathcal{L}_V^* (or \mathcal{R}_V^*), and in $O(\log n)$ time decide whether it lies inside, outside, or intersects P . Therefore, we can compute $\mathcal{L}_V^* \cap \partial P$ (or $\mathcal{R}_V^* \cap \partial P$) by a binary search in $O(\log^2 n)$ time.

2. Compute the units that intersect $\text{sector}(V)$ for a given vertex V . Let u_L, u_R respectively be the unit containing $\mathcal{L}_V^* \cap \partial P$ and the unit containing $\mathcal{R}_V^* \cap \partial P$, which can be computed when we compute $\mathcal{L}_V^* \cap \partial P$ and $\mathcal{R}_V^* \cap \partial P$. By SECTOR-CONTINUITY, the units that intersect $\text{sector}(V)$ are (roughly) the units from u_L to u_R in clockwise order. (This holds almost in every case. A degenerate case is discussed in subsection 7.2).

3. Compute the respective sectors that contain each vertex. We build two groups of *event-points*: the points in $\{\mathcal{L}_V^* \cap \partial P, \mathcal{R}_V^* \cap \partial P \mid V \text{ is a vertex of } P\}$, and the intersections between σP and ∂P . Two tags, *current-tag* and *future-tag*, are assigned to each event-point; the former one indicates the sector containing this event-point; the latter one indicates the sector containing the boundary-portion starting from this event-point and terminating at its clockwise next event-point. By a **sweeping** around ∂P , we find the sector containing each vertex utilizing the tags.

4. Compute the block containing V for a given vertex V . This is the most nontrivial part in our algorithm. Given V which lies in $\text{sector}(w)$, where w is given, we shall find (u_1^*, u_2^*) so that $\text{block}(u_1^*, u_2^*)$ contains V .

Similarly as in the proof of SECTOR-CONTINUITY, we need to introduce a few notations first. (For SECTOR-CONTINUITY, we search (u, u') such that $V \in \zeta(u, u')$; and here we search (u, u') such that $V \in \text{block}(u, u')$.)

Let $[X \circlearrowleft X']$ denote $[X \circlearrowleft X'] - \{X'\}$ and let $(X \circlearrowleft X')$ denote $[X \circlearrowleft X'] - \{X\}$.

Delimiting edges e_{pV}, e_{qV} . Two particular edges of P will be specified as e_{pV} and e_{qV} , for each vertex V . Note that the exact values of p_V and q_V however will not be defined in this overview section, because the definition is involved and needs additional notations to explain, as we will see in subsection 7.3; and also because there is no need to know the exact values p_V and q_V for understanding the following notations and facts within this section. Indeed, only in the proofs of the following facts will we look at the exact values of p_V, q_V .

We abbreviate p_V, q_V as p, q when V is clear, and call e_p, e_q the *delimiting edges*. Two crucial facts are:

- (i) $e_p \prec e_q$. Moreover, the boundary-portion $(v_p \circ v_{q+1})$ contains V .
- (ii) $u_1^* \in [v_p \circ V]$, and $u_2^* \in (V \circ v_{q+1})$. (This suggests the name “delimiting”.)

Alive pairs. For any unit pair (u, u') such that u is chasing u' , we regard it as *alive* if it satisfies the conditions given in fact (ii). In other words, it is alive if $u \in [v_p \circ V]$ and $u' \in (V \circ v_{q+1})$.

Active pairs. For any alive pair (u, u') , we regard it as *active* if $\zeta(u, u')$ intersects w . In particular, (u_1^*, u_2^*) is active due to fact (ii) and $V \in \text{sector}(w)$. This means we only need to search (u_1^*, u_2^*) among the active pairs.

Figure 15 (a) draws all the blocks of the alive pairs, where the colored blocks are blocks of the active pairs.

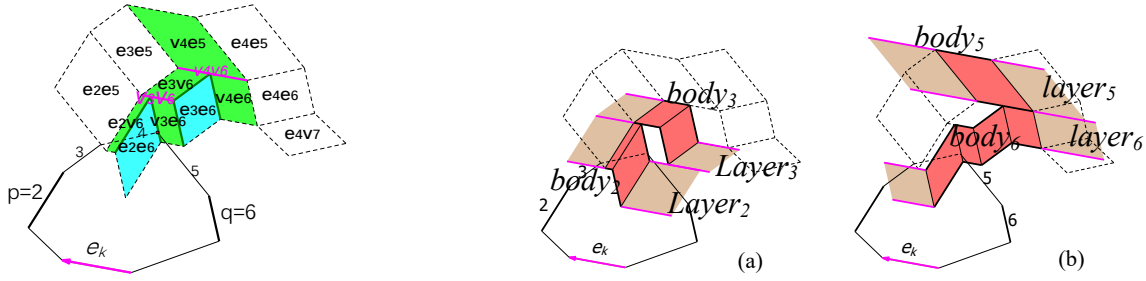


Figure 15: Illustration of cells and layers.

Next, we have to discuss two cases depending on whether w is an edge or a vertex. The edge case is more typical and the vertex case can be regarded as a degenerate case. Assume in the following w is an edge, e.g. $w = e_k$.

Cells & layers. For each active pair (u, u') , define a region $\text{cell}(u, u') := \text{block}(u, u') \cap \text{sector}(w)$ and call it a *cell*. For each edge e_j in $(v_p \circ v_{q+1})$, we define a region layer_j , called a *layer*, which contains all the cells parallel to e_j together with two more infinite strip region parallel to e_k as shown Figure 15 (b).

Note: The “cells” and “layers” are counterparts of the “roads” and “routes” (recall them in Figure 14).

Algorithm for computing u_1^* and u_2^* (overview). We prove a monotonicity between the cells within the same layer and a monotonicity between the different layers. Based on these monotonicities, in $O(\log n)$ time we can determine the relative position between any layer and V . So, in $O(\log^2 n)$ time we find the layer that contains V . In another $O(\log n)$ time we find the cell (within this layer) that contains V , which must be $\text{cell}(u_1^*, u_2^*)$.

Remark 5. In our algorithm, computing the block containing V is **highly symmetric** to computing the endpoints of $\text{sector}(V) \cap \partial P$. The biggest challenges in both of them lie in defining the delimiting edges. Both of them take $O(\log^2 n)$ time for each query. Moreover, (s, t) and (p, q) can both be computed in $O(\log n)$ time (not shown in this section). This symmetry suggests that if one of them can be optimized to $O(\log n)$ time, so may the other.

The tricky definitions of s, t and p, q are given in subsection 6.2.1 and subsection 7.3. To define p, q we need to apply once again the bounding-quadrants of the blocks and their properties introduced in subsection 2.3.

In the future, we would like to study whether the term $O(\log^2 n)$ can be optimized to $O(\log n)$ applying [4].

4 Proofs of the lemmas stated in section 2

This section introduces some facts about the Z -points and proves the seven lemmas stated in section 2.

Given point X and edge e_i , denote by $p_i(X)$ the unique line at X that is parallel to e_i .

When a point X lies in ∂P , we abbreviate $back(\mathbf{u}(X))$, $forw(\mathbf{u}(X))$ as $back(X)$, $forw(X)$ respectively.

4.1 Several facts about the Z -points (in addition to Fact 1)

Denote by D_i the unique vertex with the largest distance to ℓ_i . The uniqueness follows from the pairwise-nonparallel assumption of edges. Denote by $l_{i,j}$ the intersection of ℓ_i and ℓ_j .

Fact 2. [3] Point Z_i^j lies in $[D_i \circlearrowleft D_j] \cap (v_{j+1} \circlearrowleft v_i)$. Moreover, if it lies in some edge e_k , it lies at $(l_{i,k} + l_{j,k})/2$.

Fact 3. Point Z_i^j lies in or on the boundary of the opposite quadrant of quad_i^j .

Proof. See Figure 16 (a). Let $M = (v_i + v_{j+1})/2$. Denote by H_1 and H_2 the closed half-plane bounded by $p_i(M)$ and containing v_{j+1} , and the closed half-plane bounded by $p_j(M)$ and containing v_i . We shall prove that $Z_i^j \in H_1 \cap H_2$. Denote $e_b = back(Z_i^j)$. Because Z_i^j has the largest distance-product to (ℓ_i, ℓ_j) in P , it has a larger distance-product to (ℓ_i, ℓ_j) than all the other points on e_b . Applying this observation with the concavity of $\text{disprod}_{\ell_i, \ell_j}(\cdot)$ on segment $\overline{l_{j,b}l_{i,b}}$ (see Lemma 3 in [3]), $|l_{i,b}Z_i^j| \geq \frac{1}{2}|l_{j,b}l_{i,b}|$. So $d_{\ell_i}(Z_i^j) \geq \frac{1}{2}d_{\ell_i}(l_{j,b})$. Further since $\frac{1}{2}d_{\ell_i}(l_{j,b}) \geq \frac{1}{2}d_{\ell_i}(v_{j+1}) = d_{\ell_i}(M)$, we get $d_{\ell_i}(Z_i^j) \geq d_{\ell_i}(M)$. Thus $Z_i^j \in H_1$. Symmetrically, $Z_i^j \in H_2$. \square

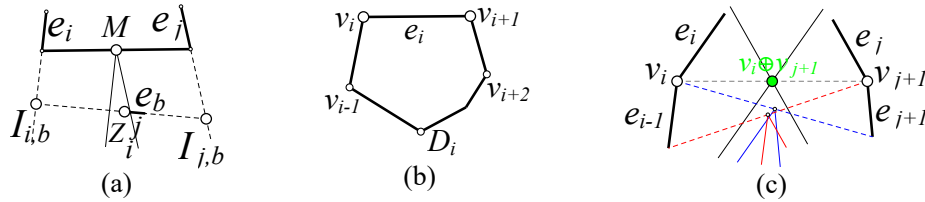


Figure 16: Picture (a) illustrates the proof of Fact 3; whereas (b) and (c) illustrate the proof of Fact 4.

Fact 4. When v_i is chasing v_{j+1} , boundary-portion $\zeta(v_i, v_{j+1})$ lies in the opposite quadrant of quad_i^j .

Proof. Case 1: $i = j$. See Figure 16 (b). By Fact 2, $Z_{i-1}^i \in (v_{i+1} \circlearrowleft D_i)$ whereas $Z_i^{i+1} \in [D_i \circlearrowleft v_i]$. This means $[Z_{i-1}^i \circlearrowleft Z_i^{i+1}] \subset (v_{i+1} \circlearrowleft v_i)$, i.e. $\zeta(v_i, v_{i+1}) \subset (v_{i+1} \circlearrowleft v_i)$. Further since $(v_{i+1} \circlearrowleft v_i)$ is contained in the opposite quadrant of quad_i^i , boundary-portion $\zeta(v_i, v_{i+1})$ is contained in the opposite quadrant of quad_i^i .

Case 2: $i \neq j$. See Figure 16 (c). Let γ be the intersection of ∂P and the opposite quadrant of quad_i^j . Let $\rho = [v_{j+1} \circlearrowleft v_i]$. We claim: (i) Z_{i-1}^j and Z_i^{j+1} both lie in γ , and (ii) $Z_{i-1}^j \leq_\rho Z_i^{j+1}$.

Clearly, γ is contained in ρ . So (i) and (ii) together imply that $Z_{i-1}^j \leq_\gamma Z_i^{j+1}$. This means $[Z_{i-1}^j \circlearrowleft Z_i^{j+1}]$, i.e. $\zeta(v_i, v_{j+1})$, lies in γ and hence in the opposite quadrant of quad_i^j .

Claim (ii) follows from Fact 1 – the bi-monotonicity of the Z -points. We prove claim (i) in the following. We only show the proof of point Z_{i-1}^j ; the proof of the other point Z_i^{j+1} is symmetric and omitted. Since v_i is chasing v_{j+1} , we get $e_{i-1} \prec e_j$. This implies that point $(v_{i-1} + v_{j+1})/2$ lies in the opposite quadrant of quad_i^j . Further since this point is the apex of the opposite quadrant of quad_{i-1}^j , we get (a): the opposite quadrant of quad_{i-1}^j and its boundary are contained in the opposite quadrant of quad_i^j . By Fact 3, we get (b): Z_{i-1}^j lies in or on the boundary of the opposite quadrant of quad_{i-1}^j . Together, Z_{i-1}^j lies in the opposite quadrant of quad_i^j and thus lies in γ . \square

4.2 LOCAL-REVERSIBILITY OF f and LOCAL-MONOTONICITY OF f (Lemmas 1 and 2)

Proof of Lemma 1. Take distinct tuples $A = (A_1, A_2, A_3)$ and $B = (B_1, B_2, B_3)$ from $\mathcal{T}(u, u')$. According to (8), we have: (i) $A_3 \in u, A_1 \in u'$; (ii) $B_3 \in u, B_1 \in u'$; and (iii) $A_2, B_2 \in \zeta(u, u')$. We shall prove that $f(A) \neq f(B)$.

First, assume $A_2 = B_2$ and $(A_1, A_3) \neq (B_1, B_3)$. Because $(A_1, A_3) \neq (B_1, B_3)$ and by (i) and (ii), A_1A_3 and B_1B_3 are distinct line segments connecting u, u' . Further since all the line segments connecting u, u' have different midpoints, $(A_3 + A_1)/2 \neq (B_3 + B_1)/2$. Therefore, $A_3 + A_1 - A_2 \neq B_3 + B_1 - B_2$, namely, $f(A) \neq f(B)$.

Next, consider the case where $A_2 \neq B_2$. By (iii), $\zeta(u, u')$ contains both A_2 and B_2 and hence is not a single point. This means at least one of u, u' is a vertex. If u, u' are both vertices, $(A_1 + A_3)/2 = u \oplus u' = (B_1 + B_3)/2$, and combining this with $A_2 \neq B_2$ would result $f(A) \neq f(B)$. So, we assume u, u' are an edge and a vertex. Without loss of generality, assume $(u, u') = (v_i, e_j)$; the case $(u, u') = (e_i, v_j)$ is symmetric.

We know A_2 and B_2 both lie in $\zeta(v_i, e_j)$ according to (iii), whereas $\zeta(v_i, e_j) = [Z_{i-1}^j \circlearrowleft Z_i^j] \subseteq [v_{j+1} \circlearrowleft D_j]$ according to Fact 2. Moreover, all the points in $[v_{j+1} \circlearrowleft D_j]$ have different distances to ℓ_j . Altogether, A_2 and B_2 have different distances to ℓ_j . However, $(A_1 + A_3)/2$ and $(B_1 + B_3)/2$ have the same distance to ℓ_j because they both lie in $v_i \oplus e_j$. Together, $f(A)$ and $f(B)$ have different distances to ℓ_j . Therefore, $f(A) \neq f(B)$. \square

Proof of Lemma 2. Denote $(J_X, K_X, L_X) = f_{u, u'}^{-1}(X)$ for any point X in $\text{block}(u, u')$. Note that $J_X \in u', K_X \in \zeta(u, u')$ and $L_X \in u$ since $(J_X, K_X, L_X) \in \mathcal{T}(u, u')$. We shall prove that when X travels (in clockwise) along a boundary-portion ρ that lies in $\text{block}(u, u')$, function K_X moves along ∂P in clockwise non-strictly.

The result is trivial for the case where u, u' are both edges. Because in this case K_X is invariant. It always equals $Z_u^{u'}$. The result on the case where u, u' are both vertex is easy to prove, because in this case $\text{block}(u, u')$ is a curve, and we only need to show that when X moves along $\text{block}(u, u')$, function K_X moves along $\zeta(u, u')$ in clockwise, which is obvious. In the following, we focus on the case where u, u' are a vertex and an edge.

Without loss of generality, assume $(u, u') = (v_i, e_j)$. Abbreviate $d_{\ell_j}(\cdot)$ by $d(\cdot)$. We first state three arguments.

- (i) When point X travels along ρ in clockwise, $d(X)$ (non-strictly) decreases.
- (ii) For any point X in $\text{block}(v_i, e_j) \cap \partial P$, the sum $d(X) + d(K_X)$ is a constant.
- (iii) If the position of a dynamic point Y is restricted to $\zeta(v_i, e_j)$, and we observe that $d(Y)$ (non-strictly) increases during the movement of Y , we can conclude that Y moves in clockwise (non-strictly) along $\zeta(v_i, e_j)$.

Altogether, we can obtain the monotonicity property of K_X as follows. Since X travels along ρ , $d(X)$ non-strictly decreases due to (i). So, $d(K_X)$ non-strictly increases due to (ii). Finally, applying (iii) for $Y = K_X$, point K_X travels along $\zeta(v_i, e_j)$ in clockwise non-strictly. We prove (i), (ii), and (iii) in the following.

Proof of (i): It suffices to prove two facts: (a) When X travels along $[v_i \circlearrowleft v_{j+1}]$ in clockwise, $d(X)$ non-strictly decreases. (b) When a boundary-portion ρ lies $\text{block}(v_i, e_j)$, it must lie in $[v_i \circlearrowleft v_{j+1}]$. Because v_i is chasing e_j , we get $e_i \prec e_j$, which implies (a). The proof of (b) is given in the following.

See Figure 7 (b). Let H denote the half-plane delimited by the extended line of $\overline{v_i v_{j+1}}$ and not containing e_i . By Fact 2, Z_i^j and Z_{i-1}^j both lie in $(v_{j+1} \circlearrowleft v_i)$. Therefore, $\zeta(v_i, e_j) = [Z_i^j \circlearrowleft Z_{i-1}^j]$ is contained in H . Since $\zeta(v_i, e_j) \subset H$ whereas $v_i \oplus e_j$ lies in the opposite half-plane of H , applying (6), $\text{block}(v_i, e_j)$ lies in the opposite half-plane of H . So, $\text{block}(v_i, e_j) \cap \partial P \subseteq [v_i \circlearrowleft v_{j+1}]$. Further since $\rho \subseteq \text{block}(v_i, e_j) \cap \partial P$, we get (b).

Proof of (ii): Since $f(J_X, K_X, L_X) = X$, we get $(X + K_X)/2 = (J_X + L_X)/2$. Because $J_X \in u'$ and $L_X \in u$, point $(J_X + L_X)/2 \in u \oplus u' = v_i \oplus e_j$. Therefore, $(X + K_X)/2 \in v_i \oplus e_j$. Hence $d((X + K_X)/2)$ is a constant. Since $X, K_X \in \partial P$, they lie on the same side of ℓ_j , so $d(X) + d(K_X) = 2d((X + K_X)/2)$. Together, we get (ii).

Proof of (iii): By Fact 2, $\zeta(v_i, e_j) = [Z_{i-1}^j \circlearrowleft Z_i^j] \subseteq [v_{j+1} \circlearrowleft D_j]$, which implies that $d(Y)$ strictly increases when Y travels along $\zeta(v_i, e_j)$. This simply implies (iii). \square

4.3 Peculiarity and monotonicity of the bounding-quadrants (Lemmas 6 and 7)

We add one more notation before the next proofs. For edge pair (e_i, e_j) such that $e_i \preceq e_j$, denote by hp_i^j the **open** half-plane delimited by the extended line of $\overrightarrow{v_i v_{j+1}}$ and lies on the left side of $\overrightarrow{v_i v_{j+1}}$. Notice that $\text{quad}_i^j \subseteq \text{hp}_i^j$.

Proof of Lemma 6. Assume that $e_a \preceq e_{a'}, e_b \preceq e_{b'}$ and $e_a, e_{a'}, e_b, e_{b'}$ are not contained in any inferior portion. We shall prove that $\text{quad}_a^{a'} \cap \text{quad}_b^{b'}$ lies in the interior of P . We have to analyze several cases.

In the first three cases shown below, $\text{quad}_a^{a'} \cap \text{quad}_b^{b'}$ will be empty and hence it will lie in the interior of P .

Case 1 $a = a'$. Since $e_a, e_{a'}, e_b, e_{b'}$ are not contained in any inferior portion, $e_a \prec e_b$ and $e_{b'} \prec e_a$. See Figure 17 (a). Denote by H the half plane delimited by $\rho_a(M)$ and on the right of e_a , where M is the apex of $\text{quad}_b^{b'}$. Since $M = (v_b + v_{b'+1})/2$, this point lies in or on the right of e_a . Therefore, (1) H is disjoint with $\text{quad}_a^{a'}$. Since $e_a \prec e_b$, the part of boundary of $\text{quad}_b^{b'}$ that is parallel to e_b lies in H . Since $e_{b'} \prec e_a$, the part of boundary of $\text{quad}_b^{b'}$ that is parallel to $e_{b'}$ also lies in H . Together, the entire boundary of $\text{quad}_b^{b'}$ lies in H , and hence (2) $\text{quad}_b^{b'} \subseteq H$. Combining (1) and (2), the subregion $\text{quad}_b^{b'}$ of H is disjoint with $\text{quad}_a^{a'}$.

Case 2 $b = b'$. This case is symmetric to Case 1.

Case 3 $e_a, e_{a'}, e_b, e_{b'}$ are distinct and lie in clockwise order on ∂P . See Figure 17 (b). Make four rays $r_a, r_{a'}, r_b, r_{b'}$, which originate at $v_{a'+1}, v_a, v_{b'+1}, v_b$, respectively, and which have their directions the same as $e_a, e_{a'}, e_b, e_{b'}$, respectively. Let Π_1 be the region bounded by $r_{a'}, \overline{v_a v_{a'+1}}, r_a$ and containing $\text{quad}_a^{a'}$. Let Π_2 be the region bounded by $r_{b'}, \overline{v_b v_{b'+1}}, r_b$ and containing $\text{quad}_b^{b'}$. Assume that Π_1, Π_2 do not contain their boundaries. Since $e_a, e_{a'}, e_b, e_{b'}$ are not containing in any inferior portion, $e_{b'} \prec e_a$ whereas $e_{a'} \prec e_b$. This implies that Π_1, Π_2 are disjoint. Therefore, $\text{quad}_a^{a'}, \text{quad}_b^{b'}$ are disjoint, since they are respectively subregions of Π_1, Π_2 .

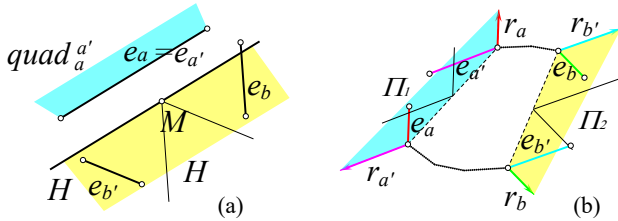


Figure 17: Trivial cases in proving the peculiarity.

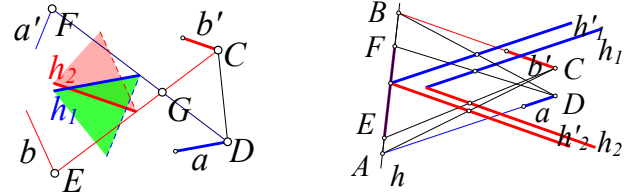


Figure 18: Nontrivial cases in proving the peculiarity.

When none of the preceding (trivial) cases occur, only two cases remain: either $e_a \prec e_b \preceq e_{a'} \prec e_{b'} \prec e_a$, or, $e_b \prec e_a \preceq e_{b'} \prec e_{a'} \prec e_b$. Assume the first case occurs without loss of generality; the other case is symmetric.

See Figure 18. Let $C = v_{b'+1}, D = v_a, E = v_b, F = v_{a'+1}$. Let G denote the intersection of CE and DF . Obviously, $\triangle EFG$ lies in P . So, proving that $\text{quad}_a^{a'} \cap \text{quad}_b^{b'}$ lies in the interior of P reduces to proving that it lies in the interior of $\triangle EFG$, which further reduces to proving the following two facts:

- i. $\text{quad}_a^{a'} \cap \text{quad}_b^{b'}$ lies in both $\text{hp}_a^{a'}$ and $\text{hp}_b^{b'}$. (See the definition of hp at the beginning of this subsection.)
- ii. $\text{quad}_a^{a'} \cap \text{quad}_b^{b'}$ lies in half-plane h , where h denotes the **open** half-plane bounded by the extended line of \overline{EF} and containing G . (So, h is the complementary half-plane of $\text{hp}_a^{a'}$.)

We have $\text{quad}_a^{a'} \subseteq \text{hp}_a^{a'}$ and $\text{quad}_b^{b'} \subseteq \text{hp}_b^{b'}$, which imply (i). One of the two (open) half-planes defining $\text{quad}_a^{a'}$ is parallel to e_a , denoted by h_1 . One of the two (open) half-planes defining $\text{quad}_b^{b'}$ is parallel to $e_{b'}$, denoted by h_2 . See h_1, h_2 in the figure. Clearly, $\text{quad}_a^{a'} \cap \text{quad}_b^{b'} \subseteq h_1 \cap h_2$. So proving (ii) reduces to proving that $h_1 \cap h_2 \subseteq h$.

Next, see the right picture of Figure 18. Assume that the extended line of \overline{EF} intersects $\ell_a, \ell_{b'}$ at A, B respectively. Denote by h'_1 the open half-plane bounded by $p_a((D+B)/2)$ and containing e_a , and h'_2 the open half-plane bounded by $p_{b'}((A+C)/2)$ and containing $e_{b'}$. Because P is convex, points E, F both lie in \overline{AB} . Since F lie in \overline{AB} , we know $(D+F)/2$ lies in or on the boundary of h'_1 , which implies $h_1 \subseteq h'_1$ because h_1 is parallel to h'_1 and has $(D+F)/2$ on its boundary. Since E lie in \overline{AB} , we know $(C+E)/2$ lies in or on the boundary of h'_2 , which implies $h_2 \subseteq h'_2$ because h_2 is parallel to h'_2 and has $(C+E)/2$ on its boundary. It remains to show that $h'_1 \cap h'_2 \subseteq h$. By the definition of h'_1, h'_2 , their boundaries pass through $(A+B)/2$. Combining this with the facts that h'_1 is parallel to e_a and h'_2 is parallel to $e_{b'}$, as well as $e_{b'} \prec e_a$, we obtain that $h'_1 \cap h'_2 \subseteq h$. \square

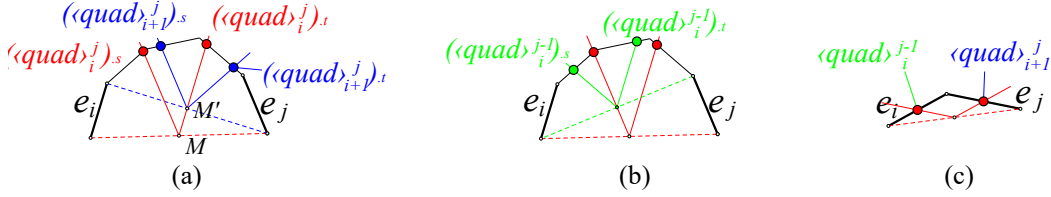


Figure 19: Illustration of the proof of the monotonicity of $\langle \text{quad} \rangle$.

Proof of Lemma 7. (Recall this lemma contains two parts.) First, for $e_i \prec e_j$ and $\rho = [v_i \circ v_{j+1}]$, we shall prove:

$$\langle \text{quad} \rangle_i^{j-1}.s \leq_\rho \langle \text{quad} \rangle_i^j.s \leq_\rho \langle \text{quad} \rangle_{i+1}^j.s, \quad (15)$$

$$\langle \text{quad} \rangle_i^{j-1}.t \leq_\rho \langle \text{quad} \rangle_i^j.t \leq_\rho \langle \text{quad} \rangle_{i+1}^j.t. \quad (16)$$

When $j = i + 1$, the following (trivial) facts together imply (15) and (16). See Figure 19 (c).

- (i) $\langle \text{quad} \rangle_i^{j-1}$ contains a single point, which is the midpoint of e_i .
- (ii) $\langle \text{quad} \rangle_{i+1}^j$ contains a single point, which is the midpoint of e_j .
- (iii) $\langle \text{quad} \rangle_i^j$ starts at the midpoint of e_i and terminates at the midpoint of e_j .

Now, assume $j \neq i + 1$. See Figure 19 (a). Let $M = (v_i + v_{j+1})/2$ and $M' = (v_{i+1} + v_{j+1})/2$.

Compare $\langle \text{quad} \rangle_i^j.s$ and $\langle \text{quad} \rangle_{i+1}^j.s$. Clearly, their distance to ℓ_j are respectively equal to the distance from M, M' to that line. Moreover, since MM' is parallel to e_i whereas $e_i \prec e_j$, point M is further to ℓ_j than M' . Together, $\langle \text{quad} \rangle_i^j.s$ is further to ℓ_j than $\langle \text{quad} \rangle_{i+1}^j.s$. This means $\langle \text{quad} \rangle_i^j.s \leq_\rho \langle \text{quad} \rangle_{i+1}^j.s$.

Compare $\langle \text{quad} \rangle_i^j.t$ and $\langle \text{quad} \rangle_{i+1}^j.t$. Because segments $M'(\langle \text{quad} \rangle_i^j).t$ and $M'(\langle \text{quad} \rangle_{i+1}^j).t$ are parallel to e_i, e_{i+1} respectively, whereas $e_i \prec e_{i+1}$, it follows that $\langle \text{quad} \rangle_i^j.t \leq_\rho \langle \text{quad} \rangle_{i+1}^j.t$.

Symmetrically, $\langle \text{quad} \rangle_i^{j-1}.s \leq_\rho \langle \text{quad} \rangle_i^j.s$ and $\langle \text{quad} \rangle_i^{j-1}.t \leq_\rho \langle \text{quad} \rangle_i^j.t$. See Figure 19 (b).

Next, consider the second part of the lemma. For a list of m boundary-portions $\langle \text{quad} \rangle_{u'_1}^{u'_1}, \dots, \langle \text{quad} \rangle_{u'_m}^{u'_m}$ where (1) units u_1, \dots, u_m lie in clockwise order, (2) units u'_1, \dots, u'_m lie in clockwise order, and (3) u_k is chasing u'_k for $1 \leq k \leq m$, we shall prove that their starting points lie in clockwise order and so do their terminal points.

Denote $a_k = \text{forw}(u_k)$ and $a'_k = \text{back}(u'_k)$ for $1 \leq k \leq m$. According to the assumptions (1), (2), and (3), we have: (i) the edges a_1, \dots, a_m lie in clockwise order, and (ii) the edges a'_1, \dots, a'_m lie in clockwise order, and (iii) $a_k \preceq a'_k$ for $1 \leq k \leq m$. According to these facts and by applying inequalities (15) and (16), we get

- the starting points of $\langle \text{quad} \rangle_{a'_1}^{a'_1}, \dots, \langle \text{quad} \rangle_{a'_m}^{a'_m}$ lie in clockwise order around ∂P , and
- the terminal points of $\langle \text{quad} \rangle_{a'_1}^{a'_1}, \dots, \langle \text{quad} \rangle_{a'_m}^{a'_m}$ lie in clockwise order around ∂P .

We complete the proof of the second part by recalling (12), which defines $\langle \text{quad} \rangle_{u'_k}^{u'_k} := \langle \text{quad} \rangle_{a'_k}^{a'_k}$. \square

4.4 Two relations between blocks and bounding-quadrants (Lemmas 4 and 5)

Proof of Lemma 4. We shall prove $\text{block}(u, u') \subset \text{quad}_u^{u'}$. Recall $\text{quad}_u^{u'} := \text{quad}_{\text{forw}(u)}^{\text{back}(u')}$. So, it reduces to proving

$$\text{block}(e_i, e_j) \subset \text{quad}_i^j, \quad \text{block}(v_i, v_{j+1}) \subset \text{quad}_i^j, \quad \text{block}(e_i, v_{j+1}) \subset \text{quad}_i^j, \quad \text{block}(v_i, e_j) \subset \text{quad}_i^j.$$

- Proof of $\text{block}(e_i, e_j) \subset \text{quad}_i^j$. See Figure 20 (a). By Fact 3, Z_i^j lies in or on the boundary of the opposite quadrant of quad_i^j . By the definition of quad_i^j , clearly $e_i \oplus e_j \subset \text{quad}_i^j$. Together, the 2-scaling of $e_i \oplus e_j$ with respect to Z_i^j , which equals $\text{block}(e_i, e_j)$ due to (7), is contained in quad_i^j .
- Proof of $\text{block}(v_i, v_{j+1}) \subset \text{quad}_i^j$. See Figure 20 (b). By Fact 4, $\zeta(v_i, v_{j+1})$ lies in the opposite quadrant of quad_i^j . So, its reflection with respect to $(v_i + v_{j+1})/2$, which equals $\text{block}(v_i, v_{j+1})$ due to (6), is in quad_i^j .

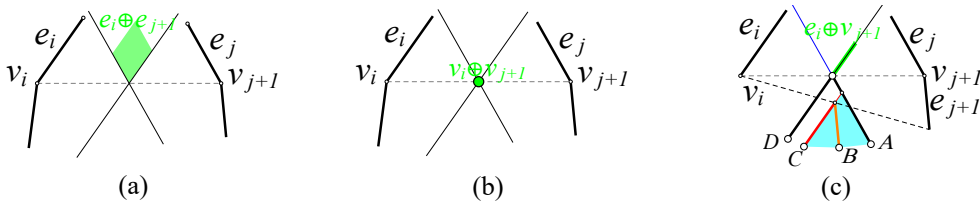


Figure 20: Illustration of the proof of Lemma 4

- Proof of $\text{block}(e_i, v_{j+1}) \subset \text{quad}_i^j$. See Figure 20 (c). Denote by H_1 the closed half-plane delimited by line $p_j((v_i + v_{j+1})/2)$ and not containing e_j , and H_2 the closed half-plane delimited by line $p_i((v_i + v_{j+1})/2)$ and not containing e_i . The colored region in Figure 20 (c) shows $H_1 \cap H_2$. We claim (i) $\zeta(e_i, v_{j+1}) \subset H_1 \cap H_2$. As a corollary of (i), the reflection of $\zeta(e_i, v_{j+1})$ with respect to any point in $e_i \oplus v_{j+1}$ lies in quad_i^j . By (6), $\text{block}(e_i, v_{j+1})$ is the union of such reflections of $\zeta(e_i, v_{j+1})$. Together, $\text{block}(e_i, v_{j+1}) \subset \text{quad}_i^j$.

We prove (i) in the following. Notice that the intersection between ∂P and the opposite quadrant of quad_i^j is a boundary-portion, denoted by $(A \circ D)$. Similarly, the intersection between ∂P and the opposite quadrant of quad_i^{j+1} is a boundary-portion, denoted by $(B \circ C)$. We point out three facts:

- (a) $[B \circ C] \subset [A \circ D]$. (b) $Z_i^j \in [A \circ D]$ and $Z_i^{j+1} \in [B \circ C]$. (c) $Z_i^j \leq_\gamma Z_i^{j+1}$, where $\gamma = [A \circ D]$.

Fact (a) follows from the fact that $e_i \prec e_{j+1}$, which follows from the assumption that e_i is chasing v_{j+1} . Fact (b) is an application of Fact 3. Fact (c) is an application of the bi-monotonicity of Z -points (Fact 1). Combining facts (a), (b), and (c) would result $[Z_i^j \circ Z_i^{j+1}] \subseteq [A \circ C]$, which implies (i).

The proof of the last formula $\text{block}(v_i, e_j) \subset \text{quad}_i^j$ is symmetric to the preceding proof and is omitted. \square

We introduce one more fact about the Z -points before proving Lemma 5.

Fact 5. Consider any edge pair $(e_a, e_{a'})$ for which $e_a \prec e_{a'}$. Let $e_b = \text{back}(Z_a^{a'})$ and $e_f = \text{forw}(Z_a^{a'})$.

1. The ray r which originates from v_a and has direction opposite to $e_{a'}$ (assume it does not include its originate) lies on the right of e_k , for every e_k in $\{e_{a'}, \dots, e_b\}$. See Figure 21 (a).
2. The ray r which originates from $v_{a'+1}$ and has direction the same as e_a (assume it does not include its originate) lies on the right of e_k , for every e_k in $\{e_f, \dots, e_a\}$. See Figure 21 (b).

These two claims are obviously symmetric; so we only show the proof of the first one in the following.

Proof. By Fact 2, $Z_a^{a'} \in (v_{a'+1} \circ v_a)$. This implies that $e_b \neq e_{a'}$. Moreover, we claim that e_b cannot be chasing $e_{a'}$. Suppose to the opposite that $e_b \prec e_{a'}$. Then, $d_{a'}(v_b) > d_{a'}(Z_a^{a'})$ and $d_a(v_b) > d_a(Z_a^{a'})$, which means v_b has a larger distance-product to lines $(\ell_a, \ell_{a'})$ than $Z_a^{a'}$, contradicting the definition of $Z_a^{a'}$. Therefore, $e_{a'} \prec e_b$.

Consider any e_k in $e_{a'+1}, \dots, e_b$. As $e_{a'} \prec e_b$, it holds that (i) $e_{a'} \prec e_k$. Since P lies in the closed half-plane delimited by ℓ_k and lying on the right of e_k , we get (ii) v_a (namely, the originate of r) lies on the right of e_k or lies in ℓ_k . Also recall that (iii) the direction of $e_{a'}$ is opposite to that of r . Altogether, ray r lies on the right of e_k .

It is clear that r lies on the right of $e_{a'}$ as well. So the result holds for $e_k \in \{e_{a'}, \dots, e_b\}$. \square

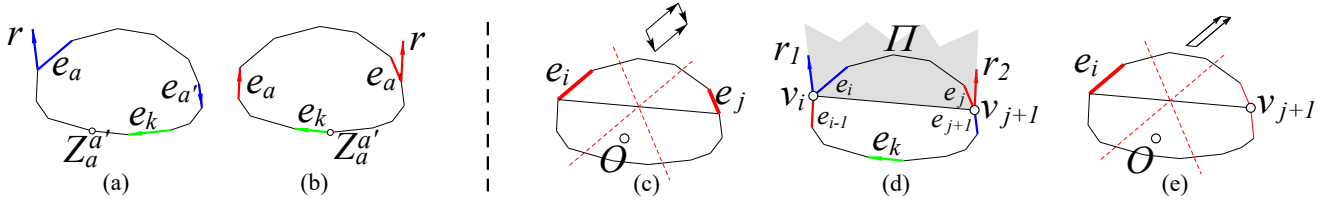


Figure 21: Illustration of the proof of Lemma 5

Proof of Lemma 5. Fix any point O in P that lies in the opposite quadrant of $\text{quad}_u^{u'}$. We shall prove: (i) when a point X travels along any border of $\text{block}(u, u')$, it moves (strictly) in clockwise around O .

- Case 1: both u, u' are edges. By Lemma 4, $\text{block}(u, u') \subset \text{quad}_u^{u'}$. As a corollary, the opposite quadrant of $\text{quad}_u^{u'}$, including O , are on the right of each border of $\text{block}(u, u')$ (see Figure 21 (c)), which implies (i).
- Case 2: both u, u' are vertices, e.g., $(u, u') = (v_i, v_{j+1})$. Recall that the unique border of $\text{block}(u, u')$ equals the reflection of $\zeta(u, u')$ with respect to $(v_i + v_{j+1})/2$. Let O' be the reflection of O with respect to $(v_i + v_{j+1})/2$. It reduces to proving the mirror consequence as follows:

(i') when a point X travels along $\zeta(u, u')$, it moves (strictly) in clockwise around O' .

See Figure 21 (d). It further reduces to proving that O' lies on the right of any e_k such that $e_k \cap \zeta(u, u') \neq \emptyset$. Let r_1 be the ray at v_i which has opposite direction to e_{j+1} . Let r_2 be the ray at v_{j+1} which has the same direction as e_{i-1} . Let Π denote the region on the right of r_1 , the left of r_2 , and the left of $\overrightarrow{v_i v_{j+1}}$.

Consider any e_k that intersects $\zeta(u, u')$. Since $\zeta(u, u')$ starts at Z_{i-1}^j , edge e_k is in $\{\text{forw}(Z_{i-1}^j), \dots, e_{i-1}\}$. Applying Fact 5 (part 2) at $(a, a') = (i-1, j)$, ray r_2 is on the right of e_k . Since $\zeta(u, u')$ terminates at Z_i^{j+1} , edge e_k is in $\{e_{j+1}, \dots, \text{back}(Z_i^{j+1})\}$. Applying Fact 5 (part 1) at $(a, a') = (i, j+1)$, ray r_1 is on the right of e_k . Together, Π is on the right of e_k . (To be clear, assume π contains r_1, r_2 but not segment $v_i v_{j+1}$.)

Because O lies in the opposite quadrant of $\text{quad}_u^{u'}$, it lies on the right of $\overrightarrow{v_i v_{j+1}}$. Because O lies in P , it lies on the right of e_{i-1} (or on ℓ_{i-1}) and on the right of e_{j+1} (or on ℓ_{j+1}). As a corollary, $O' \in \Pi$.

Combining the above two results, O' is on the right of e_k , thus we complete the proof for this case.

- Case 3: u, u' are an edge and a vertex, e.g. $u = e_i, u' = v_{j+1}$. Recall that in this case $\text{block}(u, u')$ has four borders; two of which are congruent to the only edge in u, u' ; whereas the other two are reflections of $\zeta(u, u')$. See Figure 21 (e). Applying the technique developed in Case 1, we can prove the part of result (i) that is associated with the former two borders. Applying the technique developed in Case 2, we can prove the part of result (i) that is associated with the latter two borders. (For proving the second part, a useful trick is that we only need to show O lies on the right of each oriented segment of the lower border. This simply implies that O lies on the right of each oriented segment of the other border reflected from $\zeta(u, u')$.) Since the proof is almost the same as the proofs for the above two cases, we do not give them in detail.

\square

4.5 The lemma which shows that \mathcal{C} interleaves ∂P under some conditions (Lemma 3)

Proof of Lemma 3. We refer to $\beta_1, \alpha_1, \dots, \beta_q, \alpha_q$ as the 1st, 2nd, etc., the $2q$ -th fragment; $q \geq 3$. We shall prove that the concatenation of these $2q$ fragments, i.e. curve \mathcal{C} , interleaves ∂P , when the following conditions hold:

(a) The concatenation of $\alpha_{i-1}, \beta_i, \alpha_i$ interleaves ∂P (for $1 \leq i \leq q$). (b) There are $S_1, T_1, \dots, S_q, T_q$ lying in clockwise order around ∂P such that $\beta_i \cap \partial P \subset [S_i \circ T_i]$ whereas $\alpha_i \cap \partial P \subset [S_i \circ T_{i+1}]$ (for $1 \leq i \leq q$).

We assume that at least one fragment in $\alpha_1, \dots, \alpha_q$ intersects ∂P . The case where none of them intersects ∂P is much easier (almost trivial) and can be proved similarly. Without loss of generality, assume that α_q intersects ∂P .

Let \mathcal{D} denote the concatenation of the first $2q - 1$ fragments. Since \mathcal{C} is the concatenation of α_q and \mathcal{D} , to show that it interleaves ∂P reduces to proving three facts:

(i) α_q interleaves ∂P . (ii) \mathcal{D} interleaves ∂P . (iii) We can find two points A, B on ∂P such that the points in $\alpha_q \cap \partial P$ are restricted to $[A \circ B]$ whereas the points in $\mathcal{D} \cap \partial P$ are restricted to $[B \circ A]$.

(Note that in (iii), we abuse the notation a little bit so that $[B \circ A]$ means the entire ∂P when $A = B$.)

Proof of (i): This one simply follows from condition (a).

Proof of (ii): We need some notations. Regard S_1 as the starting point of ∂P . For two points A, A' on ∂P , we say that A lies *behind* A' if $A = A'$ or, A will be encountered later than A' traveling around ∂P starting from S_1 . We say that fragment γ lies *behind* fragment γ' , if all of the points in $\gamma \cap \partial P$ lie behind all of the points in $\gamma' \cap \partial P$.

According to condition (a), each fragment interleaves ∂P . Therefore, proving (ii) reduces to proving that

the k -th fragment lies behind the first $k - 1$ fragments, for $1 < k < 2q$.

We prove this observation in the following.

Case 1: $k = 2$. Applying conditions (a) and (b), the concatenation of β_1, α_1 interleaves ∂P and has all its intersections with ∂P restricted to $[S_1 \circ T_2]$. This means α_1 (i.e. the 2nd fragment) lies behind β_1 (i.e. the 1st fragment).

Case 2: $k > 2$ and k is odd. Assume the k -th fragment is β_i . By condition (b), the first $k - 2$ fragments have all their intersections with ∂P restricted to $[S_1 \circ T_{i-1}]$. However, $\beta_i \cap \partial P \subset [S_i \circ T_i]$. So, the k -th fragment β_i lies behind the first $k - 2$ fragments. Applying the technique for proving Case 1, fragment β_i lies behind the $(k - 1)$ -th fragment α_{i-1} . Together, the k -th fragment lies behind all the first $k - 1$ fragments.

Case 3: $k > 2$ and k is even. Assume the k -th fragment is α_i . Similar to Case 1, α_i lies behind the $(k - 1)$ -th and $(k - 2)$ -th fragments β_i, α_{i-1} . Following the ideas given in Case 2, α_i lies behind the first $k - 3$ fragments. (To be more clear, $\alpha_i \cap \partial P \subset [S_i \circ T_{i+1}]$ whereas the first $k - 3$ fragments having all their intersections with ∂P restricted to $[S_1 \circ T_{i-1}]$.) Together, the k -th fragment lies behind all the first $k - 1$ fragments.

Proof of (iii): We simply choose the first and last points of $\alpha_q \cap \partial P$ to be points A, B . Recall that $\alpha_q \cap \partial P \neq \emptyset$; so A, B are well defined. Assume that $A \neq B$ in the following, otherwise fact (iii) is trivial.

By the definition of A and B , points $\alpha_q \cap \partial P$ are contained in $[A \circ B]$. So, we only need to prove that $\mathcal{D} \cap \partial P \subset [B \circ A]$, namely, each fragment beside α_q has all its intersections with ∂P restricted to $[B \circ A]$.

By condition (a), the concatenation of $\alpha_q, \beta_1, \alpha_1$, or $\alpha_{q-1}, \beta_q, \alpha_q$ interleaves ∂P . So, for the four fragments $\alpha_1, \beta_1, \alpha_{q-1}, \beta_q$, their intersections with ∂P do not lie in $(A \circ B)$, and hence can only lie in $[B \circ A]$.

Next, consider any fragment γ other than $\alpha_q, \beta_1, \alpha_1, \alpha_{q-1}, \beta_q$. Applying condition (b), the points in $\gamma \cap \partial P$ lie in $[S_2 \circ T_{q-1}]$. Therefore, it reduces to proving that $[S_2 \circ T_{q-1}] \subset [B \circ A]$. The proof is as follows.

Applying condition (b), $\alpha_q \cap \partial P$ are contained in $[S_q \circ T_1]$, and so $[A \circ B] \subset [S_q \circ T_1]$.

Since $S_1, T_1, \dots, S_q, T_q$ lie in clockwise order around ∂P , $[S_q \circ T_1] \subset [T_{q-1} \circ S_2]$.

Together, $[A \circ B] \subset [T_{q-1} \circ S_2]$. Equivalently, $[S_2 \circ T_{q-1}] \subset [B \circ A]$. □

5 Proofs of BLOCK-DISJOINTNESS and INTERLEAVITY-OF- f

This section proves BLOCK-DISJOINTNESS and INTERLEAVITY-OF- f (recall a sketch in section 3).

5.1 Preliminary: some observations

Recall that $(e_c, e_{c'})$ is *extremal* if $e_c \prec e_{c'}$ and $[v_c \circ v_{c'+1}]$ is not contained in any other inferior portions, and recall that $\Delta(c, c')$ is defined as $\{(u, u') \mid \text{unit } u \text{ is chasing } u', \text{ and } \text{forw}(u), \text{back}(u') \in \{e_c, e_{c+1}, \dots, e_{c'}\}\}$.

Fact 6. *There exist at least three extremal pairs.*

Proof. Obviously there must be at least one extremal pair. This can be made stronger as follows. For any edge pair (e_i, e_j) such that $e_i \prec e_j$, there is an extremal pair $(e_{i'}, e_{j'})$ such that $[v_{i'} \circ v_{j'+1}]$ contains e_i and e_j .

Assume (e_i, e_j) is extremal. Choose any edge e_k that does not lie in $[v_i \circ v_{j+1}]$. Obviously,

$$e_i \prec e_j, e_j \prec e_k \text{ and } e_k \prec e_i.$$

Starting from (e_k, e_i) , we find extremal pair (e_a, e_b) so that $[v_a \circ v_{b+1}]$ contains e_k, e_i . Notice that $[v_a \circ v_{b+1}]$ is inferior and thus cannot contain e_j . Starting from (e_j, e_k) , we find extremal pair (e_c, e_d) so that $[v_c \circ v_{d+1}]$ contains e_j, e_k . Notice that $[v_c \circ v_{d+1}]$ is inferior and thus cannot contain e_i . Thus we get three extremal pairs. \square

For any set S of unit pairs, denote $BLOCK[S] = \{\text{block}(u, u') \mid (u, u') \in S\}$.

Lemma 8. *Assume $(e_c, e_{c'})$ is extremal. Let $O = (v_c + v_{c'+1})/2$. Consider any $\text{block}(u, u') \in BLOCK[\Delta(c, c')]$.*

1. *Region $\text{block}(u, u')$ does not intersect the opposite quadrant of $\text{quad}_c^{e'}$.*
2. *When point X travels along any border of $\text{block}(u, u')$, it moves in clockwise around O .*

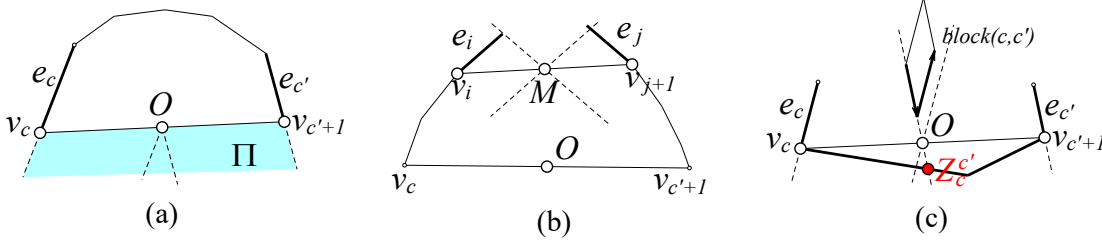


Figure 22: Illustration of the proof of Lemma 8.

Proof. Let $e_i = \text{forw}(u)$ and $e_j = \text{back}(u')$. Because $(u, u') \in \Delta(c, c')$ and applying the definition of $\Delta(c, c')$,

$$e_i, e_j \text{ belong to } \{e_c, \dots, e_{c'}\} \text{ and } e_i \preceq e_j. \quad (17)$$

Recall that hp_i^j is the open half-plane delimited by the extended line of $\overline{v_i v_{j+1}}$ and lies on the left side of $\overline{v_i v_{j+1}}$. Let Π denote the region that lies on the right of $e_c, e_{c'}$ and $\overline{v_c v_{c'+1}}$. According to (17) and the definition of hp_i^j , half-plane hp_i^j is disjoint with Π . Further since $\text{block}(u, u') \subset \text{quad}_u^{u'} = \text{quad}_i^j \subseteq \text{hp}_i^j$, region $\text{block}(u, u')$ is disjoint with Π . Further since the opposite quadrant of $\text{quad}_c^{e'}$ is a subregion of Π , we get part 1 of this lemma.

We prove part 2 in the following. First of all, assume that $(u, u') \neq (e_c, e_{c'})$.

When $(u, u') \neq (e_c, e_{c'})$, we claim that $(i, j) \neq (c, c')$. Suppose $(i, j) = (c, c')$. Then, (u, u') is one of $(e_c, e_{c'})$, $(e_c, v_{c'+1})$, $(v_c, e_{c'})$, $(v_c, v_{c'+1})$. Since $(e_c, e_{c'})$ is extremal, e_c is not chasing $v_{c'+1}$, v_c is not chasing $e_{c'}$, and v_c is not chasing $v_{c'+1}$. Yet u is chasing u' . Together, (u, u') can only be $(e_c, e_{c'})$. This contradicts the assumption.

See Figure 22 (b). Let $M = (v_i + v_{j+1})/2$. Consider the distance to ℓ_j . Because (17), $d_{\ell_j}(v_c) \geq d_{\ell_j}(v_i)$ and $d_{\ell_j}(v_{c'+1}) \geq d_{\ell_j}(v_{j+1})$. Notice that at least one of these inequalities is unequal since $(i, j) \neq (c, c')$. So,

$$d_{\ell_j}(v_c) + d_{\ell_j}(v_{c'+1}) > d_{\ell_j}(v_i) + d_{\ell_j}(v_{j+1}).$$

The left and right sides equal to $2 \cdot d_{\ell_j}(O)$ and $2 \cdot d_{\ell_j}(M)$, respectively. So $d_{\ell_j}(O) > d_{\ell_j}(M)$. Symmetrically, $d_{\ell_i}(O) > d_{\ell_i}(M)$. Therefore, O lies in the opposite quadrant of quad_i^j , namely, it lies in the opposite quadrant of $\text{quad}_u^{u'}$. Further since $O \in P$, applying the monotonicity of the borders (Lemma 5), we get part 2.

When $(u, u') = (e_c, e_{c'})$, part 2 still holds. However, if X travels along the two lower borders of $\text{block}(e_c, e_{c'})$, it is possible that the orientation of OX keeps invariant during the traveling process. This occurs when $Z_c^{c'}$ lies on the boundary of the opposite quadrant of $\text{quad}_c^{c'}$ as shown in Figure 22 (c). (See Fact 3 for more information.) \square

Note 2. In most cases, X moves in clockwise around O *strictly*; namely, the orientation of OX strictly increases. This is true for almost all borders; the only possible exceptions are the lower borders of $\text{block}(e_c, e_{c'})$.

5.2 Proof of the BLOCK-DISJOINTNESS

Recall *local pairs* and *global pairs* introduced in section 3. To prove the BLOCK-DISJOINTNESS, we prove:

(I) When $\text{block}(u, u')$, $\text{block}(v, v')$ are a global pair, their intersection lies in the interior of P .

(II) When $\text{block}(u, u')$, $\text{block}(v, v')$ are a local pair, their intersection is empty!

As shown in section 3, argument (I) easily follows from the peculiarity of the bounding-quadrants (Lemma 6).

Argument (II) is obviously equivalent to the following fact.

Fact 7. For extremal pair $(e_c, e_{c'})$, the blocks in $\text{BLOCK}[\Delta(c, c')]$ are pairwise-disjoint.

As mentioned in section 3, we will prove Fact 7 by using the monotonicity of the borders (Lemma 5 and its successor Lemma 8). First, we prove the following intermediate fact.

Fact 8. For $(e_a, e_{a'})$ in $\Delta(c, c')$, all blocks in $\text{BLOCK}[\text{U}(a, a')]$ are pairwise-disjoint, where

$$\text{U}(a, a') = \{(u, u') \mid u \text{ is chasing } u', \text{ and } u, u' \text{ lie in } (v_a \circ v_{a'+1})\}.$$

We introduce some notations for the proof of the above fact.

Tiling. For a set S of unit pairs, we call $\text{BLOCK}[S]$ a tiling if all the blocks in $\text{BLOCK}[S]$ are pairwise-disjoint.

A quadrant region $\text{SWEPT}_O(X, Y)$. For distinct points O, X, Y , imaging that a ray originated at O rotates from OX to OY in clockwise, we denote by $\text{SWEPT}_O(X, Y)$ the region swept by this ray.

Proof of Fact 8. We prove this fact by using induction on the number of edges k in $(v_a \circ v_{a'})$.

Initial: $k = 2$, i.e., $a' = a + 1$. $\text{BLOCK}[\text{U}(a, a')]$ contains only one block, $\text{block}(e_a, e_{a+1})$, so the claim is trivial.

Induction: $k > 2$. Divide the unit pairs in $\text{U}(a, a')$ into four parts distinguished by whether $\text{U}(a, a' - 1)$, $\text{U}(a + 1, a')$ respectively contain them. Formally,

$$\begin{aligned} U_{10} &= \text{U}(a, a' - 1) - \text{U}(a + 1, a'), & U_{01} &= \text{U}(a + 1, a') - \text{U}(a, a' - 1), \\ U_{11} &= \text{U}(a, a' - 1) \cap \text{U}(a + 1, a'), & U_{00} &= \text{U}(a, a') - \text{U}(a, a' - 1) - \text{U}(a + 1, a'). \end{aligned}$$

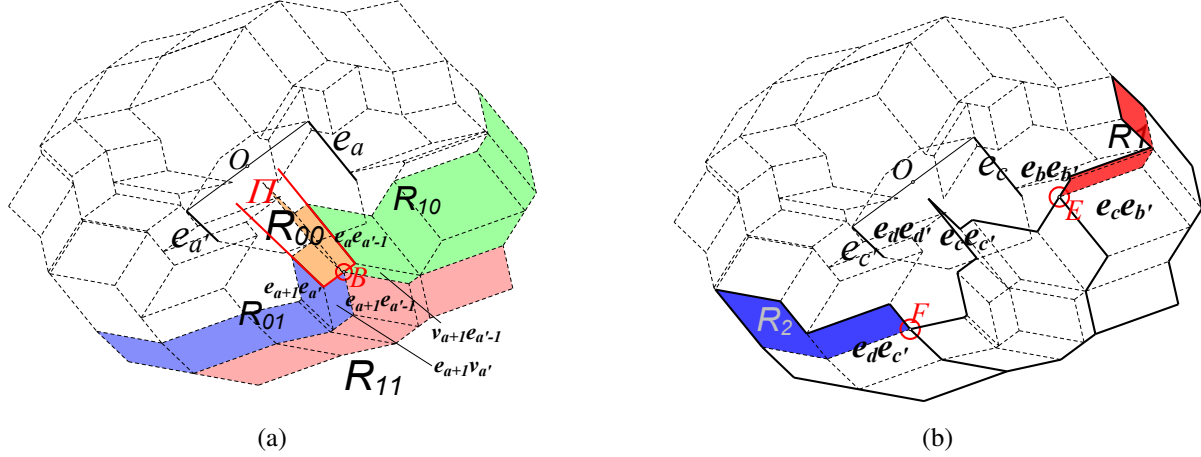


Figure 23: Illustration of the proofs of the BLOCK-DISJOINTNESS

By the induction hypothesis, $BLOCK[U_{01}]$, $BLOCK[U_{10}]$, $BLOCK[U_{11}]$ are tilings. Moreover, since $U_{00} = \{(e_a, e_{a'}), (v_{a+1}, e_{a'}), (e_a, v_{a'}), (v_{a+1}, v_{a'})\}$ only contains four unit pairs, by the definition of the blocks, $BLOCK[U_{00}]$ is also a tiling (see Figure 3; details omitted). So, we only need to prove that $R_{00}, R_{01}, R_{10}, R_{11}$ are pairwise-disjoint, where $R_{00}, R_{01}, R_{10}, R_{11}$ denotes the regions occupied by $BLOCK[U_{00}], BLOCK[U_{01}], BLOCK[U_{10}], BLOCK[U_{11}]$, respectively. It further reduces to proving the following four statements:

- (i) R_{11}, R_{10} are disjoint. (ii) R_{11}, R_{01} are disjoint.
- (iii) R_{01}, R_{10} are disjoint. (iv) R_{00} is disjoint with the other three regions.

See Figure 23 (a). Statement (i) holds because $BLOCK[U(a, a' - 1)]$ is a tiling. Statement (ii) holds because $BLOCK[U(a + 1, a')]$ is a tiling. We prove the other two statements in the following.

Proof of (iii): Let $O = (v_a + v_{a'+1})/2$. Let A be an arbitrary point in the opposite quadrant of $\text{quad}_c^{c'}$, and let B be the terminal point of the lower border of $\text{block}(v_{a+1}, e_{a'-1})$; equivalently, B is the starting point of the lower border of $\text{block}(e_{a+1}, v_{a'})$. Our key observation is the following:

$$R_{10} \subset \text{SWEPT}_O(A, B), \text{ whereas } R_{01} \subset \text{SWEPT}_O(B, A). \quad (18)$$

The part $R_{10} \subset \text{SWEPT}_O(A, B)$ is due to two reasons. 1. When a point X travels along the oriented borders in $BLOCK[U_{10}]$, it eventually reaches B . 2. While X is tracking down these borders, OX keeps rotating in clockwise according to Lemma 8. The part $R_{01} \subset \text{SWEPT}_O(B, A)$ is due to two similar reasons.

Further since $\text{SWEPT}_O(B, A)$ is disjoint with $\text{SWEPT}_O(A, B)$, we obtain statement (iii).

Proof of (iv): Let Π denote the region bounded by: C_1 - the right lower border of $\text{block}(e_a, e_{a'-1})$, C_2 - the left lower border of $\text{block}(e_{a+1}, e_{a'})$, and C_3 - the lower border of $\text{block}(v_{a+1}, v_{a'})$. Observe that (1) R_{00} is contained in Π ; and (2) the united region of R_{10}, R_{01}, R_{11} is also bounded by C_1, C_2 and C_3 and hence is disjoint with Π . Together, we get statement (iv). The proofs of the last two observations are trivial yet burdensome and hence are omitted. \square

Next, we prove Fact 7 and thus complete our proof of the BLOCK-DISJOINTNESS.

Proof of Fact 7. For convenience, let $(e_b, e_{b'}), (e_d, e_{d'})$ respectively denote the previous and next extremal pair of $(e_c, e_{c'})$ in the frontier-pair-list. We divide $\Delta(c, c')$ into three parts:

$$U_1 = (\Delta(c, c') - U(c, c')) \cap U(b, b'), \quad U_2 = (\Delta(c, c') - U(c, c')) \cap U(d, d'), \quad U_3 = U(c, c').$$

Fact 9. β_i begins with the bottom border of $\text{block}(e_{a_i}, e_{a'_i})$ and ends with the bottom border of $\text{block}(e_{b_i}, e_{b'_i})$.

This fact simply follows the definition of β_i and is illustrated by the right picture of Figure 24.

Recall $\langle \text{quad} \rangle$ in (12). Using a_i, a'_i, b_i, b'_i defined above, we further define $2q$ points $S_1, \dots, S_q, T_1, \dots, T_q$ as follows. See the middle picture of Figure 24 for an illustration.

$$S_i = \text{the starting point of } \langle \text{quad} \rangle_{a'_i}^{a'_i}, \quad T_i = \text{the terminal point of } \langle \text{quad} \rangle_{b_i}^{b'_i}. \quad (22)$$

Step 2. Verify these $2q$ points lying in order and prove the three conditions (9), (10), and (11).

Proof of the fact that $S_1, T_1, \dots, S_q, T_q$ lie in clockwise order around ∂P . Consider any pair of neighboring extremal pairs $(e_{c_i}, e_{c'_i}), (e_{c_{i+1}}, e_{c'_{i+1}})$. Following Definition 7 and the definition in (21), we have

edges $e_{b_i}, e_{b'_i}, e_{a_{i+1}}, e_{a'_{i+1}}$ are not in any inferior portion.

According to this observation and the peculiarity of the bounding-quadrants (Lemma 6), $\langle \text{quad} \rangle_{b_i}^{b'_i}$ and $\langle \text{quad} \rangle_{a_{i+1}}^{a'_{i+1}}$ are disjoint (although their endpoints may coincide), for any i ($1 \leq i \leq q$). Combining this with (22) and the monotonicity of $\langle \text{quad} \rangle$ (Lemma 7), the q boundary-portions $(S_1 \circ T_1), \dots, (S_q \circ T_q)$ are pairwise-disjoint and lie in clockwise order. Therefore, $S_1, T_1, \dots, S_q, T_q$ lie in clockwise order. \square

Proof of condition (9). Notice that the concatenation of $\alpha_{i-1}, \beta_i, \alpha_i$ is exactly $\sigma(c_i, c'_i)$. We shall prove that for each extremal pair $(e_c, e_{c'})$, the curve $\sigma(c, c')$ interleaves ∂P . For ease of discussion, assume that $\sigma(c, c')$ and ∂P have a finite number of intersecting points. Denote these points by l_1, \dots, l_x , and assume that

(i) I_1, \dots, I_x are sorted according to their priority on $\sigma(c, c')$.

Denote $O = (v_c + v_{c'})/2$. Since (i) and by applying Lemma 8, rays OI_1, \dots, OI_x are in clockwise order. Further, because O lies in P , we get

(ii) l_1, \dots, l_x lie in clockwise order around ∂P .

Since l_1, \dots, l_x are all the intersecting points between $\sigma(c, c')$ and ∂P , facts (i) and (ii) together imply that: starting from I_1 , regardless of whether we travel along $\sigma(c, c')$ (following its positive direction) or travel around ∂P (in clockwise), we meet the points in $\sigma(c, c') \cap \partial P$ in identical order. In other words, $\sigma(c, c')$ interleaves ∂P . \square

Recall condition (10) states that $\beta_i \cap \partial P \subset [S_i \circ T_i]$.

Proof of condition (10). Consider any frontier block whose bottom border is a fraction of β_i , e.g. $\text{block}(u, u')$, we shall prove that (I) the intersecting points between ∂P and the bottom border of $\text{block}(u, u')$ lie in $[S_i \circ T_i]$.

Denote by $\overline{\langle \text{quad} \rangle}_u^{u'}$ the closed set of $\langle \text{quad} \rangle_u^{u'}$, which contains $\langle \text{quad} \rangle_u^{u'}$ and its endpoints. By Lemma 4, $\text{block}(u, u') \subset \overline{\langle \text{quad} \rangle}_u^{u'}$. So, the bottom border of $\text{block}(u, u')$ lie in the closed set of $\overline{\langle \text{quad} \rangle}_u^{u'}$. Therefore, the intersecting points between ∂P and the bottom border of $\text{block}(u, u')$ are contained in $\overline{\langle \text{quad} \rangle}_u^{u'}$. By the monotonicity of the $\langle \text{quad} \rangle$ (Lemma 7) and the definition (22) of S_i, T_i , we get $\overline{\langle \text{quad} \rangle}_u^{u'} \subseteq [S_i \circ T_i]$. Together, we get (I). \square

Condition (11) can be proved the same way as condition (10); so proof omitted.

Step 3. Complete the proof of INTERLEAVITY-OF- f by applying Lemma 3. Since the conditions of Lemma 3 are all satisfied, applying this lemma we obtain that σP interleaves ∂P .

6 Proof: two more properties of $\text{Nest}(P)$ (MONOTONICITY-OF- f & SECTOR-CONTINUITY)

This section proves MONOTONICITY-OF- f and SECTOR-CONTINUITY (recall a sketch in section 3).

6.1 Proof of the MONOTONICITY-OF- f

We first give some terminologies and then prove the MONOTONICITY-OF- f .

See Figure 25. Let K_1, \dots, K_m denote all the intersecting points between σP and ∂P , and assume that they lie in clockwise order around ∂P . Points K_1, \dots, K_m divide ∂P into m portions; each of which is called a K -portion.

Top borders. Recall the four borders of $\text{block}(e_i, e_{i+1})$. We define the *top border* of $\text{block}(e_i, e_{i+1})$ as the concatenation of those two borders that are not the lower borders (recall the lower borders in subsection 2.1). Recall the unique border of $\text{block}(v_i, v_{i+1})$. We define this border to be the *top border* of $\text{block}(v_i, v_{i+1})$.

Outer boundary of $f(\mathcal{T})$. See Figure 26. We define the *outer boundary* of $f(\mathcal{T})$ as the concatenation of the top borders of $\text{block}(e_1, e_2), \text{block}(v_2, v_3), \dots, \text{block}(e_n, e_1), \text{block}(v_1, v_2)$, which is closed by observing that the terminal point of the top border of one block equals the starting point of the top border of its next block.

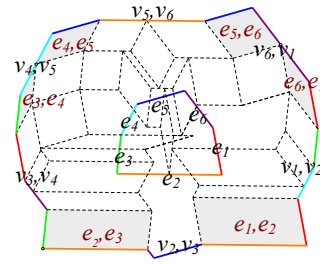
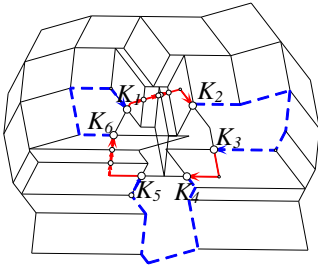


Figure 25: Illustration of the K -points and K -portions.

Figure 26: Illustration of the outer boundary.

Fact 10. (1) All the top borders defined above lie outside P . (2) The outer boundary of $f(\mathcal{T})$ is a simple closed curve whose interior contains P . (3) For any K -portion, it either lies in $f(\mathcal{T})$ or lies outside $f(\mathcal{T})$.

Proof. (1) The top border of $\text{block}(v_i, v_{i+1})$ is $\text{block}(v_i, v_{i+1})$ itself, and by Lemma 4 it lies in quad_i^i and hence lies outside P . The top border of $\text{block}(e_i, e_{i+1})$ is the concatenation of two borders; one is parallel to e_i and the other is parallel to e_{i+1} . Following from the fact $\text{block}(e_i, e_{i+1}) \subset \text{quad}_i^{i+1}$, the former border lies on the left of e_i whereas the latter one lies on the left of e_{i+1} ; so both borders lie outside P . Therefore, the top borders lie outside P .

(2) We already know the outer boundary is closed. Combining part 1 with the BLOCK-DISJOINTNESS, two top borders do not intersect. Therefore, the outer boundary is simple and contains P in its interior (see Figure 26).

(3) Clearly, $f(\mathcal{T})$ has an annular shape which is bounded by its inner and outer boundaries. Combining the above result on the outer boundary with the INTERLEAVITY-OF- f of the inner boundary, we obtain part 3. \square

Extend the definition of f_2^{-1} . Recall $f_2^{-1}(\cdot)$ in Theorem 1. So far, it is defined on $f(\mathcal{T}) \cap \partial P$, but **not** on the K -points. This is implied by Fact 11 below. However, to prove the monotonicity of $f_2^{-1}(\cdot)$, it is convenient to also define f_2^{-1} on the K -points. Below we show a natural way to extend the definition of f_2^{-1} on to those K -points.

Consider any K -point K_i . Assume it comes from the bottom border of $\text{block}(u, u')$. Recall the extended definition of $f_{u,u'}^{-1,2}(\cdot)$ above Definition 5. We simply define $f_2^{-1}(K_i) := f_{u,u'}^{-1,2}(K_i)$.

Fact 11. K_1, \dots, K_m are not contained in $f(\mathcal{T}) \cap \partial P$.

Proof. Without loss of generality, assume some K -point K_i comes from the bottom border of the frontier block $\text{block}(u, u')$. We first argue that u, u' cannot both be vertices. For a contradiction, suppose they are both vertices. Then, u' must be the clockwise next vertex of u since $\text{block}(u, u')$ is a frontier block (this can be observed from Algorithm 1). Then, by Fact 10, $\text{block}(u, u')$ lies outside P , so its bottom border (which is the block itself) has no intersection with ∂P . This means K_i cannot come from the bottom border of $\text{block}(u, u')$. Contradictory.

Therefore, u, u' comprise at least one edge. Then, according to Definitions 2 and 3, the lower borders and bottom border of $\text{block}(u, u')$ are not contained in $\text{block}(u, u')$. This further implies that K_i is not contained in $f(\mathcal{T})$. \square

Proof of the MONOTONICITY-OF- f . We shall prove the circularly monotone property of $f^{-2}(X)$. We state two observations first. (Recall function g from σP to ∂P in Definition 5.)

(i) The value of $f_2^{-1}()$ is continuous at the K -points.

(ii) Function g is circularly monotone on curve σP (see Figure 8 (c)).

The way we extend $f_{u,u'}^{-1,2}()$ onto the lower border of $\text{block}(u, u')$ implies observation (i). Also according to this extension, $f_{u,u'}^{-1,2}()$ is monotone on the lower border of $\text{block}(u, u')$, which implies observation (ii).

We then state two more observations.

(iii) Points $f_2^{-1}(K_1), \dots, f_2^{-1}(K_m)$ lie in clockwise order around ∂P .

(iv) Function $f_2^{-1}()$ is monotone on any K -portion that lies in $f(\mathcal{T})$. In other words, when point X travels along such a K -portion, $f_2^{-1}(X)$ moves in clockwise order around ∂P non-strictly.

Proof of (iii): Since K_1, \dots, K_m lie in clockwise around ∂P , they lie in clockwise around σP due to the INTERLEAVITY-OF- f , and thus $g(K_1), \dots, g(K_m)$ lie in clockwise around ∂P according to observation (ii). Furthermore, notice that $f_2^{-1}(K_i) = g(K_i)$, we obtain observation (iii).

Proof of (iv): This observation follows from the LOCAL-MONOTONICITY OF f (Lemma 2); because when X travels along a K -portion that lies in $f(\mathcal{T})$, it travels inside some blocks (see Figure 25).

We now complete the proof. By Fact 10, $f(\mathcal{T}) \cap \partial P$ consists of those K -portions lying in $f(\mathcal{T})$. Imagine that a point X travels around $f(\mathcal{T}) \cap \partial P$ in clockwise; observation (iv) assures that $f_2^{-1}(X)$ is monotone inside each K -portion, whereas observations (i) and (iii) assure that $f_2^{-1}(X)$ is monotone between the K -portions. \square

6.2 Proof of the SECTOR-CONTINUITY

Outline of this subsection. Assume V is a fixed vertex.

1. Prove that $\text{sector}(V)$ equals the 2-scaling of $(\bigcup_{(u,u') \in \Lambda_V} u \oplus u')$ with respect to V , where

$$\Lambda_V = \{(u, u') \mid u \text{ is chasing } u', \text{ and } \zeta(u, u') \text{ contains } V\}.$$

Moreover, define delimiting edges e_{s_V}, e_{t_V} .

2. Prove a few crucial properties of e_{s_V}, e_{t_V} . (see subsection 6.2.1)
3. Define $\mathcal{L}_V, \mathcal{R}_V, \text{mid}_V$ based on e_{s_V} and e_{t_V} (as shown in section 3). Then, prove a structural property of Λ_V applying mid_V . (see subsection 6.2.2)
4. Define $\text{mid}_V^*, \mathcal{L}_V^*, \mathcal{R}_V^*$ as the 2-scalings of $\text{mid}_V, \mathcal{L}_V, \mathcal{R}_V$ with respect to V , respectively. Prove that mid_V^* is the closed set of $\text{sector}(V)$. Based on this result, prove that $\mathcal{L}_V^*, \mathcal{R}_V^*$ are boundaries of $\text{sector}(V)$ and further prove the SECTOR-CONTINUITY. (see subsection 6.2.3)

Proof of the above formula of sector(V).

$$\begin{aligned}
\text{sector}(V) &= f(\{(X_1, X_2, X_3) \in \mathcal{T} \mid X_2 = V\}) \quad (\text{By definition (5)}) \\
&= f\left(\bigcup_{u \text{ is chasing } u'} \{(X_1, X_2, X_3) \mid X_1 \in u', X_2 = V, X_2 \in \zeta(u, u'), X_3 \in u\}\right) \\
&= f\left(\bigcup_{u \text{ is chasing } u', V \in \zeta(u, u')} \{(X_1, V, X_3) \mid X_3 \in u, X_1 \in u'\}\right) \\
&= \bigcup_{(u, u') \in \Lambda_V} f(\{(X_1, V, X_3) \mid X_3 \in u, X_1 \in u'\}) \\
&= \bigcup_{(u, u') \in \Lambda_V} \text{2-scaling of } (u \oplus u') \text{ with respect to } V \\
&= \text{2-scaling of } \left(\bigcup_{(u, u') \in \Lambda_V} u \oplus u'\right) \text{ with respect to } V.
\end{aligned}$$

□

A relation \leq_V between the edges. We say e_i is *smaller than* e_j or e_j is *larger than* e_i (with respect to V), if e_i would appear earlier than e_j when we enumerate all the edges of P in clockwise order from $forw(V)$ to $back(V)$. Denote by $e_i \leq_V e_j$ if e_i is smaller than or identical to e_j .

The following definition is crucial to this subsection.

Definition 8 (Delimiting edges e_{s_V} & e_{t_V}). Recall that D_i is the furthest vertex to ℓ_i . For any edge e_i , denote

$$\begin{aligned}
\omega_i^+ &= \bigcup_{e_j: e_i < e_j} [v_{i+1} \circlearrowleft Z_i^j] = [v_{i+1} \circlearrowleft Z_i^{back(D_i)}], \\
\omega_i^- &= \bigcup_{e_k: e_k < e_i} [Z_k^i \circlearrowleft v_i] = [Z_{forw(D_i)}^i \circlearrowleft v_i].
\end{aligned} \tag{23}$$

We define e_{s_V}, e_{t_V} respectively as the smallest edge e_i such that ω_i^+ contains V , and the largest edge e_i such that ω_i^- contains V . Throughout this subsection, “smallest” or “largest” is with respect to relation \leq_V introduced above. See Figure 27 for an illustration for this definition. We abbreviate s_V, t_V as s, t .

Note: Clearly, $V \in \omega_{back(V)}^+$, so there is at least one element in $\{\omega_i^+\}$ which contains V . So s_V is well defined.

Note: Clearly, $V \in \omega_{forw(V)}^-$, so there is at least one element in $\{\omega_i^-\}$ which contains V . So t_V is well defined.

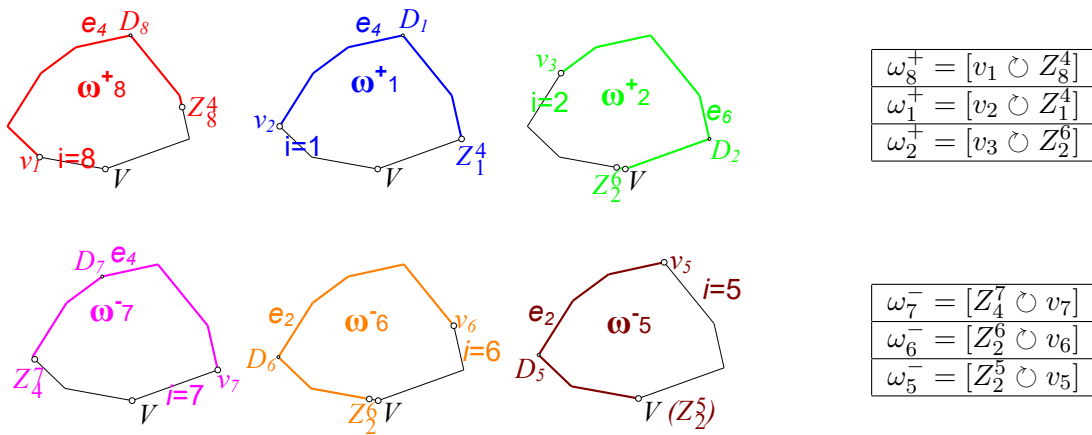


Figure 27: Demonstration of the definitions of s_V and t_V . Here, $s_V = 2, t_V = 5$.

6.2.1 Crucial properties of e_{s_V}, e_{t_V}

Fact 12. $e_s \preceq e_t$ and the inferior portion $[v_s \circ v_{t+1}]$ does not contain V .

Proof. Assume $V = v_1$ for simplicity. This proof is divided into three parts as shown below.

Part 1): prove that $e_s \leq_V e_t$. To this end, we first state an observation:

(i) $e_s \leq_V e_{s^*}$ and $e_{t^*} \leq_V e_t$, where $e_{s^*} = \text{forw}(D_n)$ and $e_{t^*} = \text{back}(D_1)$.

Proof of (i): See Figure 28 (a). By Fact 2, $Z_{s^*}^n$ lies in $(V \circ v_{s^*})$. Therefore, $V \in [v_{s^*+1} \circ Z_{s^*}^n]$. Moreover, $[v_{s^*+1} \circ Z_{s^*}^n] \subseteq \omega_{s^*}^+$ by the definition of $\omega_{s^*}^+$. Therefore, $V \in \omega_{s^*}^+$, which implies $e_s \leq_V e_{s^*}$ due to the definition of s . Symmetrically, $V \in \omega_{t^*}^-$ and thus $e_{t^*} \leq_V e_t$.

We now use the above observation to prove that $e_s \leq_V e_t$.

Case 1 $D_1 \neq D_n$. In this case $e_{s^*} \leq_V e_{t^*}$. Combining with observation (i), we get $e_s \leq_V e_t$.

Case 2 $D_1 = D_n$. See Figure 28 (b). In this case $Z_{t^*}^{s^*}$ is defined since e_{s^*} is the next edge of e_{t^*} .

Case 2.1 $Z_{t^*}^{s^*}$ lies in $[V \circ D_1]$. In this subcase, we argue that $e_s \leq_V e_{t^*}$. Since $V \in [D_1 \circ Z_{t^*}^{s^*}]$, whereas $[D_1 \circ Z_{t^*}^{s^*}] = [v_{t^*+1} \circ Z_{t^*}^{s^*}] \subseteq \omega_{t^*}^+$, we get $V \in \omega_{t^*}^+$, which implies that $e_s \leq_V e_{t^*}$ according to the definition of s . Combining $e_s \leq_V e_{t^*}$ with $e_{t^*} \leq_V e_t$ stated in observation (i), we get $e_s \leq_V e_t$.

Case 2.2 $Z_{t^*}^{s^*}$ lies in $[D_1 \circ V]$. In this subcase, we argue that $e_{s^*} \leq_V e_t$. The proof is symmetric to Case 2.1 and omitted. Combining $e_{s^*} \leq_V e_t$ with $e_s \leq_V e_{s^*}$ stated in observation (i), we get $e_s \leq_V e_t$.

Part 2): prove that $[v_s \circ v_{t+1}]$ does not contain V .

By the definition of ω^+ , we get $V \notin \omega_{\text{forw}(V)}^+$, which means $e_s \neq \text{forw}(V)$, i.e. $V \neq v_s$. Symmetrically, $V \neq v_{t+1}$. In addition, applying $e_s \leq_V e_t$, we get $V \notin (v_s \circ v_{t+1})$. Altogether, $V \notin [v_s \circ v_{t+1}]$.

Part 3): prove that $e_s \preceq e_t$. For a contradiction, suppose that $e_t \prec e_s$, as shown in Figure 28 (c).

Denote $e_a = \text{back}(D_s)$ and $e_b = \text{forw}(D_t)$. If $D_s \neq D_t$, denote $\rho = [D_s \circ D_t]$; otherwise, let ρ denote the entire boundary of P and assume that it starts and terminates at D_s . Consider points Z_s^a and Z_b^t , which lie in ρ according to Fact 1. We claim that (I) $Z_b^t \leq_\rho Z_s^a$ and (II) $Z_s^a <_\rho Z_b^t$, which lead to a contradiction.

Proof of (I). By definition of s , we have $V \in \omega_s^+ = [v_{s+1} \circ Z_s^a]$. This means $V \leq_\rho Z_s^a$. By definition of t , we have $V \in \omega_t^- = [Z_b^t \circ v_t]$. This means $Z_b^t \leq_\rho V$. Together, we get (I).

Proof of (II). Let $M = (v_s + v_{t+1})/2$. Recall that $p_i(X)$ denotes the unique line at point X that is parallel to e_i . Let A be the intersection of $p_s(M)$ and $[v_{t+1} \circ v_s]$, and B the intersection of $p_t(M)$ and $[v_{t+1} \circ v_s]$. We claim that $Z_s^a <_\rho A <_\rho B <_\rho Z_b^t$, which implies (II). The inequality $A <_\rho B$ follows from the assumption $e_t \prec e_s$. We prove $Z_s^a <_\rho A$ in the next paragraph; the proof of $B <_\rho Z_b^t$ is symmetric and omitted.

Proof of $Z_s^a <_\rho A$. Denote by h the open half-plane delimited by $p_s(M)$ and containing v_{t+1} . By the definition of D_s , it is further than v_{t+1} on the distance to ℓ_s , so the mid point of v_s and D_s is contained in h . Therefore the opposite quadrant of quad_s^a , together with its boundary, are contained in h . However, Z_s^a lies in or on the boundary of the opposite quadrant of quad_s^a (by Fact 3). Therefore, $Z_s^a \in h$, which implies that $Z_s^a <_\rho A$. \square

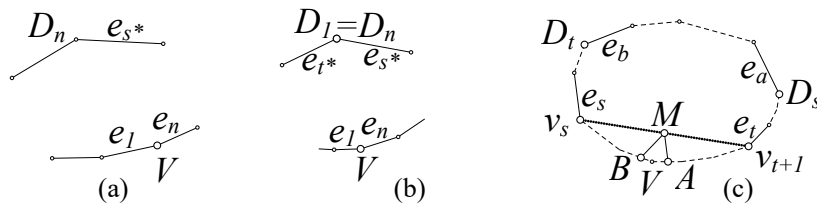


Figure 28: Illustration of the proof of the relation between e_s, e_t and V

Fact 13. For $(u, u') \in \Lambda_V$, units u, u' both lie in $[v_s \circ v_{t+1}]$.

Proof. Let $e_a = \text{back}(u), e_{a'} = \text{back}(u'), e_b = \text{forw}(u), e_{b'} = \text{forw}(u')$. Assume $(u, u') \in \Lambda_V$. Then, $V \in \zeta(u, u')$. Notice that $V \in \zeta(u, u') = [Z_{a'}^+ \circ Z_b^+] \subseteq [v_{b+1} \circ Z_b^+] \subseteq \omega_b^+$. So, $V \in \omega_b^+$. This implies that $e_s \leq_V e_b$ by the definition of s . Symmetrically, $V \in \omega_{a'}^-$, which implies that $e_{a'} \leq_V e_t$ by the definition of t .

Since u is chasing u' , we have $\text{forw}(u) \preceq \text{back}(u')$. Together, $e_s \leq_V \text{forw}(u) \preceq \text{back}(u') \leq_V e_t$. Further since $e_s \preceq e_t$ (By Fact 12), $e_s \leq_V \text{forw}(u) \leq_V \text{back}(u') \leq_V e_t$, hence u and u' both lie in $[v_s \circ v_{t+1}]$. \square

Fact 14. (1) $V \in \omega_i^+$ if and only if $e_s \leq_V e_i$. (2) $V \in \omega_j^-$ if and only if $e_j \leq_V e_t$,

Proof. We only give the proof of Claim 1. Claim 2 is symmetric.

The ‘‘only if’’ part follows from the definition of s . We shall prove that $V \in \omega_i^+$ for $e_i \in \{e_s, e_{s+1}, \dots, \text{back}(V)\}$. We prove it by induction. Recall that $\omega_i^+ = [v_{i+1} \circ Z_i^{\text{back}(D_i)}]$. Initially, let $i = s$. We know $[v_{s+1} \circ Z_s^{\text{back}(D_s)}]$ contains V by the definition of s . Next, consider $\omega_{i+1}^+ = [v_{i+2} \circ Z_{i+1}^{\text{back}(D_{i+1})}]$. See Figure 29 (a). By the bi-monotonicity of the Z -points, $Z_{i+1}^{\text{back}(D_{i+1})}$ lies in $[Z_i^{\text{back}(D_i)} \circ v_{i+1}]$. This implies that ω_{i+1}^+ contains V . \square

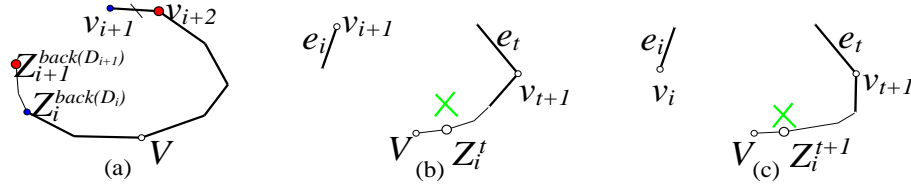


Figure 29: Illustrations of the proofs of Fact 14 and Fact 15.

6.2.2 Definition of mid_V and a structural property of Λ_V

Recall set Δ_V , region mid_V and its two boundaries $\mathcal{L}_V, \mathcal{R}_V$ defined in section 3 (see Figure 14).

Lemma 9. $(u, u') \in \Lambda_V$ if and only if $(u, u') \in \Delta_V, u \oplus u' \subseteq \text{mid}_V$, and u is chasing u' .

Note: Although $e_s \preceq e_t$, set Δ_V sometimes may contain unit pair (u, u') such that u is not chasing u' . For example, $(v_s, v_{t+1}) \in \Delta_V$, but it is possible that v_s is not chasing e_{t+1} .

Before proving Lemma 9, we state some additional observations of s, t in Fact 15.

Fact 15. Denote $\rho = [v_{t+1} \circ v_s]$.

1. For e_i in $[v_s \circ v_{t+1}]$ and $e_i \neq e_t$, when $Z_i^t <_\rho V$, we have $e_i \prec e_{t+1}$.
2. For e_i in $[v_s \circ v_{t+1}]$, when $e_i \prec e_{t+1}$, we have $Z_i^{t+1} \in (V \circ v_i)$.
3. For e_j in $[v_s \circ v_{t+1}]$ and $e_j \neq e_s$, when $Z_s^j >_\rho V$, we have $e_{s-1} \prec e_j$.
4. For e_j in $[v_s \circ v_{t+1}]$, when $e_{s-1} \prec e_j$, we have $Z_{s-1}^j \in (v_{j+1} \circ V)$.

We only show the proof of parts 1 and 2. Parts 3 and 4 are symmetric to parts 1 and 2, respectively.

Proof of part 1. For a contradiction, suppose that $e_i \not\prec e_{t+1}$, as shown in Figure 29 (b). This means $D_i = v_{t+1}$, which further implies $\omega_i^+ = [v_{i+1} \circ Z_i^t]$. Combining this equation with the assumption $Z_i^t <_\rho V$, we see ω_i^+ does not contain V . Since e_i lies in $[v_s \circ v_{t+1}]$, we know $e_s \leq_V e_i$ and so ω_i^+ contains V by Fact 14. Contradictory. \square

Proof of part 2. For a contradiction, suppose that Z_i^{t+1} does not lie in $(V \circ v_i)$. Then, it must lie in $[v_{t+1} \circ V]$ according to Fact 2, as shown in Figure 29 (c). So $[Z_i^{t+1} \circ v_i]$ contains V . Further since $[Z_i^{t+1} \circ v_i] \subseteq \omega_{t+1}^-$, we get $V \in \omega_{t+1}^-$. This means e_t is not the largest edge such that ω_t^- contains V , contradicting the definition of e_t . \square

Proof of Lemma 9. According to Fact 13, $\Lambda_V \subseteq \Delta_V$. Thus it reduces to proving that for each $(u, u') \in \Delta_V$ such that u is chasing u' ,

$$\zeta(u, u') \text{ contains } V \Leftrightarrow u \oplus u' \subseteq \text{mid}_V. \quad (24)$$

First, consider the trivial case $s = t$, where (v_s, v_{t+1}) is the only element in Δ_V so that u is chasing u' (v_i is always chasing v_{i+1} .) By definition, mid_V equals $v_s \oplus v_{t+1}$. It remains to show that $\zeta(v_s, v_{t+1})$ contains V . By Fact 15.2 and 15.4, $Z_s^{t+1} \in (V \circ v_s)$ whereas $Z_{s-1}^t \in (v_{t+1} \circ V)$. So, $V \in [Z_{s-1}^t \circ Z_s^{t+1}]$, i.e. $V \in \zeta(v_s, v_{t+1})$.

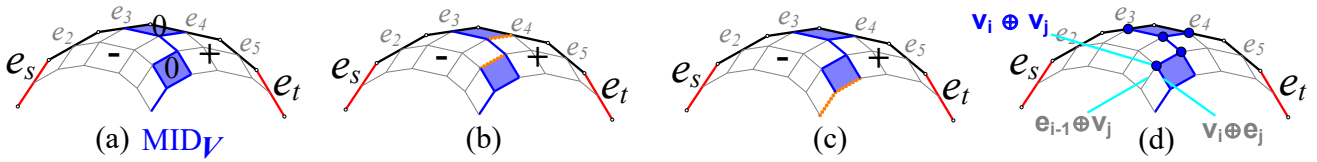


Figure 30: Illustration of Statement (24).

Assume now $s \neq t$. Let $\rho = [v_{t+1} \circ v_s]$. Take an arbitrary unit pair $(u, u') \in \Delta_V$ such that u is chasing u' .

Case 1: u, u' are both edges. By definition of mid_V , $u \oplus u' \subseteq \text{mid}_V \Leftrightarrow [u \oplus u'$ is marked by '0'] $\Leftrightarrow Z_u^{u'} = V$. By definition of $\zeta(u, u')$ in (2), $V \in \zeta(u, u') \Leftrightarrow Z_u^{u'} = V$. Together, (24) holds.

Case 2.1: $(u, u') = (e_i, v_j)$ where $j \neq t+1$. See the dotted segments in Figure 30 (b). We have $u \oplus u' \subseteq \text{mid}_V \Leftrightarrow [e_i \oplus e_{j-1}$ is marked by '0/-' whereas $e_i \oplus e_j$ is marked by '0/+'] $\Leftrightarrow [Z_i^{j-1} \leq_\rho V \leq_\rho Z_i^j] \Leftrightarrow V \in \zeta(e_i, v_j)$. In particular, the first " \Leftrightarrow " is by the definition of mid_V , the last " \Leftrightarrow " is by the definition of $\zeta(u, u')$.

Case 2.2: $(u, u') = (e_i, v_{t+1})$. See the dotted segments in Figure 30 (c). We have $u \oplus u' \subseteq \text{mid}_V \Leftrightarrow [e_i \oplus e_t$ is marked by '0/-'] $\Leftrightarrow Z_i^t \leq_\rho V \Leftrightarrow V \in \zeta(u, u')$. Here, the last " \Leftrightarrow " is non-obvious and is proved in the following. Since $u = e_i$ is chasing $u' = v_{t+1}$, we know $e_i \prec e_{t+1}$. Therefore, by Fact 15.2, $Z_i^{t+1} \in (V \circ v_i)$. This implies that $Z_i^t \leq_\rho V \Leftrightarrow V \in [Z_i^t \circ Z_i^{t+1}]$. In other words, $Z_i^t \leq_\rho V \Leftrightarrow V \in \zeta(u, u')$.

Case 2.3: u is a vertex and u' is an edge. This is symmetric to Case 2.1 or Case 2.2.

Case 3.1: $(u, u') = (v_s, v_{t+1})$. (This does not necessarily occur since v_s may not be chasing v_{t+1} .) Since u is chasing u' , we have $e_{s-1} \prec e_t$ and $e_s \prec e_{t+1}$. By Fact 15.2 and 15.4, Z_{s-1}^t lies in $(v_{t+1} \circ V)$, whereas Z_s^{t+1} lies in $(V \circ v_s)$. Therefore, V lies in $[Z_{s-1}^t \circ Z_s^{t+1}] = \zeta(v_s, v_{t+1})$. Moreover, $v_s \oplus v_{t+1}$ must be contained in mid_V . Thus (24) holds.

Case 3.2: $(u, u') = (v_i, v_j)$ where $i \neq s$ and $j \neq t+1$. See the dots in Figure 30 (d) for illustrations. We have $v_i \oplus v_j \subseteq \text{mid}_V \Leftrightarrow [e_{i-1} \oplus v_j \subseteq \text{mid}_V$ or $v_i \oplus e_j \subseteq \text{mid}_V] \Leftrightarrow [V \in \zeta(e_{i-1}, v_j)$ or $V \in \zeta(v_i, e_j)] \Leftrightarrow [V \in \zeta(v_i, v_j)]$. The last second " \Leftrightarrow " applies the results in Case 2. The last " \Leftrightarrow " applies the fact that $\zeta(v_i, v_j)$ is the concatenation of $\zeta(e_{i-1}, v_j)$ and $\zeta(v_i, e_j)$.

Case 3.3: $[u = v_s$ and u' is a vertex other than $v_{t+1}]$ or $[u' = v_{t+1}$ and u is a vertex other than $v_s]$. The proof of this case is similar to those of Case 3.1 and Case 3.2 and is omitted.

\square

6.2.3 Proof of the enhanced version of SECTOR-CONTINUITY

For convenience, denote

$$\frac{1}{2}\text{sector}(V) = \frac{1}{2}\text{-scaling of sector}(V) \text{ with respect to } V = \bigcup_{(u,u') \in \Lambda_V} u \oplus u'. \quad (25)$$

Lemma 10. *Let ϵ_V = the union of $\{u \oplus u' \mid (u, u') \in \Delta_V, u \text{ is not chasing } u'\}$, then*

$$\frac{1}{2}\text{sector}(V) = \text{mid}_V - \epsilon_V. \quad (26)$$

Moreover, mid_V is the closed set of $\frac{1}{2}\text{sector}(V)$. So mid_V^* is the closed set of $\text{sector}(V)$.

Proof. Regions $\frac{1}{2}\text{sector}(V)$, mid_V , ϵ_V are all unions of some regions in $\{u \oplus u' \mid (u, u') \in \Delta_V\}$. Obviously, the regions in $\{u \oplus u' \mid (u, u') \in \Delta_V\}$ are pairwise-disjoint. Therefore, proving (26) reduces to proving that for any $(u, u') \in \Delta_V$,

$$\begin{aligned} u \oplus u' \subseteq \frac{1}{2}\text{sector}(V) &\Leftrightarrow [u \oplus u' \subseteq \text{mid}_V \text{ and } u \oplus u' \not\subseteq \epsilon_V]; \text{ equivalently,} \\ [(u, u') \in \Lambda_V] &\Leftrightarrow [u \text{ is chasing } u' \text{ and } u \oplus u' \subseteq \text{mid}_V], \end{aligned}$$

which holds according to Lemma 9.

Next, we show that mid_V is the closed set of $\frac{1}{2}\text{sector}(V)$.

For simplification, assume that $s \neq t$; the case $s = t$ is trivial. Denote

$$\begin{aligned} \epsilon_V^{(1)} &= \text{the union of } \{u \oplus u' \mid (u, u') \in \Delta_V, u \text{ is not chasing } u', \text{ and } u = v_s\}, \\ \epsilon_V^{(2)} &= \text{the union of } \{u \oplus u' \mid (u, u') \in \Delta_V, u \text{ is not chasing } u', \text{ and } u' = v_{t+1}\}. \end{aligned}$$

Because $e_s \preceq e_t$, when $(u, u') \in \Delta_V$ and u is not chasing u' , either $u = v_s$ or $u' = v_{t+1}$. Therefore, $\epsilon_V = \epsilon_V^{(1)} \cup \epsilon_V^{(2)}$. In addition, we point out the following obvious facts.

- (I) $\epsilon_V^{(1)} \subseteq \alpha$, where α denotes the unique route that terminates at the midpoint of e_s .
- (II) $\epsilon_V^{(2)} \subseteq \beta$, where β denotes the unique route that terminates at the midpoint of e_t .

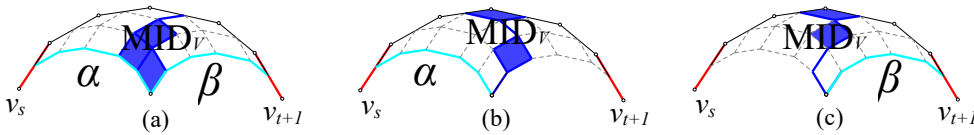


Figure 31: mid_V is the closed set of $\frac{1}{2}\text{sector}(V)$.

Next, we discuss three different cases.

Case 1: $Z_s^t = V$. See Figure 31 (a). In this case, by the definition of mid_V , for any subregion R of $\alpha \cup \beta$, the closed set of $\text{mid}_V - R$ equals mid_V . In particular, ϵ_V is a subset of $\alpha \cup \beta$ by (I) and (II), so the closed set of $\text{mid}_V - \epsilon_V$ (i.e. the closed set of $\frac{1}{2}\text{sector}(V)$) is mid_V .

Case 2: $Z_s^t <_\rho V$. By Fact 15.1, $e_s \prec e_{t+1}$. So every unit in $[v_s \circlearrowleft v_{t-1}]$ beside v_s is chasing v_{t+1} . (v_s may be chasing or not.) So, $\epsilon_V^{(2)} \subseteq \epsilon_V^{(1)}$. So, $\epsilon_V = \epsilon_V^{(1)} \cup \epsilon_V^{(2)} = \epsilon_V^{(1)} \subseteq \alpha$. Therefore, the closed set of $\text{mid}_V - \epsilon_V$ (i.e. the closed set of $\frac{1}{2}\text{sector}(V)$) is mid_V . See Figure 31 (b).

Case 3: $V <_\rho Z_s^t$. This case is symmetric to Case 2. See Figure 31 (c). We omit its proof. □

Recall that the 2-scaling of $\mathcal{L}_V, \mathcal{R}_V, \text{mid}_V$ with respect to V are respectively defined to be $\mathcal{L}_V^*, \mathcal{R}_V^*, \text{mid}_V^*$. In Figure 4, the red and blue curves indicate $\mathcal{L}_{v_1}^*, \dots, \mathcal{L}_{v_n}^*$ and $\mathcal{R}_{v_1}^*, \dots, \mathcal{R}_{v_n}^*$ respectively.

Since $\mathcal{L}_V, \mathcal{R}_V$ are boundaries of mid_V , curves $\mathcal{L}_V^*, \mathcal{R}_V^*$ are boundaries of mid_V^* . Further by Lemma 10, $\mathcal{L}_V^*, \mathcal{R}_V^*$ are boundaries of $\text{sector}(V)$. To prove the SECTOR-CONTINUITY, we prove the following enhanced lemma.

Lemma 11. *If the common starting point of $\mathcal{L}_V^*, \mathcal{R}_V^*$ lies in P , then, \mathcal{L}_V^* has a unique intersecting point with ∂P and so does \mathcal{R}_V^* and $\text{sector}(V) \cap \partial P$ is a boundary-portion from $\mathcal{L}_V^* \cap \partial P$ to $\mathcal{R}_V^* \cap \partial P$. (This does not mean $\text{sector}(V) \cap \partial P = [\mathcal{L}_V^* \cap \partial P \cup \mathcal{R}_V^* \cap \partial P]$; endpoints may not be contained.) Otherwise, $\text{sector}(V) \cap \partial P$ is empty.*

Proof. Recall the roads and routes in section 3. For each road or route, call its 2-scaling with respect to V a *scaled-road* or *scaled-route*. Assume that each scaled-road (or scaled-route) has the same direction as its corresponding unscaled road (or route). We have two observations:

- (i) The 2-scaling of $[v_s \cup v_{t+1}]$ with respect to V lies in the exterior of P .
- (ii) If we travel along a given scaled-route, we eventually get outside P and never return to P since then. Therefore, there is exactly one intersection between this scaled-route and ∂P if its starting point lies inside P ; and no intersection otherwise.

Proof of (i): This observation follows from the relation $V \notin [v_s \cup v_{t+1}]$ stated in Fact 12.

Proof of (ii): Because all of the routes terminate at $[v_s \cup v_{t+1}]$, the scaled-routes terminate at the 2-scaling of $[v_s \cup v_{t+1}]$ with respect to V . Further by observation (i), the scaled-routes terminate at the exterior of P . Therefore, we will eventually get outside P traveling along any scaled-route. Moreover, any road $e_i \oplus v_j$ where $(e_i, v_j) \in \Delta_V$ has a property that we do not return to P from outside P traveling along the 2-scaling of $e_i \oplus v_j$. This follows from observations (ii.1) and (ii.2) below. The roads in $\{v_i \oplus e_j \mid (v_i, e_j) \in \Delta_V\}$ also have this property due to similar reasons. Further since the scaled-routes consist of these scaled-roads, we obtain observation (ii).

- (ii.1) The 2-scaling of $e_i \oplus v_j$ with respect to V is a translation of e_i that lies on the right of $\overrightarrow{v_{t+1}v_i}$. (Regard that the translation of e_i has the same direction as e_i .)
- (ii.2) When we travel along a translation of e_i that lies on the right of $\overrightarrow{v_{t+1}v_i}$, we will not go into P from outside P .

Proof of (ii.1): $e_i \oplus v_j$ lies on the right of $\overrightarrow{v_{t+1}v_i}$, whereas V lies on its left; thus we get observation (ii.1).

Proof of (ii.2): Since $e_s \preceq e_t$ and $(e_i, v_j) \in \Delta_V$, we get $e_i \prec e_t$, which implies observation (ii.2).

Let S_V^* denote the common starting point of all scaled-routes (including \mathcal{L}_V^* and \mathcal{R}_V^*). Equivalently, S_V^* is the 2-scaling of $v_s \oplus v_{t+1}$ with respect to V . The following observation follows from observations (i) and (ii).

- (iii) If S_V^* lies in P , then $\text{mid}_V^* \cap \partial P = [\mathcal{L}_V^* \cap \partial P \cup \mathcal{R}_V^* \cap \partial P]$; otherwise $\text{mid}_V^* \cap \partial P$ is empty.

Proof of (iii): When S_V^* lies outside P , by (i) and (ii), all the boundaries that bound mid_V^* , including $\mathcal{L}_V^*, \mathcal{R}_V^*$ and a fraction of the 2-scaling of $[v_s \cup v_{t+1}]$ with respect to V , lie in the exterior of P . Therefore mid_V^* lies in the exterior of P , which implies that $\text{mid}_V^* \cap \partial P$ is empty. When S_V^* lies in P , the boundaries of mid_V^* have exactly two intersections with ∂P . Therefore, $\text{mid}_V^* \cap \partial P$ either equals $[\mathcal{L}_V^* \cap \partial P \cup \mathcal{R}_V^* \cap \partial P]$, or equals $[\mathcal{R}_V^* \cap \partial P \cup \mathcal{L}_V^* \cap \partial P]$. We argue that it does not equal the latter one. Notice that region mid_V^* is always on our right side when we travel along \mathcal{L}_V^* . This implies that $\text{mid}_V^* \cap \partial P \neq [\mathcal{R}_V^* \cap \partial P \cup \mathcal{L}_V^* \cap \partial P]$.

At last, we can see this lemma easily follows from observation (iii) together with Lemma 10. □

7 Computation – answer the location queries mentioned in Theorem 2

Outline. Assume V is a vertex.

1. Compute the two endpoints of $\text{sector}(V) \cap \partial P$. (see subsection 7.1)
2. Compute the (set of) units intersected by $\text{sector}(V)$. (see subsection 7.2)
3. Compute w such that $\text{sector}(W)$ contains V . (also see subsection 7.2)
4. Compute u, u' such that $\text{block}(u, u')$ contains V . (see the last two subsections)

Hint. Parts 1 and 4 (especially, part 4) are more nontrivial than parts 2 and 3. We suggest that the reader skipping subsection 7.2 for the first read. (Moreover, notice that part 1 and part 4 are highly **symmetric**; see Remark 5.)

Lemma 12 (Lemma 7 of [3]; Computational aspect of the Z -points).

1. For (e_i, e_j) in which $e_i \prec e_j$, point Z_i^j can be computed in $O(1)$ time given the unit containing this point.
2. Given i, j, k such that $e_i \prec e_j$ and $v_k \in (v_{j+1} \cup v_i)$. There are three possibilities of Z_i^j (due to Fact 2): (i) it equals v_k ; (ii) it lies in $(v_{j+1} \cup v_k)$; or (iii) it lies in $(v_k \cup v_i)$. We can distinguish them in $O(1)$ time.
3. Given edge pairs $(a_1, b_1), \dots, (a_m, b_m)$ such that $a_i \prec b_i$ ($1 \leq i \leq m$) and that a_1, \dots, a_m lie in clockwise order and b_1, \dots, b_m lie in clockwise order, we can compute $Z_{a_1}^{b_1}, \dots, Z_{a_m}^{b_m}$ altogether in $O(m+n)$ time.

7.1 Compute the two endpoints of $\text{sector}(V) \cap \partial P$

Assume the reader is familiar with the notations and results given in subsection 6.2. Especially, recall \leq_V , smallest and largest (with respect to \leq_V), s and t , and the marks ‘-/+/0’ of the regions $u \oplus u' \mid (u, u') \in \Delta_V$.

By Lemma 11, computing the endpoints of $\text{sector}(V) \cap \partial P$ means computing $\mathcal{L}_V^* \cap \partial P$ and $\mathcal{R}_V^* \cap \partial P$. In the following we show how do we compute $\mathcal{L}_V^* \cap \partial P$; computing $\mathcal{R}_V^* \cap \partial P$ is symmetric and is omitted.

Briefly, we shall find the segment piece of \mathcal{L}_V^* that intersects ∂P by a binary search, as outlined in section 3.

An explicit definition for \mathcal{L}_V . To describe our algorithm, we need an explicit definition of \mathcal{L}_V as follows.

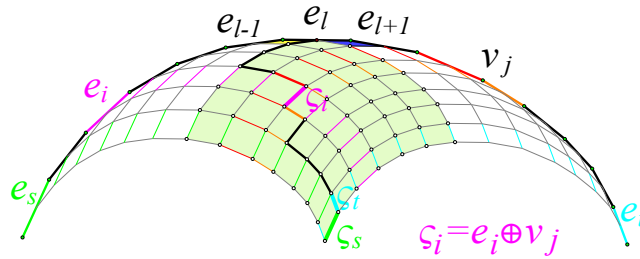


Figure 32: Notations used in the algorithm for computing $\mathcal{L}_V^* \cap \partial P$.

We first introduce an edge e_l . See Figure 32. It is defined as the unique edge in $[v_s \cup v_{t+1}]$ such that

- I For e_i such that $e_s \leq_V e_i \leq_V e_{l-1}$, region $e_i \oplus e_{i+1}$ is marked by ‘-’.
- II For e_i such that $e_l \leq_V e_i \leq_V e_{t-1}$, region $e_i \oplus e_{i+1}$ is marked by ‘+/0’.

Since \mathcal{L}_V divides the regions marked by ‘-’ from those marked by ‘+/0’, it terminates at the midpoint of e_l .

We then introduce two types of roads.

A-type roads. For any edge e_i in $[v_s \odot v_l]$, let e_j denote the smallest edge in $[v_{l+1} \odot v_{t+1}]$ such that $e_i \oplus e_j$ is marked by ‘0/+’ (or denote $e_j = e_{t+1}$ if no such edge exists); define $\varsigma_i = e_i \oplus e_j$ and call it an *A-type road*.

B-type roads. For any edge e_j in $[v_{l+1} \odot v_{t+1}]$, let e_i denote the smallest edge in $[v_s \odot v_l]$ such that $e_i \oplus e_j$ is marked by ‘0/+’ (or denote $e_i = e_l$ if no such edge exists); define $\varsigma_j = v_i \oplus e_j$ and call it a *B-type road*.

Explicitly, \mathcal{L}_V can be defined as the route that consists of all the A-type and B-type roads.

The following observations of these A-type and B-type roads are obvious.

A *The order of the A-type roads in \mathcal{L}_V is determined, and equals to $\varsigma_s, \varsigma_{s+1}, \dots, \varsigma_{l-1}$.*

B *The order of the B-type roads in \mathcal{L}_V is determined, and equals to $\varsigma_t, \varsigma_{t-1}, \dots, \varsigma_{l+1}$.*

Lemma 13. 1. *We can compute s, t, l in $O(\log n)$ time.*

2. *When ς_i is defined (in other words, e_i lies in $[v_s \odot v_{t+1}]$ and $e_i \neq e_l$), we can compute the endpoints of ς_i in $O(\log n)$ time. Moreover, we can distinguish the following in $O(\log n)$ time: ς_i^* intersects ∂P , or ς_i^* lies in the interior of P , or ς_i^* lies in the exterior of P , where ς_i^* denotes the 2-scaling of ς_i with respect to V .*

3. *Recall that S_V^* denotes the starting point of \mathcal{L}_V^* . We can compute S_V^* in $O(1)$ time. Moreover, if S_V^* lies in P , we can compute $\mathcal{L}_V^* \cap \partial P$ in $O(\log^2 n)$ time.*

Proof. 1. First, we show how do we compute s ; the value of t can be computed symmetrically.

We need two facts. (The first one is Fact 14 part (1).)

(i) *For every edge e_i , it holds that $e_s \leq_V e_i$ if and only if ω_i^+ contains V .*

(ii) *Given an edge e_i , we can determine whether ω_i^+ contains V in $O(1)$ time.*

Proof of (ii). To determine whether ω_i^+ contains V is to determine the relation between Z_i^j and V , where $e_j = \text{back}(D_i)$, which can be determined in $O(1)$ time by Lemma 12 part 2.

Applying facts (i) and (ii), s can be determined in $O(\log n)$ time by a binary search.

Next, we show how to compute l . By Lemma 12, we can determine whether $e_i \oplus e_{i+1}$ is marked by ‘-’, ‘0’, or ‘+’ in $O(1)$ time. So, based on properties I and II stated above, we can compute l in $O(\log n)$ time by a binary search.

2. First, we show how do we compute road ς_i . Assume that $e_s \leq_V e_i \leq_V e_{l-1}$; otherwise $e_{l+1} \leq_V e_i \leq_V e_t$ and it is symmetric. It reduces to finding the edge e_j defined in the paragraph ‘‘A-type roads’’ above. According to the bi-monotonicity of the Z -points (Fact 1), e_j is the unique edge such that $e_i \oplus e_{j-1}$ is marked by ‘-’ while $e_i \oplus e_j$ is marked by ‘+0’. As we can compute each mark in $O(1)$ time, we can search j in $O(\log n)$ time.

After computing ς_i , we easily obtain ς_i^* . We then distinguish the relation between ς_i^* and ∂P . First, compute whether the endpoints of ς_i^* lie in P , which takes only $O(\log n)$ time because P is convex. If both the endpoints lie in P , segment ς_i^* lies in P ; if both lie outside P , segment ς_i^* lies outside P ; otherwise, ς_i^* intersects ∂P .

3. Finally, we show how do we compute the (potential) intersecting point $\mathcal{L}_V^* \cap \partial P$.

Since \mathcal{L}_V starts at $(v_s + v_{t+1})/2$, point S_V^* is at the 2-scaling of $(v_s + v_{t+1})/2$ with respect to V , which can be computed in $O(1)$ time. Now, assume S_V^* lies in P , so \mathcal{L}_V^* has one intersection with ∂P .

We design two *subroutines*: one assumes that there is an A-type road whose 2-scaling (with respect to V) intersects ∂P , and it seeks for this road. The other is symmetric. It assumes there is a B-type road whose 2-scaling (with respect to V) intersects ∂P and seeks for this road. Clearly, one subroutine would success.

According to observations A and B stated above, the A-type roads $\varsigma_s, \varsigma_{s+1}, \dots, \varsigma_{l-1}$ are in order on \mathcal{L}_V ; so do the B-type roads. So, a binary search can be applied in designing our two subroutines. Each searching step costs $O(\log n)$ time due to part 2 of this lemma; hence the total running time is $O(\log^2 n)$. \square

7.2 Which units does $\text{sector}(V)$ intersect & which sector does V lie in?

Assuming the endpoints of $\text{sector}(V) \cap \partial P$ are known for each vertex V , we now proceed to compute the interval of units that intersect $\text{sector}(V)$ and the (unique) sector that contains V for each vertex V .

Compute the units that intersect $\text{sector}(V)$. Let $u_L = \mathbf{u}(\mathcal{L}_V^* \cap \partial P)$ and $u_R = \mathbf{u}(\mathcal{R}_V^* \cap \partial P)$. They can be computed while we compute the two endpoints of $\text{sector}(V) \cap \partial P$. In most cases the units that intersect $\text{sector}(V)$ are the units (in clockwise) from u_L to u_R . Exceptional cases are discussed in the following note.

Note 3. Sometimes an endpoint of $\text{sector}(V) \cap \partial P$ is not contained in the sector. This is because $\text{sector}(V)$ is not always a closed set (see Lemmas 10 and 11). Under a degenerate case, this endpoint may happen to lie at a vertex V^* of P , and then, by definition, we could not include V^* into the set of units that intersect $\text{sector}(V)$.

Compute the sector that contains V for each vertex V by a sweeping algorithm.

Recall the event-points and their two types of tags mentioned in section 3. We have two groups of *event-points*. One group contains the points in $\{\mathcal{L}_V^* \cap \partial P, \mathcal{R}_V^* \cap \partial P\}$; and the other contains the intersecting points between σP and ∂P , namely, the K -points (recall the K -points in subsection 6.1). Notice that all the event-points lie in ∂P .

Below we show how to define our event-points and their tags precisely. We use two procedures – an adding and a removing procedure. The removing procedure removes redundant event-points added in the first procedure.

Adding procedure. See Figure 33. The left picture exhibits the event-points in Group 1 defined below; the middle one exhibits the event-points in Group 2 defined below.

Group 1: For every vertex V for which $\text{sector}(V)$ intersects ∂P , add two event-points $\mathcal{L}_V^* \cap \partial P$ and $\mathcal{R}_V^* \cap \partial P$, and define

$$\begin{aligned} \text{Current}(\mathcal{L}_V^* \cap \partial P) &= V, & \text{Future}(\mathcal{L}_V^* \cap \partial P) &= V, \\ \text{Current}(\mathcal{R}_V^* \cap \partial P) &= V, & \text{Future}(\mathcal{R}_V^* \cap \partial P) &= \text{forw}(V). \end{aligned} \quad (27)$$

Group 2: For every $K_i \in \sigma P \cap \partial P$, add event-point K_i . Notice that σP consists of several directional line segments. Assume K_i comes from directional line segment \overrightarrow{AB} of σP . Recall g in Definition 5. Define

$$\text{Current}(K_i) = \#, \quad \text{Future}(K_i) = \begin{cases} \#, & \text{when } A \in P, B \notin P; \\ \mathbf{u}(g(K_i)), & \text{when } A \notin P, B \in P. \end{cases} \quad (28)$$

Note: The special symbol $\#$ is introduced for indicating the outside of $f(\mathcal{T})$. When $\text{Current}(E) = \#$, no sector contains event-point E . When $\text{Future}(E) = \#$, no sector contains $(E \circlearrowleft E')$, where E' denotes the clockwise next event-point of E . The reason that $\text{Current}(K_i)$ should be $\#$ is explained in Fact 11.

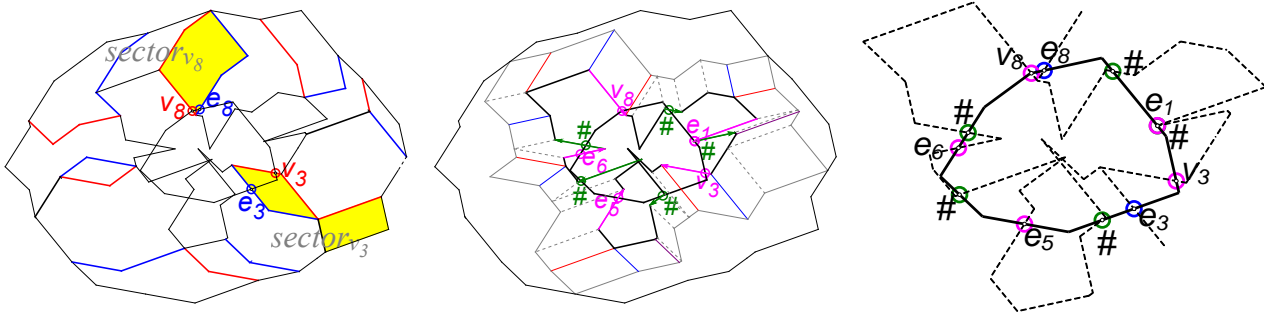


Figure 33: Definition of the *event-points*. Their *future-tags* are labeled in the figure.

Removing procedure. If there are multiple event-points locating at the same position, we keep only one of them according to the following priority: First, $\{\sigma P \cap \partial P\}$. Then, $\{\mathcal{R}_V^* \cap \partial P\}$. Last, $\{\mathcal{L}_V^* \cap \partial P\}$

As a consequence of the SECTOR-MONOTONICITY and INTERLEAVITY-OF- f , we get:

Corollary 1. *Take any point X in ∂P . If X lies at some event-point E , it belongs to $\text{sector}(\text{Current}(E))$. Otherwise, it belongs to $\text{sector}(\text{Future}(E^*))$, where E^* is the closest event-point preceding X in clockwise order.*

Note: X belongs to no sector when we say it belongs to $\text{sector}(\#)$.

Our algorithm is as follows. 1. ADD: Find all the event-points and compute their tags. 2. SORT: Sort these points in clockwise order. 3. REMOVE: Remove the redundant event-points. 4. SWEEP: For each vertex, compute the closest event-point preceding it (in clockwise) and then compute the sector containing it by applying Corollary 1.

The event-points from Group 1 and their tags can be computed efficiently as shown in subsection 7.1. In the following we show how to compute the event-points from Group 2 and compute their tags.

Lemma 14. *The polygonal curve σP consists of $O(n)$ sides and can be computed in $O(n)$ time. The points in $\sigma P \cap \partial P$ are of size $O(n)$ and can be computed in $O(n \log n)$ time. Moreover, the future-tag of each such point can be computed in $O(1)$ amortized time. (The current tags of these event-points are trivially '#'; see (28)).*

Proof. Recall frontier-pair-list and bottom borders in subsection 2.1. Proving that σP is of size $O(n)$ (namely, the bottom borders have in total $O(n)$ sides) reduces to showing that (i) the bottom borders of blocks in $\{\text{block}(u, u') \mid (u, u') \in \text{frontier-pair-list}, u, u' \text{ are both edges}\}$ have in total $O(n)$ sides, and (ii) the bottom borders of blocks in $\{\text{block}(u, u') \mid (u, u') \in \text{frontier-pair-list}, \text{at least one of } u, u' \text{ is a vertex}\}$ have in total $O(n)$ sides.

Proof of (i): Clearly, the frontier-pair-list contains $O(n)$ unit pairs, and the bottom border of $\text{block}(u, u')$ has at most two sides when u, u' are both edges. Therefore, we obtain (i).

Proof of (ii): Let $(u_1, u'_1), \dots, (u_m, u'_m)$ denote the sublist of the frontier-pair-list that contains all of the edge pairs. Let $Z_i = Z_{u_i}^{u'_i}$ for short. Combining the following two observations, we obtain (ii). 1. For any two neighboring edge pairs, e.g. (u_i, u'_i) and (u_{i+1}, u'_{i+1}) , there is another unit pair (denoted by u, u') in the frontier-pair-list between (u_i, u'_i) and (u_{i+1}, u'_{i+1}) (see Figure 8 (b)), and the bottom border of $\text{block}(u, u')$ is exactly the reflection of $[Z_i \circlearrowleft Z_{i+1}]$. 2. Boundary-portions $[Z_1 \circlearrowleft Z_2], \dots, [Z_m \circlearrowleft Z_1]$ form a partition of ∂P . This is because Z_1, \dots, Z_m lie in clockwise order ∂P , which is due to the bi-monotonicity of the Z -points (Fact 1), as shown in Figure 8 (c).

Next, we show that σP can be computed in $O(n)$ time. We compute σP in three steps; each costs $O(n)$ time. (Step 1) Compute the frontier-pair-list by Algorithm 1. (Step 2) Compute Z_1, \dots, Z_m . This cost $O(n + m) = O(n)$ time by Lemma 12 part 3 since they lie in clockwise order. (Step 3) Construct each side in the bottom border of each frontier block. Each side can be constructed in $O(1)$ time according to the definition of bottom borders.

To compute $\sigma P \cap \partial P$, we can try each side of σP and compute its intersection with ∂P . According to the common computational geometric result, by $O(n)$ time preprocessing, the intersection between a segment and the boundary of a fixed convex polygon P can be computed in $O(\log n)$ time. Thus, this takes $O(n \log n)$ time.

To compute the future-tag of each intersection K_i in $\sigma P \cap \partial P$ reduces to computing $\mathbf{u}(g(K_i))$, due to (28). Notice that (1) $\mathbf{u}(g(\cdot))$ has the property that it is identical within any side of σP (by the definition of g), and (2) while computing σP , we can compute the value of $\mathbf{u}(g(\cdot))$ for each side of σP . Therefore, by sweeping around σP , we can compute $\mathbf{u}(g(K_i))$ for all the intersections K_i in $\sigma P \cap \partial P$ in linear time. \square

Running time analysis of the sweeping algorithm. The ADD step requires $O(n \log^2 n)$ time for Group 1 (as shown in subsection 7.1), and $O(n \log n)$ time for Group 2 (by Lemma 14). Also according to Lemma 14, there are in total $O(n)$ event-points. So the SORT step runs in $O(n \log n)$ time (or even in $O(n)$ time). The REMOVE and SWEEP steps are trivial and they cost $O(n)$ time. Therefore, the algorithm runs in $O(n \log^2 n)$ time.

Remark 6. There is an $O(n)$ time algorithm for computing $\sigma P \cap \partial P$, improving the one given in the proof of Lemma 14. We sketch it in the following. Initially, choose a pair of edges, one from σP and one from ∂P . In each iteration, compute their intersection and change one edge to its clockwise next one. The selection of edge-to-change follows a specific (and involved) rule. We can prove that, by selecting good initial edges and rule, the algorithm does not miss any intersection in $\sigma P \cap \partial P$. The analysis is complicated. So we do not present it in detail.

7.3 Two delimiting edges e_{p_V}, e_{q_V} for block locating

Fix V to be a vertex. Let $\text{block}(u_1^*, u_2^*)$ denote the block containing V . Recall section 3 for a sketch on how do we compute (u_1^*, u_2^*) . It mentioned that we have to find two **delimiting edges** e_{p_V}, e_{q_V} so that

$$e_p \prec e_q. \text{ Moreover, } (v_p \circlearrowleft v_{q+1}) \text{ contains } V. \quad (29)$$

$$u_1^* \in [v_p \circlearrowleft V), \text{ and } u_2^* \in (V \circlearrowleft v_{q+1}]. \quad (30)$$

This subsection shows how to find (e_{p_V}, e_{q_V}) satisfying (29) and (30) by utilizing the bounding-quadrants of the blocks. Although it is rather short, this subsection contains the most important ideas for proving Theorem 2.

Assume $V = v_i$ henceforth for convenience. Denote

$$\nabla_V := \{(u, u') \mid \text{unit } u \text{ is chasing unit } u', u \in (D_i \circlearrowleft V), u' \in (V \circlearrowleft D_{i-1})\}. \quad (31)$$

Fact 16. $(u_1^*, u_2^*) \in \nabla_V$.

Proof. By the definition of ∇_V , it reduces to proving that $u_1^* \in (D_i \circlearrowleft V)$ while $u_2^* \in (V \circlearrowleft D_{i-1})$.

Let $e_a = \text{forw}(u_1^*), e_{a'} = \text{back}(u_2^*)$. Since u_1^* is chasing u_2^* , we have $e_a \preceq e_{a'}$. By Lemma 4, $V \in \text{block}(u_1^*, u_2^*) \subset \text{quad}_{u_1^*}^{u_2^*} = \text{quad}_a^{a'} \subseteq \text{hp}_a^{a'}$, hence $V = v_i \in (v_a \circlearrowleft v_{a'+1})$. Together, $e_a \prec e_i$ and $e_{i-1} \prec e_{a'}$.

Since $e_a \prec e_i, e_a \in (D_i \circlearrowleft V)$, i.e. $\text{forw}(u_1^*) \in (D_i \circlearrowleft V)$. So, $u_1^* \in [D_i \circlearrowleft V)$.

Since $e_{i-1} \prec e_{a'}, e_{a'} \in (V \circlearrowleft D_{i-1})$, i.e. $\text{back}(u_2^*) \in (V \circlearrowleft D_{i-1})$. So, $u_2^* \in (V \circlearrowleft D_{i-1}]$.

In the following we further argue that $u_1^* \neq D_i$ and $u_2^* \neq D_{i-1}$. Because $e_{a'} \in (V \circlearrowleft D_{i-1})$, it also lies in $(V \circlearrowleft D_i)$. So, $e_{a'} \preceq \text{back}(D_i)$. Therefore, $\text{back}(D_i) \not\prec e_{a'}$, i.e. $\text{back}(D_i) \not\prec \text{back}(u_2^*)$. Therefore, D_i is not chasing u_2^* . This means that $u_1^* \neq D_i$ because u_1^* must be chasing u_2^* . Symmetrically, $u_2^* \neq D_{i-1}$. \square

Following the definition of chasing and due to the definition of ∇_V , all elements (u, u') in ∇_V constitute into a ‘‘staircase’’ structure when they are filled into a 2-dimensional matrix (as shown in Figure 34 (b)), where elements with the same u are in the same row and rows are sorted from top to bottom according to the clockwise order of u , whereas elements with the same u' are in the same column and columns are sorted from right to left according to the clockwise order of u' . See also Figure 34 (c) for an illustration of the ‘‘staircase’’ structure.

We define the ‘‘corners of this staircase’’ as the corner pairs. Formally, $(e_x, e_{x'})$ in ∇_V is a **corner pair**, if neither $(e_{x-1}, e_{x'})$ nor $(e_x, e_{x'+1})$ belongs to ∇_V . (This concept is similar to extremal pair introduced in Definition 7.) Denote by $\text{CP}_1, \dots, \text{CP}_k$ the corner pairs, which are sorted so that CP_1 is at topmost and CP_k at leftmost.

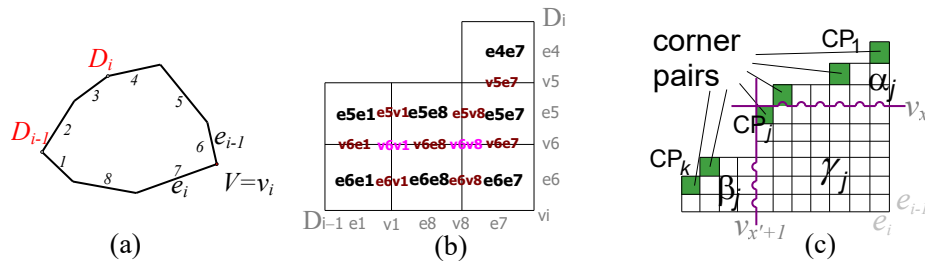


Figure 34: An illustration of set ∇_V and its corner pairs.

As demonstrated below, we are going to pick a corner pair of ∇_V to be (e_p, e_q) . The exact definition of p, q relies on an interesting observation of ∇_V (Fact 17 below). We need some notations.

Subsets $\alpha_j, \beta_j, \gamma_j$ of ∇_V . Consider $CP_j = (e_x, e_{x'})$. If we cut ∇_V along the horizontal line corresponding to v_x and the vertical line corresponding to $v_{x'+1}$, we get three chunks; the unit pairs in the top chunk are in α_j ; those in the left chunk are in β_j ; and the rest form a rectangular shape and they are in γ_j . Formally,

$$\alpha_j = \{(u, u') \in \nabla_V \mid u \text{ lies in } (D_i \circ v_x)\},$$

$$\beta_j = \{(u, u') \in \nabla_V \mid u' \text{ lies in } (v_{x'+1} \circ D_{i-1})\},$$

$$\gamma_j = \{(u, u') \in \nabla_V \mid u \text{ lies in } [v_x \circ V], u' \text{ lies in } (V \circ v_{x'+1})\}.$$

See the illustration of subsets α_j, β_j and γ_j in Figure 34 (c). For convenience, denote $\alpha_{k+1} = \nabla_V$.

Recall $\langle \text{quad} \rangle_u^{u'}$ in Definition 6. For any subset S of ∇_V , denote $\langle \text{quad} \rangle[S] = \bigcup_{(u, u') \in S} \langle \text{quad} \rangle_u^{u'}$.

Fact 17. $\langle \text{quad} \rangle[\alpha_{j+1}] \cap \langle \text{quad} \rangle[\beta_j] = \emptyset$ ($1 \leq j \leq k$).

Before proving Fact 17, we state explicit formulas for $\langle \text{quad} \rangle[\alpha_j]$ and $\langle \text{quad} \rangle[\beta_j]$. Let a_j, b_j ($1 < j \leq k$) respectively denote the edge pairs at the upper right and lower left corners of α_j ; Let c_j, d_j ($1 \leq j < k$) respectively denote the edge pairs at the upper right and lower left corners of β_j ; see Figure 35 (a). Recall that $\rho.s$ and $\rho.t$ denote the starting and terminal point of boundary-portion ρ . Applying the monotonicity of $\langle \text{quad} \rangle$ (Lemma 7), we have

$$\langle \text{quad} \rangle[\alpha_j] = (\langle \text{quad} \rangle[a_j].s \circ \langle \text{quad} \rangle[b_j].t), \text{ for any } 1 < j \leq k. \quad (32)$$

$$\langle \text{quad} \rangle[\beta_j] = (\langle \text{quad} \rangle[c_j].s \circ \langle \text{quad} \rangle[d_j].t), \text{ for any } 1 \leq j < k. \quad (33)$$

Proof of Fact 17. When $j = k$, set β_j is empty and the equation is trivial.

Next, we assume that $j < k$. We state the following observations.

$$\langle \text{quad} \rangle[a_{j+1}].s, \langle \text{quad} \rangle[b_{j+1}].s, \langle \text{quad} \rangle[c_j].s, \langle \text{quad} \rangle[d_j].s \text{ lie in clockwise order.} \quad (34)$$

$$\langle \text{quad} \rangle[a_{j+1}].t, \langle \text{quad} \rangle[b_{j+1}].t, \langle \text{quad} \rangle[c_j].t, \langle \text{quad} \rangle[d_j].t \text{ lie in clockwise order.} \quad (35)$$

$$\langle \text{quad} \rangle[a_{j+1}] \text{ has no overlap with } \langle \text{quad} \rangle[d_j]. \quad (36)$$

$$\langle \text{quad} \rangle[b_{j+1}] \text{ has no overlap with } \langle \text{quad} \rangle[c_j]. \quad (37)$$

Proof: The first two facts follow from the monotonicity of $\langle \text{quad} \rangle$; the proof of (36) is given in the following; the proof of (37) is similar to that of (36) and omitted. Recall $V = v_i$. Notice that $a_{j+1} = (\text{forw}(D_i), e_i)$ and $d_j = (e_{i-1}, \text{back}(D_{i-1}))$. Observing that edges $\text{forw}(D_i), e_i, e_{i-1}, \text{back}(D_{i-1})$ do not lie in any inferior portion, applying the peculiarity of the bounding-quadrants (Lemma 6), $\text{quad}_{\text{forw}(D_i)}^i \cap \text{quad}_{i-1}^{\text{back}(D_{i-1})}$ lie in the interior of P . So, $\text{quad}_{\text{forw}(D_i)}^i \cap \partial P$ is disjoint with $\text{quad}_{i-1}^{\text{back}(D_{i-1})} \cap \partial P$. This further implies (36).

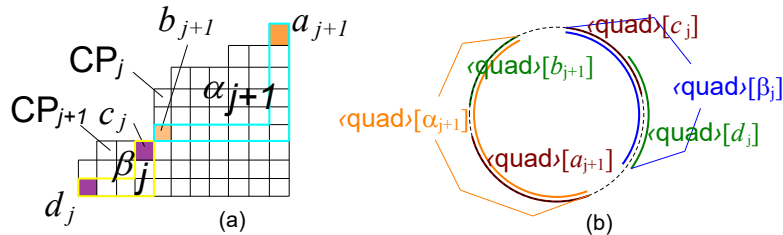


Figure 35: Illustration of the proof of Fact 17.

See Figure 35 (b). Combining the observations, $\langle \text{quad} \rangle[a_{j+1}].s$, $\langle \text{quad} \rangle[b_{j+1}].s$, $\langle \text{quad} \rangle[b_{j+1}].t$, $\langle \text{quad} \rangle[c_j].s$, $\langle \text{quad} \rangle[d_j].s$, $\langle \text{quad} \rangle[d_j].t$ lie in clockwise order around ∂P . In particular, points $\langle \text{quad} \rangle[a_{j+1}].s$, $\langle \text{quad} \rangle[b_{j+1}].t$, $\langle \text{quad} \rangle[c_j].s$, $\langle \text{quad} \rangle[d_j].t$ lie in clockwise order around ∂P . So $(\langle \text{quad} \rangle[a_{j+1}].s \circ \langle \text{quad} \rangle[b_{j+1}].t)$ is disjoint with $(\langle \text{quad} \rangle[c_j].s \circ \langle \text{quad} \rangle[d_j].t)$. Further, by (32) and (33), $\langle \text{quad} \rangle[a_{j+1}]$ is disjoint with $\langle \text{quad} \rangle[\beta_j]$. \square

We state a trivial fact before showing the definition of p_V and q_V .

(i) If (u_1^*, u_2^*) belongs to some set S , then $V \in \langle \text{quad} \rangle[S]$.

Proof. $V \in \text{block}(u_1^*, u_2^*) \cap \partial P \subseteq \text{quad}_{u_1^*}^{u_2^*} \cap \partial P \subseteq \langle \text{quad} \rangle_{u_1^*}^{u_2^*} \subseteq \bigcup_{(u, u') \in S} \langle \text{quad} \rangle_u^{u'} = \langle \text{quad} \rangle[S]$. \square

Definition 9 (Delimiting edges e_{p_V} and e_{q_V}). Recall that $(u_1^*, u_2^*) \in \nabla_V$ (see Fact 16). So $V \in \langle \text{quad} \rangle[\nabla_V]$ by fact (i) above. Further, since $\emptyset = \alpha_1 \subset \dots \subset \alpha_{k+1} = \nabla_V$, there must be a unique index in $1, \dots, k$, denoted by h , such that $V \notin \langle \text{quad} \rangle[\alpha_h]$ but $V \in \langle \text{quad} \rangle[\alpha_{h+1}]$. We choose the corner pair CP_h to be (e_{p_V}, e_{q_V}) .

By defining p_V, q_V this way, we can verify that (29) and (30) are satisfied.

Proof of (29). Since $(e_p, e_q) \in \nabla_V$, we get $e_p \prec e_q$ and $V \in (v_p \circ v_{q+1})$ by (31). \square

Proof of (30). By the definition of h , we know $V \notin \langle \text{quad} \rangle[\alpha_h]$ and $V \in \langle \text{quad} \rangle[\alpha_{h+1}]$.

Since $V \notin \langle \text{quad} \rangle[\alpha_h]$, we know $(u_1^*, u_2^*) \notin \alpha_h$ due to fact (i). Since $V \in \langle \text{quad} \rangle[\alpha_{h+1}]$, we get $V \notin \langle \text{quad} \rangle[\beta_h]$ according to Fact 17, which further implies that $(u_1^*, u_2^*) \notin \beta_h$ due to fact (i).

However, by Fact 16, $(u_1^*, u_2^*) \in \nabla_V = \alpha_h \cup \beta_h \cup \gamma_h$. So (u_1^*, u_2^*) must belong to γ_h , i.e. $(u_1^*, u_2^*) \in \{(u, u') \in \nabla_V \mid u \text{ lies in } [v_p \circ V], u' \text{ lies in } (V \circ v_{q+1})\}$. This implies (30). \square

Lemma 15. Given $1 \leq j \leq k$, in $O(1)$ time we can determine whether V lies in $\langle \text{quad} \rangle[\alpha_j]$. As a corollary, we can compute h and thus compute (e_p, e_q) (using definition 9) in $O(\log n)$ time.

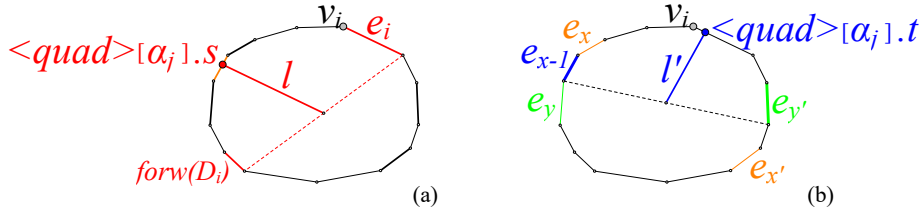


Figure 36: Compute e_p, e_q .

Proof. The case $j = 1$ is trivial since $\langle \text{quad} \rangle[\alpha_j] = \emptyset$. Assume that $j > 1$. Assume $\text{CP}_j = (e_x, e_{x'})$, $\text{CP}_{j-1} = (e_y, e_{y'})$. (We can compute CP_j and CP_{j-1} in $O(1)$ time. Except for the first and last element of CP , the other corner pairs are extremal pairs. Yet we can obtain a list of extremal pairs beforehand and use it to compute CP_j .)

Recall that (i) $\langle \text{quad} \rangle[\alpha_j] = (\langle \text{quad} \rangle[a_j].s \circ \langle \text{quad} \rangle[b_j].t)$, by (32), where a_j, b_j are respectively the edge pairs at the upper right and lower left corners of α_j . Observe that $a_j = (\text{forw}(D_i), e_i)$ and $b_j = (e_{x-1}, e_{y'})$. According to Definition 6, (ii) $\langle \text{quad} \rangle[a_j].s$ is at the intersection between l and $[D_i \circ v_{i+1}]$, where l denotes the line at $(D_i + v_{i+1})/2$ parallel to e_i (see Figure 36 (a)), and (iii) $\langle \text{quad} \rangle[b_j].t$ is at the intersection between l' and $[v_{x-1} \circ v_{y'+1}]$, where l' denotes the line at $(v_{x-1} + v_{y'+1})/2$ parallel to e_{x-1} (see Figure 36 (b)). Altogether, $V \in \langle \text{quad} \rangle[\alpha_j]$ if and only if V lies in the open half-plane delimited by l' and containing e_{x-1} . Further, since in $O(1)$ time we can compute l' and find the side of l' that contains V , we can determine whether $V \in \langle \text{quad} \rangle[\alpha_j]$ in $O(1)$ time, as claimed above. \square

7.4 Find the block that contains V

Fix a vertex V . Given w such that $V \in \text{sector}(w)$, and p_V, q_V such that (29) and (30) hold, we now compute (u_1^*, u_2^*) so that $\text{block}(u_1^*, u_2^*)$ contains V . (Unit w and indices p_V, q_V are computed in subsections 7.2 and 7.3.)

Recall the sketch of our algorithm in section 3 and recall the following notations. A unit pair (u, u') in which u is chasing u' is *alive* if $u \in [v_p \circ V)$ and $u' \in (V \circ v_{q+1}]$. Moreover, it is *active* if it is alive and $\zeta(u, u')$ intersects w . Furthermore, for each active pair (u, u') , define $\text{cell}(u, u') := \text{block}(u, u') \cap \text{sector}(w)$ and call it a *cell*.

Fact 18. (u_1^*, u_2^*) is active, and $\text{cell}(u_1^*, u_2^*)$ is the unique cell that contains V .

Proof. We know (u_1^*, u_2^*) is alive due to (30).

Assume $f^{-1}(V) = (X_1, X_2, X_3)$. Because $V \in \text{block}(u_1^*, u_2^*)$, we know $X_3 \in u_1^*$ and $X_1 \in u_2^*$. Because $(X_1, X_2, X_3) \in \mathcal{T}$, point $X_2 \in \zeta(\mathbf{u}(X_3), \mathbf{u}(X_1))$. Together, $X_2 \in \zeta(u_1^*, u_2^*)$. Because $V \in \text{sector}(w)$, we know $X_2 \in w$. Therefore, $\zeta(u_1^*, u_2^*)$ intersects w (at X_2), which means that (u_1^*, u_2^*) is active.

Since $\text{block}(u_1^*, u_2^*)$ and $\text{sector}(w)$ both contain V , their intersection $\text{cell}(u_1^*, u_2^*)$ contains V .

At last, we argue that $\text{cell}(u_1^*, u_2^*)$ is the unique cell that contains V . If, to the opposite, V lies in two distinct cells, it lies in two distinct blocks, which contradicts BLOCK-DISJOINTNESS. \square

By Fact 18, it reduces to finding the cell that contains V . Next, there are two cases, depending on whether w is an edge or a vertex. We first concentrate on the typical case where w is an edge. Assume $w = e_k$.

Outline. We first prove some observations of the cells (e.g., a monotonicity as stated in Fact 21), define those regions called layers, and prove a monotonicity between the layers (Fact 22), and then present our algorithm.

7.4.1 Basic observations

Active edges. An edge e_j in $(v_p \circ V)$ is *active* if there is at least one unit u such that (e_j, u) is active; an edge e_j in $(V \circ v_{q+1})$ is *active* if there is at least one unit u such that (u, e_j) is active.

Fact 19. 1. For $e_j \in (v_p \circ V)$ that is active, the units in $\{u \mid (e_j, u) \text{ is active}\}$ are consecutive. The clockwise first and last such units can be found in $O(\log n)$ time. For $e_j \in (V \circ v_{q+1})$ that is active, the units in $\{u \mid (u, e_j) \text{ is active}\}$ are consecutive. The clockwise first and last such units can be found in $O(\log n)$ time.

2. The active edges in $(v_p \circ V)$ are consecutive. The clockwise first and last such edges can be computed in $O(\log n)$ time. Similarly, the active edges in $(V \circ v_{q+1})$ are consecutive. The clockwise first and last such edges can be computed in $O(\log n)$ time.

Proof. For any edge e_j in $(v_p \circ V)$, denote $b(j) = \begin{cases} q+1 & \text{if } e_j \prec e_{q+1}; \\ q & \text{otherwise.} \end{cases}$ Denote $b = b(j)$ when j is clear.

Assume $V = v_i$. Denote $\Pi_j = (\zeta(e_j, e_i), \zeta(e_j, v_{i+1}), \dots, \zeta(e_j, v_b), \zeta(e_j, e_b))$. We state two observations:

(i) $\Pi_j = (Z_j^i, [Z_j^i \circ Z_j^{i+1}], \dots, [Z_j^{b-1} \circ Z_j^b], Z_j^b)$. (By definition of $\zeta(e_j, u)$)

(ii) Z_j^i, \dots, Z_j^b lie in clockwise order on $\rho = [v_{b+1} \circ v_j]$. (By bi-monotonicity of the Z -points)

Proof of part 1. Assume $e_j \in (v_p \circ V)$; the case where $e_j \in (V \circ v_{q+1})$ is symmetric. By observations (i) and (ii), the elements in Π_j that intersect e_k are consecutive. This simply implies that $U = \{u \mid (e_j, u) \text{ is active}\}$ consists of consecutive units. Computing the first unit in U reduces to computing h such that $Z_j^{h-1} \leq_\rho v_k <_\rho Z_j^h$, which can be computed in $O(\log n)$ time using Lemma 12 and binary search. The last unit in U can be computed similarly.

Proof of part 2. Let π_j be the union of all portions in Π_j , which equals $[Z_j^i \circlearrowleft Z_j^{b(j)}]$ due to observations (i) and (ii). Applying the bi-monotonicity of the Z -points (fact 1), the starting points of π_p, \dots, π_{i-1} lie in clockwise order around ∂P , and so do their terminal points. So, the ones in π_p, \dots, π_{i-1} that intersect e_k are consecutive. This means the active edges in $(v_p \circlearrowleft V)$ are consecutive, since e_j is active if and only if π_j intersects e_k . Computing the first and last active edges in $(v_p \circlearrowleft V)$ reduces to computing the first and last elements in π_p, \dots, π_{i-1} that intersect e_k . By Lemma 12, in $O(1)$ time we can determine whether π_j is contained in $[v_{b(j)+1} \circlearrowleft v_k]$ or in $[v_{k+1} \circlearrowleft v_j]$, or intersects e_k . So, by a binary search, in $O(\log n)$ time we can compute these two edges. \square

Fact 20. *Given an active pair (e_j, u) (or (u, e_j)), region $\text{cell}(e_j, u)$ (or $\text{cell}(u, e_j)$) is a parallelogram with two sides congruent to e_j , and it can be computed in $O(1)$ time.*

Proof. Assume (e_j, u) is active. This means $\zeta(e_j, u)$ intersects with e_k , and

$$\text{cell}(e_j, u) = f(\{(X_1, X_2, X_3) \mid X_1 = u, X_2 \in \zeta(e_j, u) \cap e_k, X_3 \in e_j\}). \quad (38)$$

Case 1: u is an edge, e.g. $u = e_{j'}$. Since $\zeta(e_j, u) = Z_j^{j'}$ and it intersects e_k , point $Z_j^{j'}$ lies in e_k and hence can be computed in $O(1)$ time according to Lemma 12. Then, $\text{cell}(e_j, e_{j'})$ is the 2-scaling of $e_j \oplus e_{j'}$ with respect to $Z_j^{j'}$, which is a parallelogram with two sides congruent to e_j and which can be computed in $O(1)$ time.

Case 2: u is a vertex, e.g. $u = v_{j'}$. First, we argue that $\zeta(e_j, v_{j'})$ is not a single point. Suppose to the opposite that $\zeta(e_j, v_{j'})$ is a single point. Then, its two endpoints $Z_j^{j'-1}, Z_j^{j'}$ must be identical, and must lie in e_k since $\zeta(e_j, v_{j'})$ intersects e_k . However, by Fact 2, when $Z_j^{j'-1}, Z_j^{j'}$ lie in e_k , they lie at $(l_{j,k} + l_{j'-1,k})/2, (l_{j,k} + l_{j',k})/2$, respectively, which do not coincide because $l_{j'-1,k} \neq l_{j',k}$. Contradictory. Following this argument, $\zeta(e_j, u) \cap e_k$ is a segment that is not a single point. Combining this fact with (38), $\text{cell}(e_j, v_{j'})$ is a parallelogram with two sides congruent to e_j . (To see this more clearly, we refer to Figure 7 (c).) Moreover, applying Lemma 12, segment $\zeta(e_j, v_{j'}) \cap e_k$ can be computed in $O(1)$ time, and thus $\text{cell}(e_j, v_{j'})$ can be computed in $O(1)$ time.

The proof of the claim on $\text{cell}(u, e_j)$ is symmetric and omitted. \square

7.4.2 Monotonicity of cells, definition of layers, and monotonicity of layers

Fact 21. *See Figure 15 (a) and (b) for illustrations of the following statements (and see the proof below).*

1. *For e_j in $(v_p \circlearrowleft V)$ that is active, $\text{cell}(e_j, u_s), \dots, \text{cell}(e_j, u_t)$ are contiguous and lie monotonously in the opposite direction of e_k , where u_s, \dots, u_t list the units in $\{u \mid (e_j, u) \text{ is active}\}$ in clockwise order.*
2. *For e_j in $(V \circlearrowleft v_{q+1})$ that is active, $\text{cell}(u_s, e_j), \dots, \text{cell}(u_t, e_j)$ are contiguous and lie monotonously in the opposite direction of e_k , where u_s, \dots, u_t list the units in $\{u \mid (u, e_j) \text{ is active}\}$ in clockwise order.*

Definition 10 (Layers). *See Figure 15 and Figure 37 (b). We define two types of layers.*

- (A) *Let e_j be an active edge in $(v_p \circlearrowleft V)$. Assume $\{u \mid (e_j, u) \text{ is active}\} = \{u_s, \dots, u_t\}$ (in clockwise order). Let body_j denote the region united by regions $\text{cell}(e_j, u_s), \dots, \text{cell}(e_j, u_t)$.*

*Clearly, body_j is a region with two borders congruent to e_j since the cells have borders congruent to e_j (according to Fact 20). By removing these two borders, we can get an extension of body_j which contains two strip regions parallel to e_k . This extension is defined as layer_j and is called an **A-type layer**.*

- (B) *Let e_j be an active edge in $(V \circlearrowleft v_{q+1})$. Assume $\{u \mid (u, e_j) \text{ is active}\} = \{u_s, \dots, u_t\}$ (in clockwise order). Let body_j denote the region united by regions $\text{cell}(u_s, e_j), \dots, \text{cell}(u_t, e_j)$.*

*Clearly, body_j is a region with two borders congruent to e_j since the cells have borders congruent to e_j (according to Fact 20). By removing these two borders, we can get an extension of body_j which contains two strip regions parallel to e_k . This extension is defined as layer_j and is called a **B-type layer**.*

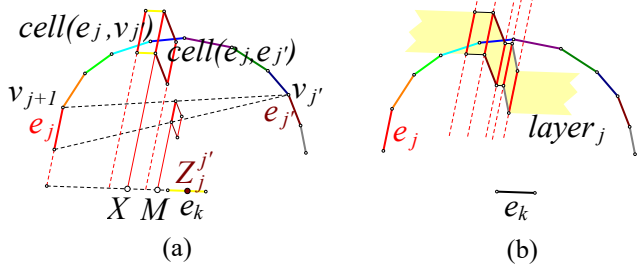


Figure 37: Monotonicity of cells & definition of layers.

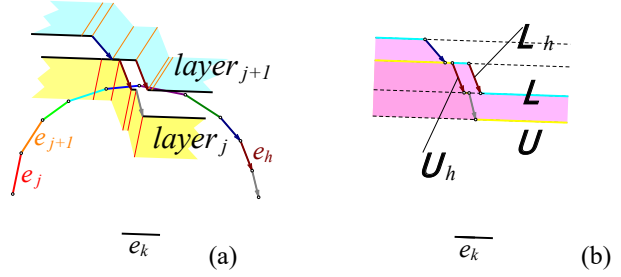


Figure 38: Monotonicity of layers.

Proof of Fact 21. We show how to prove part 1; the proof of part 2 is symmetric and omitted.

See Figure 37 (a). Let us consider the projections of these cells along direction e_j onto ℓ_k , it reduces to proving that these projections are pairwise-disjoint and are arranged in order. Take two incident units in $\{u_s, \dots, u_t\}$, e.g. $v_{j'}$ and $e_{j'}$. (For incident units $e_{j'}, v_{j'+1}$, the proof is similar.) Let M be the projection of $(v_{j+1} + v_{j'})/2$; and X the reflection of $Z_j^{j'}$ with respect to M . We state that the projection of $\text{cell}(e_j, e_{j'})$ terminates at X while the projection of $\text{cell}(e_j, v_{j'})$ starts at X . This follows the definition of cells. More details are trivial and omitted. \square

Fact 22. (1) All the layers lie in the closed half-plane delimited by ℓ_k and containing P . More importantly, (2) all the A-type layers are pairwise-disjoint and lie monotonously in the direction perpendicular to e_k . Symmetrically, all the B-type layers have the same monotonicity.

Proof. (1) Denote by H the half-plane bounded by ℓ_k and containing P . Proving that all layers lie in H reduces to proving that all cells lie in H , which further reduces to proving that $\text{sector}(e_k) \subset H$. Now, let X be an arbitrary point in $\text{sector}(e_k)$, we shall prove $X \in H$. Notice that there is $(X_1, X_2, X_3) \in \mathcal{T}$ such that $X_2 \in e_k$ and $f(X_1, X_2, X_3) = X$. Because $X_1, X_3 \in \partial P$, point $(X_1 + X_3)/2$ lies in H . Since $X_2 \in e_k$, point X_2 lies on the boundary of H . Together, the 2-scaling of $(X_1 + X_3)/2$ with respect to X_2 , which equals X , lies in H .

(2) Each layer has two boundaries; we refer to them as the *lower border* and the *upper border*, so that the lower one is closer to ℓ_k than the upper one. Assume that layer_j and layer_{j+1} are consecutive A-type layers. See Figure 38 (a). We shall prove that the upper border of layer_j (denoted by \mathcal{U}) lies between ℓ_k and the lower border of layer_{j+1} (denoted by \mathcal{L}). Make an auxiliary line parallel to ℓ_k at each vertex of the two borders; these auxiliary lines cut the plane into *slices*, as shown in Figure 38 (b). It reduces to proving that (i) in each slice, the region under \mathcal{U} is contained in the region under \mathcal{L} . Now, consider any slice that intersects both \mathcal{U} and \mathcal{L} (e.g. the middle one in the figure). (The proof for other slices are similar and easier.) Then, there is an edge e_h , such that the part of \mathcal{U} that lies in this slice (labeled by \mathcal{U}_h in the figure) and the part of \mathcal{L} that lies in this slice (labeled by \mathcal{L}_h) are both translations of e_h . Applying the monotonicity of cells within layer_h (Fact 21), we have a monotonicity between these two translations of e_h that implies statement (i). We can prove the monotonicity of the B-type layers symmetrically. \square

7.4.3 Algorithm for computing u_1^*, u_2^*

Lemma 16. 1. Given an active edge e_j , we can do the following tasks in $O(\log n)$ time:

- (a) Determine whether V lies in layer_j ; if not, determine which side of layer_j it lies on.
- (b) Determine whether V lies in body_j ; if so, find the unique cell in body_j containing V .

2. We can compute u_1^*, u_2^* in $O(\log^2 n)$ time.

Proof. 1. Assume $e_j \in (v_p \circlearrowleft V)$; otherwise $e_j \in (V \circlearrowleft v_{q+1})$ and it is symmetric. By Fact 20, the cells in $\{\text{cell}(e_j, u) \mid (e_j, u) \text{ is active}\}$ are parallelograms with two sides parallel to e_j . Those sides parallel to e_j can be

extended so that they divide the plane into several regions as shown in Figure 37 (b). We refer to each such region as a *chop* and denote the one containing $\text{cell}(e_j, u)$ by chop_u . Notice that

- (1) We can compute the first and last unit in $\{u \mid (e_j, u) \text{ is active}\}$ in $O(\log n)$ time (Fact 19).
- (2) We can compute chop_u in $O(1)$ time, since $\text{cell}(e_j, u)$ can be computed in $O(1)$ time (Fact 20).
- (3) The chops have the same monotonicity as their corresponding cells. (see Fact 21)

Altogether, by a binary search, we can find the chop that contains V , which costs $O(\log n)$ time. After the chop containing V has been computed, we can easily solve tasks (a) and (b) in $O(1)$ time.

2. We design two *subroutines*. One assumes that V is contained in an A -layer (i.e. it assumes that u_1^* is an edge), the other assumes that V is contained in a B -layer (i.e. it assumes that u_2^* is an edge). We describe the first one in the following; the other is symmetrical. First, compute the first and last active edges $e_g, e_{g'}$ in $(v_p \circlearrowleft V)$, which costs $O(\log n)$ time by Fact 19.2. Then, using part 1 (a) and a binary search, find the only A -layer in $\text{layer}_g, \dots, \text{layer}_{g'}$ that contains V . If failed, terminate this subroutine. Otherwise, assume that layer_j contains V , check whether body_j contains V using part 1 (b). If so, we find the cell containing V and thus obtain (u_1^*, u_2^*) . It costs $O(\log^2 n)$ time.

CORRECTNESS: If u_1^* is an edge, the first subroutine obtains (u_1^*, u_2^*) ; if u_2^* is an edge, the second subroutine obtains (u_1^*, u_2^*) ; however, in a degenerate case, u_1^*, u_2^* can both be vertices, and the two subroutines both fail to find (u_1^*, u_2^*) . (This case is indeed degenerate because it implies a parallelogram inscribed in P with three corners lying on the vertices.) Nevertheless, our algorithms can handle the degenerate case using the following modification.

MODIFICATION: When u_1^*, u_2^* are both vertices, V lies on the boundary of some $\text{cell}(u, u')$ such that at least one of u, u' is an edge (see fact (i) below). *We first find a cell that contains V or its boundary contains V . If we only find a cell whose boundary contains V , we use $O(1)$ extra time to find the cell that contains V which is nearby.*

- (i) If $(v_j, v_{j'})$ is active and $X \in \text{cell}(v_j, v_{j'})$, at least one of following holds. 1. $(v_j, e_{j'-1})$ is active and X lies in the boundary of $\text{cell}(v_j, e_{j'-1})$. 2. $(e_j, v_{j'})$ is active and X lies in the boundary of $\text{cell}(e_j, v_{j'})$.

Proof of (i): Denote $M = (v_j + v_{j'})/2$ and denote by X' the reflection of X with respect to M . Because $\text{cell}(v_j, v_{j'})$ is the reflection of $\zeta(v_j, v_{j'}) \cap e_k$ with respect to M , point X' lies in $\zeta(v_j, v_{j'}) \cap e_k$. Notice that $\zeta(v_j, v_{j'})$ is the concatenation of $\zeta(v_j, e_{j'-1})$ and $\zeta(e_j, v_{j'})$. Point X' lies in $\zeta(v_j, e_{j'-1}) \cap e_k$ or $\zeta(e_j, v_{j'}) \cap e_k$. In the former case, $(v_j, e_{j'-1})$ is active and the reflection of X' with respect to M (which equals X) lies on the boundary of $\text{cell}(v_j, e_{j'-1})$; in the latter case, $(e_j, v_{j'})$ is active and X lies on the boundary of $\text{cell}(e_j, v_{j'})$. \square

Remark 7 (Similarities between computing $\text{sector}(V) \cap \partial P$ and answering Vertex-in-Block query). *We locate among A -type and B -type roads or layers. Roads (of the same type) admit good monotonicities, so as the layers.*

Compute the block containing V when V lies in $\text{sector}(v_k)$

In the above we assume w is an edge. We now discuss the easier case where w is vertex. Assume $w = v_k$.

In fact, by regarding v_k as a sufficiently small edge, this case can be regarded as a special case of the edge case (where w is an edge). But we can design a more simple solution to the vertex case, as shown below.

Let (X_1, X_2, X_3) denote the preimage of V under function f . Clearly, u_1^*, v_k, u_2^* are respectively the units containing X_3, X_2, X_1 . Moreover, due to (30), $[v_p \circlearrowleft V)$ contains u_1^* ; and $(V \circlearrowleft v_{q+1}]$ contains u_2^* . Therefore,

$$X_1 \in (V \circlearrowleft v_{q+1}], X_2 = v_k, X_3 \in [v_p \circlearrowleft V), \text{ and } VX_1X_2X_3 \text{ is a parallelogram.}$$

Lemma 17. *There is a unique parallelogram $A_0A_1A_2A_3$ whose corners A_0, A_1, A_2, A_3 respectively lie in $V, (V \circlearrowleft v_{q+1}], v_k, [v_p \circlearrowleft V)$, and we can compute it in $O(\log^2 n)$ time.*

Applying Lemma 17, we can find (X_1, X_2, X_3) in $O(\log^2 n)$ time and thus obtain $(u_1^*, u_2^*) = (\mathbf{u}(X_3), \mathbf{u}(X_1))$.

Proof. Suppose there are two such parallelograms, $VA_1v_kA_3$ and $VB_1v_kB_3$. Because their centers coincide at $(v_k + V)/2$, quadrant $ABA'B'$ is a parallelogram. Recall that $[v_p \circ v_{q+1}]$ is an inferior portion by (29) and notice that it contains A_1, A_3, B_1, B_3 . Thus we get a parallelogram inscribed in an inferior portion, which is impossible.

Computing $A_0A_1A_2A_3$ is equivalent to finding two points A_3, A_1 respectively restricted to $[v_p \circ V], (V \circ v_{q+1}]$ so that their mid point lies at $(v_k + V)/2$, which is further equivalent to computing the intersection between $[v_p \circ V]$ and the reflection of $(V \circ v_{q+1}]$ with respect to $(v_k + V)/2$. Using standard methods in computational geometry, we can find this intersection in $O(\log^2 n)$ time by a binary search. We omit further details. \square

Acknowledgement. This work is mainly done during my Ph. D. at Tsinghua University. This work was supported by National Basic Research Program of China Grant 2007CB807900, 2007CB807901, and the National Natural Science Foundation of China Grant 61033001, 61061130540, 61073174.

The author thanks god for his amazing creation. After studying this mysterious structure, we got an impression that everything is perfect and rotating. The author thanks Haitao Wang for taking part in fruitful discussions and for many other helps, and thanks Andrew C. Yao, Jian Li, Danny Chen, Wolfgang Mulzer, Matias Korman, Donald Sheehy, Kevin Matulef, Junhui Deng, and anonymous reviewers from past conferences for many precious suggestions. Last but not least, the author appreciates the developers of Geometer's Sketchpad[®].

References

- [1] M. d. Berg, O. Cheong, M. Kreveld, and M. Overmars. *Computational Geometry: Algorithms and Applications*. Springer-Verlag TELOS, SC, CA, USA, 3rd edition, 2008.
- [2] S. Cabello, O. Cheong, and L. Schlipf. Finding largest rectangles in convex polygons. *European Workshop on Computational Geometry*, 2014.
- [3] K. Jin. Finding all maximal area parallelograms in a convex polygon. *CoRR*, abs/1711.00181, 2017.
- [4] D. Kirkpatrick and J. Snoeyink. Tentative prune-and-search for computing fixed-points with applications to geometric computation. *Fundamenta Informaticae*, 22(4):353–370, Dec. 1995.
- [5] N. Pano, Y. Ke, and J. O'Rourke. Finding largest inscribed equilateral triangles and squares. In *Proceeding of Annual Allerton Conference on Communication, Control, and Computing*, pages 869–878, 1987.
- [6] M. Sharir and S. Toledo. Extremal polygon containment problems. *Computational Geometry: Theory and Applications*, 4(2):99–118, jun 1994.
- [7] G. Ziegler. *Lectures on Polytopes*. Graduate texts in mathematics. Springer-Verlag, 1995.

A Appendix

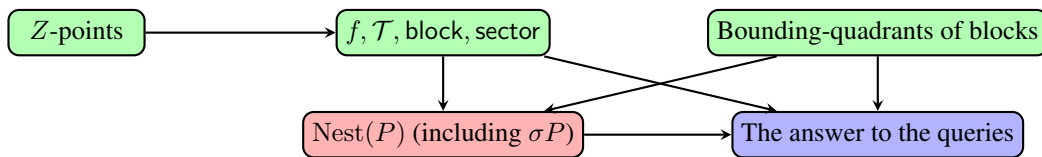


Figure 39: Key geometric objects studied in this manuscript and their relations.

Lemma 18. *The total number of segments in $\text{Nest}(P)$ is $O(n^2)$.*

Proof. By the explicit definition of \mathcal{L}_V^* , \mathcal{R}_V^* given in subsection 7.1, either of them consists of $O(n)$ segments. So it reduces to showing that (i) *the boundary-portions in $\{\zeta(u, u') \mid \text{unit } u \text{ is chasing unit } u'\}$ have in total $O(n^2)$ line segments.* For any e_i , applying the bi-monotonicity of the Z -points (Fact 1), the boundary-portions in $\{\zeta(e_i, u') \mid e_i \text{ is chasing unit } u'\}$ have in total $O(n)$ line segments. Similarly, for any e_j , the boundary-portions in $\{\zeta(u, e_j) \mid \text{unit } u \text{ is chasing } e_j\}$ have in total $O(n)$ line segments. These together imply that the number of line segments of $\{\zeta(v_i, v_j)\}$ is also $O(n^2)$ (see Figure 3). Altogether, we obtain statement (i). So the lemma holds. \square